Summer 7-7-2017

Packet Scheduling Algorithms in LTE/LTE-A cellular Networks: Multi-agent Q-learning Approach

Najem Nafiz Sirhan

Najem Nafiz Sirhan

Candidate

Department of Electrical and Computer Engineering

Department

This dissertation is approved, and it is acceptable in quality and form for publication: *Approved by the Dissertation Committee:*

Prof., Manel Martínez-Ramón

Prof., Gregory L. Heileman

Prof., Nasir Ghani

Prof., Christopher C. Lamb

Packet Scheduling Algorithms in LTE/LTE-A cellular Networks: Multi-agent Q-learning Approach

by

Najem Nafiz Sirhan

B.S., Computer Engineering, University of Jordan, Jordan, 2006
M.S., Mobile and High Speed Telecommunication Networks, Oxford Brookes University, UK, 2008

DISSERTATION

Submitted in Partial Fulfillment of the
Requirements for the Degree of

Doctor of Philosophy
Engineering

The University of New Mexico

Albuquerque, New Mexico

July, 2017

Dedication

To my father, Dr. Nafiz, for his endless love, encouragement, and financial support throughout the whole process of doing my Ph.D., in which without him, I would have not been able to do it.

To my mother, Kholoud, my brother, Bader, and my sisters, Rana and Rand, for their endless love and support.

Acknowledgments

I would like to thank my advisor, Professor Manel Martínez-Ramón, for his feedback and support.

I also would like to thank my previous advisor, Professor Gregory Heileman, for his feedback and support.

I also would like to thank Professor Nasir Ghani, and Professor Christopher Lamb, for their feedback and support.

Packet Scheduling Algorithms in LTE/LTE-A cellular Networks: Multi-agent Q-learning Approach

by

Najem Nafiz Sirhan

B.S., Computer Engineering, University of Jordan, Jordan, 2006
M.S., Mobile and High Speed Telecommunication Networks, Oxford Brookes University, UK, 2008

Ph.D., Engineering, University of New Mexico, 2017

Abstract

Spectrum utilization is vital for mobile operators. It ensures an efficient use of spectrum bands, especially when obtaining their license is highly expensive. Long Term Evolution (LTE), and LTE-Advanced (LTE-A) spectrum bands license were auctioned by the Federal Communication Commission (FCC) to mobile operators with hundreds of millions of dollars. LTE/LTE-A comes with lots of enhanced technological features, such as Carrier Aggregation (CA) and Heterogeneous Networks (HetNets) deployment. These features enable operators to provide their growing number of users with the required Quality of Service (QoS) that meets with their service demands. In-order for operators to utilise their LTE/LTE-A cellular network spectrum resources, they have to use an efficient Radio Resource Management (RRM) set of procedures, one of which are packet scheduling algorithms that play an important role in efficiently managing the spectrum resources.

Despite the fact that these packet scheduling algorithms have the ability to efficiently manage the spectrum resources, the use of them while following a fixed spectrum assignment policy does not always result in a complete spectrum utilization. This is due to the irregular usage demand by licensed users, in which this demand varies depending on time and geographical area. This causes what is called spectrum holes, which will eventually lead to spectrum underutilization. In order to solve this problem, the FCC recommends mobile operators to follow a dynamic spectrum assignment policy to allow unlicensed users to access their spectrum and use these spectrum holes without affecting the QoS of licensed users. This solution requires the use of machine learning techniques in cognitive radio.

In the first part of this dissertation, we study, analyze, and compare the QoS performance of QoS-aware/Channel-aware packet scheduling algorithms while using CA over LTE, and LTE-A heterogeneous cellular networks. This included a detailed study of the LTE/LTE-A cellular network and its features, and the modification of an open source LTE simulator in order to perform these QoS performance tests. In the second part of this dissertation, we aim to solve spectrum underutilization by proposing, implementing, and testing two novel multi-agent Q-learning-based packet scheduling algorithms for LTE cellular network. The Collaborative Competitive scheduling algorithm, and the Competitive Competitive scheduling algorithm. These algorithms schedule licensed users over the available radio resources and unlicensed users over spectrum holes. The implementation and testing was done using Matlab. The performance measurements were based on the throughput percentages that each user acquired, and the fairness level of sharing the spectrum among users. Experimental results show that both scheduling algorithms converged to almost 90% utilization of the spectrum, and provided fair shares of the spectrum among users. In conclusion, our results show that the spectrum band could be utilized by deploying efficient packet scheduling algorithms for licensed users, and can be further utilized by allowing unlicensed users to be scheduled on spectrum holes whenever they occur.

Contents

List of Figures

List of Tables

Glossary

3GPP	Third Generation Partnership Project.
AAS	Active Antenna Systems.
ABS	Almost Blank Sub-frame.
AMC	Adaptive Modulation and Coding.
ANSI	American National Standards Institute.
ARIB	Association of Radio Industries and Businesses.
ARQ	Automatic Repeat Request.
AuC	Authentication Center.
BCQI	Best CQI.
BMBS	Basic Multi-Band Scheduling.
CA	Carrier Aggregation.
CBS-CoMP	Coordinated Beam-Switching CoMP.
CC	Component Carrier.
CCSA	China Communications Standards Association.

CN	Core Network.
CoMP	Coordinated Multi-Point Operation.
CQI	Channel Quality Indicator.
CR	Cognitive Radio.
CRE	Cell Range Expansion.
CS/CB	Coordinated Scheduling and/or Beam-Forming.
CSI	Channel State Information.
D2D	Device to Device.
DCI	Downlink Control Information.
DCS	Dynamic Cell Selection.
D-ICIC	Dynamic Inter Cell Interference Coordination.
DMRS	Demodulation Reference Signal.
DQS	Disjoint Queue Scheduler.
DSA	Dynamic Spectrum Access.
DSS	Dynamic Spectrum Sharing.
eICIC	enhanced ICIC.
EMBS	Enhanced Multi-Band Scheduling.
eNodeB	Evolved NodeB.
EPC	Evolved Packet Core.

ETSI	European Telecommunications Standards Institute.
Exp-Rule	Exponential Rule.
EXP/PF	Exponential/Proportional Fairness.
FCC	Federal Communication Commission.
FCFS	First Come First Served.
FDD	Frequency Division Duplex.
FEC	Forward Error Correction.
FIFO	First In First Out.
GBR	Guaranteed Bit Rate.
GMBS	General Multi-Band Scheduling.
GPRS	General Packet Radio Service.
HARQ	Hybrid Automatic Repeat Request.
HetNets	Heterogeneous Networks.
HOL	Head of Line.
HSS	Home Subscriber Server.
IC	Independent Carrier.
ICI	Inter-Cell Interference.
ICIC	Inter-Cell Interference Coordination.
In-CC	Independent-CC.

IoT	Internet of Things.
IRC	Interference Rejection Combining.
JAL	Joint Action Learner.
JP	Joint Processing.
JQS	Joint Queue Scheduler.
JT	Joint Transmission.
JUS	Joint User Scheduler.
KMT	Kwan Maximum Throughput.
LL	Least Load.
Log-Rule	Logarithmic Rule.
LTE	Long Term Evolution.
LTE-A	LTE-Advanced.
LTP	Long Term Perspective.
LWDF	Largest Weighted Delay First.
MAC	Medium Access Control.
MARL	Multi-Agent Reinforcement Learning.
MCS	Modulation and Coding Scheme.
M-LL	Modified Least Load.
MLWDF	Modified Largest Weighted Delay First.

MME	Mobility Management Entity.
MMSE	Minimum Mean Squared Error.
MRC	Maximal Ratio Combining.
MTC	Machine-Type Communications.
MUE	Macro-Cell UE.
OFDM	Orthogonal Frequency Division Multiplexing.
PCEF	Policy Control Enforcement Function.
PCell	Primary Cell.
PCI	Physical Cell Identity.
PCRF	Policy Control and Charging Rules Function.
PDCCH	Physical Downlink Control Channel.
PDCP	Packet Data Control Protocol.
PDNs	Packet Data Networks.
PDSCH	Physical Downlink Shared Channel.
PF	Proportional Fairness.
P-GW	PDN-Gateway.
PLR	Packet Loss Rate.
PMI	Pre-coding Matrix Index.
PU	Primary User.

PUE	Pico-cell UE.
PUSCH	Physical Uplink Control Channel.
QAM	Quadrature Amplitude Modulation.
QoE	Quality of Experience.
QoS	Quality of Service.
QPSK	Quadrature Phase-Shift Keying.
QSG	Queue Side Greedy
R8/9	Release 8/9.
R10/11	Release 10/11.
R12	Release 12.
R13/14	Release 13/14.
R15	Release 15.
R16	Release 16.
RAN	Radio Access Network.
RB	Resource Block.
RF	Radio Frequency.
RL	Reinforcement Learning.
RLC	Radio Link Control.
RR	Round Robin.

RRC	Radio Resource Control.
RRH	Remote Radio Head.
RRM	Radio Resource Management.
RS	Resource Scheduler.
SCell	Secondary Cell.
SC-FDMA	Single-Carrier Frequency Division Multiple Access.
S-GW	Serving Gateway.
SINR	Signal to Interference Plus Noise Ratio.
SIPTO	Selected IP Traffic Offload.
SRUS	Separated Random User Scheduling.
SSG	Server Side Greedy.
SU	Secondary User.
TB	Transport Block.
TDD	Time Division Duplex.
TDM	Time Domain Multiplexing.
TFTs	Traffic Flow Templates.
TTA	Telecommunications Technology Association.
TTC	Telecommunications Technology Committee.
TTI	Transmission Time Interval.

TSDSI	Telecommunications Standards Development Society, India.
UMTS	Universal Mobile Telecommunication Systems.
UE	User Equipment.
UE-RS	UE-specific demodulation Reference Signal.
VoIP	Voice over IP.
Wi-Fi	wireless fidelity.
WiMAX	Worldwide Interoperability for Microwave Access

Chapter 1

Introduction

1.1 Dissertation Motivation

The increasing number of mobile subscriptions worldwide increases the demand on the LTE/LTE-A cellular network radio resources. The total number of mobile subscriptions in the first quarter of 2015 was around 7.2 billion, and it is expected to rise up to 9.2 billion by 2020, 3.7 billion of them will be LTE subscriptions. In 2014, the rate of the generated mobile data traffic worldwide per month was 3.4 ExaBytes "$3.4 * 10^{18}$ Bytes", and it is expected to rise at a compound annual growth rate of around 45%. Which means that the monthly rate will be in 2020 around 10 times of what it was in 2014. In 2014, video traffic accounted for around 45% of mobile data traffic, and this percentage is expected to rise up to 60% of all mobile data traffic by 2020 [5].

The LTE/LTE-A cellular network radio resources forms the spectrum bands that the mobile operators paid tens of millions and up to billions of dollars to operate on them when they were first auctioned by the Federal Communication Commission (FCC) [12] [13] [21].

This huge growing demand on these highly expensive radio resource indicates that the continuous improvements and evolution of telecommunication technologies is not a luxury but a necessity, and it pressure researchers and engineers in the field of telecommunication to continuously improve the utilization of these radio resources. This utilization improvement is achieved by the use of Radio Resource Management (RRM) functionalities. This is why lots of research and development studies in the area of RRM are on continuous pursed. And this is why I was motivated in this dissertation to focus on RRM with the emphasis on the packet scheduling functionality as my research topic.

Despite the fact that the use of packet scheduling algorithms could lead to an optimized scheduling decisions, there is a case in which the spectrum is still under-utilized as stated by the FCC spectrum policy task force in their spectrum efficiency report [14]. This is because the spectrum is used by licensed users only, in which their usage demands varies by time and geographical area. This sporadic usage of the spectrum indicates that there exist unused radio resources in the spectrum, which are called spectrum holes, or white spaces.

The spectrum underutilization problem could be solved by allowing unlicensed users to access the spectrum holes without affecting the QoS of the licensed users. This could be accomplished by the use of machine learning approaches in cognitive radio. Q-learning which is an example of an unsupervised machine learning approach comes with great benefit to cognitive radio systems. Q-learning helps to discover the best possible action policy for any decision process. So in the case of cognitive radio systems which have the ability to automatically detect occupied and unoccupied radio resources, Q-learning would provide the framework upon which licensed users can be scheduled over the available radio resources, and unlicensed users over the remaining radio resources, the spectrum holes. And this is why I was motivated to use multi-agent Q-learning techniques in my dissertation.

1.2 Radio Resource Management (RRM) in LTE

Radio Resource Management (RRM) refers to the whole functionality of managing the use of radio channels, co-channel interference, and other radio transmission characteristics. This management functionality is accomplished by the use of intelligent strategies and algorithms that include in their calculation multiple parameters in order to optimize the use of the available radio channels. These parameters include but are not limited to, the number of users, transmission rate per user, transmission power, QoS parameters, number of available channels, channels' conditions, and modulation and coding scheme [26] [24].

In addition to allocating the available radio resources to users, LTE uses other RRM procedures, for example, LTE uses Channel Quality Indicator (CQI) reporting, Amplitude and Modulation Coding (AMC) and power control, link adaptation, Hybrid Automatic Repeat Request (HARQ). These procedures interact with each other to further optimize the radio resource allocation, and they are hosted by the physical and medium access layers. The interaction of these procedures including the packet scheduler are shown in Fig. 1.1 [36].

The CQI reporting procedure is used to estimate the quality of the downlink channel at the eNodeB. The main objective of this reporting procedure is to help in making a tradeoff between a precise channel quality estimation and a reduced signaling overhead. The value of CQI is calculated by measuring the Signal to Interference Plus Noise Ratio (SINR) [47] [36].

The AMC procedure depends on the CQI reporting procedure, in which the value of the modulation and coding scheme (MCS) will change depending on the value of SINR, for example, if a user is having a high SINR, then the MSC value will be changed in-order to allow this user to be served with a higher bit-rate, but up to a certain threshold [47] [36].

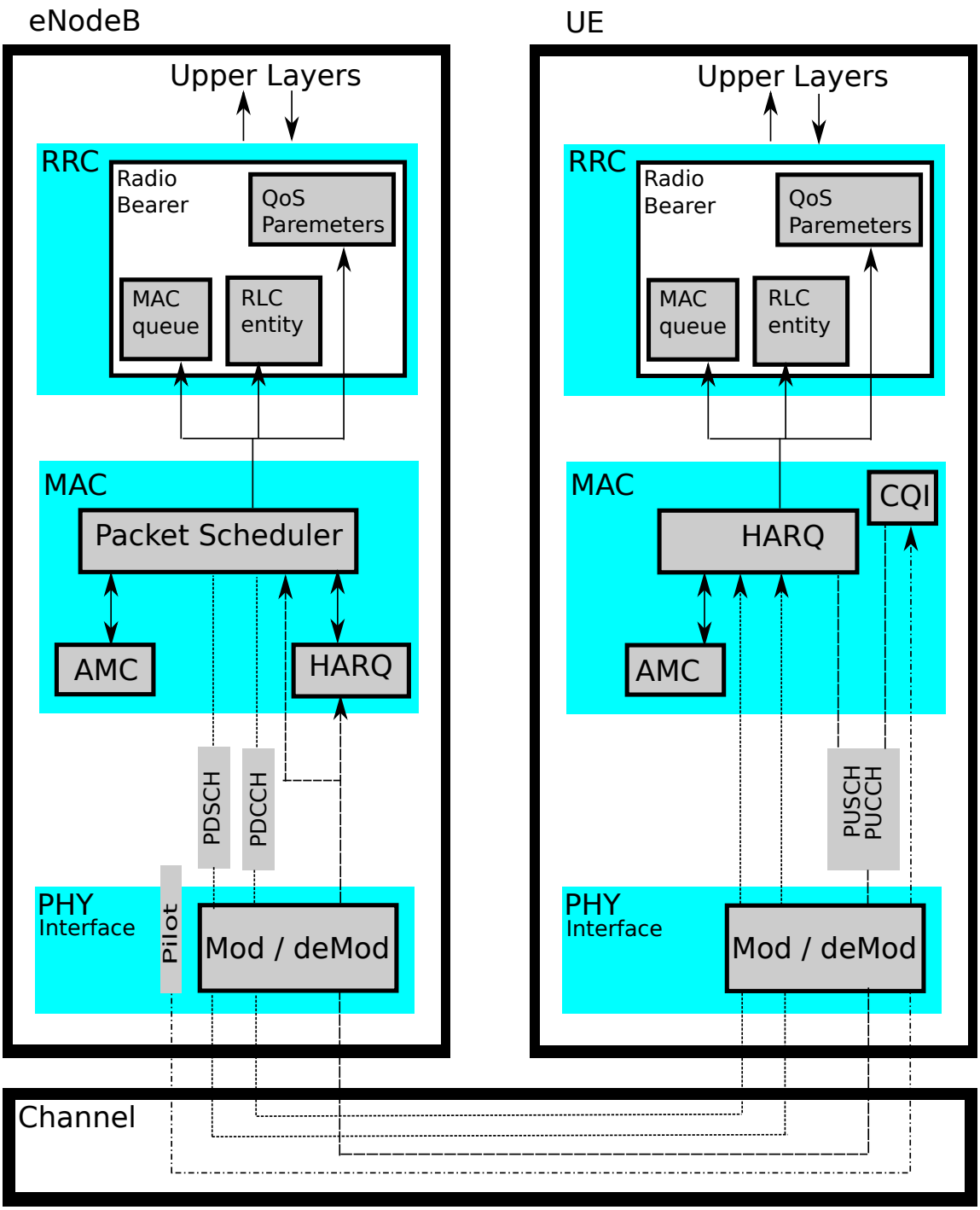

AMC: Adaptive Modulation and Coding
RLC: Radio Link Control
PDCCH: Physical Downlink Control Channel
PDSCH: Physical Downlink Shared Channel
PUSCH: Physical Uplink Schared Channel
PUCCH: Physical Uplink Control Channel
RRC: Radio Resource Control
CQI: Channel Quality Indicator
HARQ: Hybrid Automatic Repeat Request
UE: User Equipment
eNodeB: Evolved NodeB

Figure 1.1: Interaction of the main RRM procedures

The power control procedure also depends on the SINR value, in which the transmission power is adjusted to compensate for the changes of the instantaneous channel conditions [47] [36].

The HARQ procedure has two sub-procedures that works together, the Forward Error Correction (FEC), and Automatic Retransmission Request (ARQ). Its objective is to provide a better throughput by compensating for errors which occurs over wireless multi-path fading channels [51] [77].

1.3 Packet Scheduling in LTE

Packet scheduling is one of the main procedures of RRM. Packet schedulers are responsible for allocating radio resources to users' packets, and they are deployed by the Medium Access Layer (MAC) that is hosted at the eNodeB, while users' applications and connections are scheduled by the application layer.

In order to allocate radio Resource Blocks (RBs) to users, a comparison has to be made based on a previously defined metric. This metric could be seen as the priority of each user for a specific RB. This metric comparison is performed every Transmission Time Interval (TTI) in order to calculate the allocation decision which is sent to the users over the Physical Downlink Control Channel (PDCCH). One of the main characteristics of the Physical Downlink Shared Channel (PDSCH) is to be shared among all users, which means that on every TTI, which equals 1 ms, portions of the radio spectrum should be distributed among users. The user with the highest metric will be allocated this specific RB. The Physical Downlink Control Channel (PDCCH) contains the Downlink Control Information (DCI) messages that informs the users about the RBs which were allocated for data transmission on the PDSCH in the downlink direction, and the RBs that were allocated to their data transmission on the Physical Uplink Control Channel (PUSCH) in the uplink direction [36].

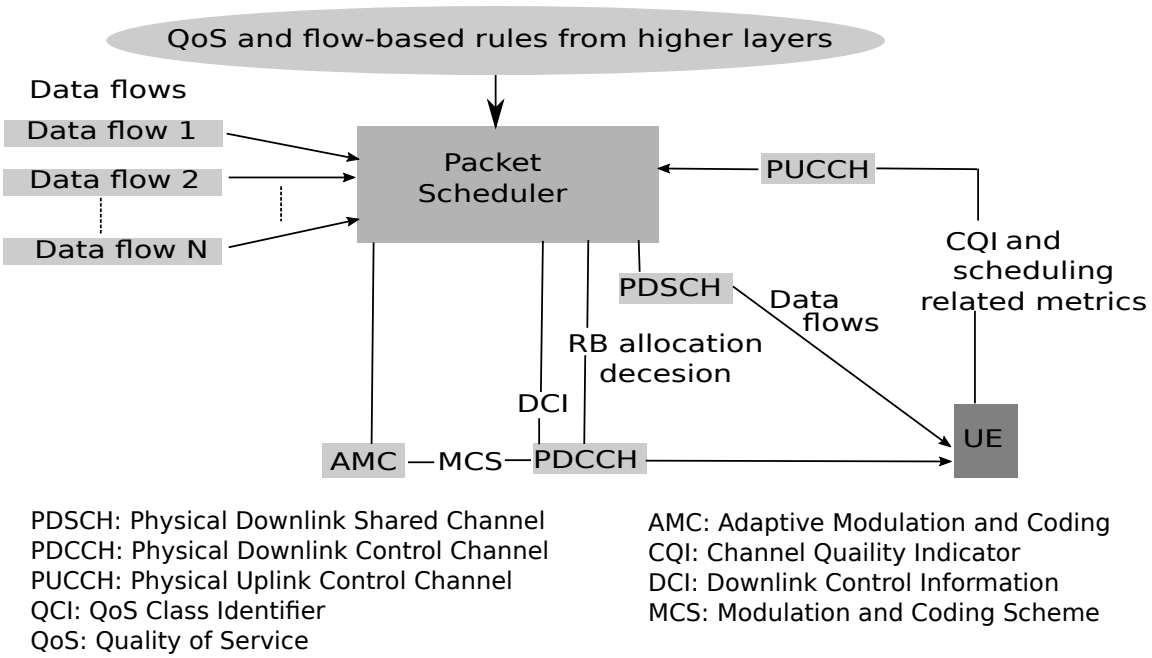

Figure 1.2: The general model of LTE scheduling.

The general model of how a downlink packet scheduler interacts with users is shown in Fig 1.2. In [36], they have divided the whole scheduling process in a sequence of operations that are repeated every TTI. First, the UE decodes the reference signal and computes the Channel Quality Indicator (CQI) then sends it back to the eNodB. Second, the CQI information is being used by the eNodeB for making the allocation decisions and filling up a RB allocating mask. Third, the Adaptive Modulation and Coding (AMC) module selects the best Modulation and Coding Scheme (MCS) that should be used for the data which will be transmitted to the scheduled users. Fourth, all the above information is sent to the UEs on the PDCCH. Finally, each UE reads the PDCCH and accesses to the proper PDSCH if it has been scheduled. This model is slightly different in the case of uplink because the eNodeB does not require extra information about the uplink channel quality.

1.4 State of the art

In the literature, there exist many packet scheduling algorithms that are based on calculating a utility function. Each of these algorithms has its own unique utility function, whether to increase the throughput, or to decrease the delay, or to improve the fairness [80]. The utility function calculation is the core process of scheduling in this type of algorithms. This is because it contains all the necessary parameters which are included in calculating the best scheduling decision that meets with the radio environment state and the users' requirements.

In addition to the packet schedulers that are based on calculating a utility function, there are other types of packet schedulers found in the literature that are based on the use of Q-learning algorithm. However, they exist in a much lesser amount.

In Q-learning-based LTE scheduling algorithms, constructing a Q-table is the core process of scheduling in this type of algorithms. Constructing and updating the Q-table depends on three main elements, the state, action, and reward. The reward is calculated after executing an action by a learning agent in a certain time and radio environment state. Assigning the reward function is crucial in the agent's learning process and in regulating its behavior. This is because calculating the reward indicates to the learning agent how much gain it can get by executing an action and how much effect it has on the environment. The repeated cycle of the agent's learning process will update and construct the Q-table, in which it will contain optimal action policies that will eventually lead to an optimized scheduling decisions.

In this section, we present the state of the arts of both scheduling types, each in a separate sub-section. In sub-section 1.4.1, we present the state of the art in the utility-based LTE packet scheduling algorithms with the focus of the Carrier Aggregation feature. And then, in subsection 1.4.2, we present the state of the art in Q-learning-based LTE packet scheduling algorithms.

1.4.1 Packet Scheduling in LTE-A with CA

The authors of [41], proposed a scheduling algorithm that allocates Component Carriers (CCs) to users dynamically, it does this by taking into account the channel and user conditions, and the network load. They stated that their scheme gives a much better network performance and user fairness. They used the aggregated value of queuing Head of Line (HOL) delay of user which is allocated to the carrier as a metric, in which they used it to determine the load of a component carrier. In-order to prove their statement they compared their dynamic scheme with the round robin static scheme in terms of throughput and delay. In terms of throughput, their dynamic reallocation achieved higher aggregated throughput which translates to better network utilization. In terms of delay, the average delay kept increasing with the static round robin scheme.

The authors of [41] applied two backlog based resource block scheduling algorithms, one was called the Queue Side Greedy (QSG) RB scheduling, and the other one was called the Server Side Greedy (SSG) RB scheduling. Their simulation focused on the QSG. The queue refers to packet queue at eNodeB and the server means the available resource blocks. In both algorithms, backlog could be represented by either, the HOL delay, or the queue length. The backlog scheme is a good indicator for the system load and priority of UE to be scheduled. And they compared the backlog based scheduler with the PF algorithm in terms of throughput and delay. In terms of throughput, the backlog had a slight better performance over the PF. In terms of delay, the backlog scheduler had a lower delay than the PF.

In LTE cellular network, the feedback about the channel quality and the achieved link adaptation is provided by the Channel Quality Indicator (CQI). Also, in LTE cellular network, the process of link adaptation technique starts by allocating all the resource blocks to the users by the scheduler. Then, the resource blocks for a single

user are built into one single transport block and modulated with Modulation and Coding Scheme (MCS) that corresponds with the lowest CQI of the resource blocks of this user. The drawbacks of this approach exists in the possibility of decreasing the number of bytes that could be transmitted over a transport block. The reason for this drawback is that the scheduler considers the user's CQI individually when assigning a resource block to it, which might not lead to an optimal assignment in terms of all CQIs of resource blocks to this user. In order to improve this, the authors of [41] proposed an intelligent link adaptation algorithm that incorporate the CQI trade off when allocating resource blocks, and dose the scheduling and link adaptation collectively. Their algorithm checks if the CQI value of a resource block that is available to a user could enhance the overall Transport Block (TB) size in accordance with the resource blocks that are already allocated to this user. If their algorithm finds out that the value of the CQI is very low for a resource block, which will result in degrading the MCS mode of the transport block built with other resource blocks. Then the algorithm will schedule this resource block to other user with a better channel condition. Their algorithm uses a function that averages the weighted CQI values. The authors also compared their algorithm with the minimum CQI in terms of average throughput and delay per user. In their comparison, they considered a 200Kbps video session that is downloaded from eNodeB to a group of users that are 1000m away over different bandwidths. Their comparison results in terms of average throughput per user, showed a slight decrease of (0.6%). In terms of average delay per user, their algorithm had a much better performance of (13%).

The authors of [42] proposed a downlink packet scheduling algorithm that is based on Proportional Fairness (PF) scheduling algorithm with a feature that reserves more resources to real time packets. Their scheduling scheme consists of a classifier which classifies users' packets into two queues, one for real time packets, and the other one for non-real time packets. The output of both queues is delivered into a transmission queue, but with different rates to represent the priority which the real time packets

have over the non-real time packets. Also, in the case of real time packets, they are delivered into the transmission queue run by run. However, in the case of the non-real time packets, they are delivered in periods, in which these periods were defined to be a specific integer multiple of a run from the first run. The transmission queue is controlled by a scheduler that schedules user k packets over the resource block j on carrier component i in scheduling runs based on a fairness vector.

The authors of [42] compared the performance of their carrier aggregation scheduler with a scheduler that is based on an Independent Carrier (IC) in terms of the system throughput, the mean delay, and the fairness. In terms of system throughput, their scheduler had a better performance especially when the system load reached its maximum value. This is because when using carrier aggregation, if the system load is large, the capability to avoid and skip temporarily faded users of their scheduler is better. In terms of mean packet delay, their scheduler achieved a lower delay for real time packets in comparison with non-real time packets. This is because their scheduler's sittings protect real time packets from the competition of non-real time packets. In addition, the mean packet delay for real time packets of both compared schedulers didn't monotonically increase. This is because in both schedulers packets with a delay more than 0.1 second will be dropped. Furthermore, their scheduler had a significant improvement for the mean packet delay of non-real time packets in case if the system load was very large. This is because the non-real time packet users have better opportunity to transmit their packets in the first carrier component. In terms of fairness, both schedulers had a high fairness index. This is due to the fact that they both used the proportional fairness algorithm.

The authors of [62] proposed a QoS-aware scheduling algorithm, and they called it Cross-CC User Migration scheme. The authors stated that their scheme reduces the effect of the unbalanced loads' problem among different CCs, and supports real-time services, taking into account the system throughput, user fairness and QoS

constraints. The structure of their scheme consists of three cooperative components, a Higher and Lower level scheduler, and Cross-CC user migration scheduler. The Higher Level Scheduler of their scheme starts by defining the amount of data that each real-time source should transmit to satisfy its delay constraint based on the delay requirements and the queue lengths. Then it calculates two types of transmission quotas frame-by-frame: the transmission quota for Head-of-Line (HoL) packets and the transmission quota from Long-Term-Perspective (LTP). Then the Lower Level Scheduler of their scheme assigns resource blocks using the Proportional Fair (PF) algorithms to fill the two defined transmission quotas based on the average data rate in PF. In order to achieve a lower packet loss probability, it offers first service for HoL packets, since these packets are more likely to face violation of the delay constraints. Finally, the Cross-CC user migration scheduler of their scheme assign more resources to the users that cannot complete their transmission quotas.

In order for the authors of [62] to prove their statement, they evaluated the performance of their scheme using a quasi-static downlink multi-cell LTE-A system-level simulator. They compared the performance of their scheme with the Two-level scheduling scheme in terms of packet loss probability, average queue length and throughput per user. In terms of packet loss probability, their scheme achieved lower probability of packet loss due to offering extra service priority to the HoL packets. In terms of average queue length, their scheme provided lower average queue length, this is because the Cross-CC user migration scheduler migrates the users at the less advantageous positions to receive more radio resource from other CCs. In terms of throughput per user, when the delay requirement was 40ms, their scheme outperformed the other scheme. However, the gain gradually decreased as the delay requirement increased which resulted in lower throughput per user.

The authors of [43] proposed a quantized water-filling packet scheduling scheme for downlink transmissions in LTE-A cellular network with carrier aggregation. Their

system environments consisted of one eNodeB and a group of users. Their system model consists of two tiers, the user grouping algorithm tier, and the quantized water-filling packet scheduling algorithm. The user grouping algorithm's input are the packets that will be sent to the users. The user grouping algorithm groups the users into different output queues according to the resources which they can share on the same carrier component. The arrived packets to various groups will be buffered into their group queues at the First In, First Out (FIFO) order, then the output of these queues will be delivered into the pseudo transmission queue *qpseudo* by the user grouping algorithm in a FIFO order. The objective of their user grouping algorithm is to minimize the mean packet delay, while maintaining the delay fairness among users in respective groups. In-order to maintain the delay fairness among users, the transmission of packets in the *qpseudo* has to follow two main rules; the First Come First Served (FCFS) discipline, and whenever a CC is assigned for a packet's transmission, all its resource blocks are fully utilized. In-order to force these two rules, the water-filling algorithm has to be applied. However, the fact that the size of the packets is not continuous and different carrier components might not be available to all users will prevent from applying the water-filling algorithm directly. So the authors designed a quantized water-filling packet scheduling algorithm as their second tier by adopting the water filling concept, which they stated in their paper that it could achieve near optimal solution to the issue of carrier component availability. They compared their algorithm with the multi-class M/G/1 queue, and their simulation results proved that their scheme had an upper bound in terms of delay.

The authors of [43] have extended their LTE-Sim [69] Simulator with multi-band scheduling algorithm for CA. And they also implemented a multi-band scheduling strategies which were able to optimally distribute radio resources among mobile users in the presence of multiple carrier components and to force a strict QoS constraints. Regarding the inter-band CA case, they are aggregating band-7 and band-20 "band-7

(UL: 2500-2570 MHz, DL: 2620-2690 MHz) and band-20 (UL: 832-862 MHz, DL: 791-821 MHz)". They did two inter-band CA scenarios, one with two carrier components of 5 MHz bandwidth each, and the other one for two carrier component of 20 MHz bandwidth each. Regarding the downlink multi-band schedulers, they have coded the General Multi-Band Scheduling (GMBS) and the Basic Multi-Band Scheduling (BMBS) which were proposed in previous work. And they enhanced the BMBS to the Enhanced Basic Multi-Band Scheduling (EMBS) and coded it. Then, they compared the performance of the EMBS scheduling algorithm while applying the two carrier aggregation scenarios, the 5 MHz and the 20 MHz with the case of not using the carrier aggregation for the two bandwidth scenarios; the 5 MHz and the 20 MHz. Their comparison was in terms of Packet Loss Rate (PLR), packet delay, and goodput. The results of comparing the average cell PLR, as a function of the number of users for cell radius of 1500 m with a PLR performance target of 1% showed that while using the EMBS for bandwidth of 5 MHz, the PLR values were the lowest. And while the system had a bandwidth of 20 MHz without the use of CA, the PLR values were the highest. The results of comparing the average delay in a cell as a function of the number of users showed that while using the EMBE for bandwidth of 5 MHz, the delay values were the lowest. And while the system had a bandwidth of 20 MHz without the use of CA, the delay values were the highest. The results of comparing the average cell supported goodput as a function of the number of users showed that while using the EMBS for bandwidth of 20 MHz, the goodput was almost as twice as it was while the system had a bandwidth of 20 MHz without the use of CA. And the gooput had the lowest similar values when the system had a bandwidth of 5 MHz with and without the use of CA. The results of comparing the average cell supported goodput as a function of the cell radius with PLR $<= 1\%$ showed that changing the cell radius didn't affect the goodput values.

The authors of [65] built a simulation tool using C++ programming language in-order to run tests on three common scheduling algorithms, the Round Robin

(RR), PF, and the Max rate in terms of system throughput and fairness. Their tests included two scenarios, one with the use of Independent-CC (In-CC), and the other with the use of Cross-CC. Their simulation model contains a three pre-processing modules. The user mobility module, the multi-path gains generator module, and the traffic generator module that run independently before the main program. The user mobility module generates a file which contains locations of every user for the simulation time. The multi-path gain generator module generates the multi-path gain for every TTI and for each CC by using the speed and carrier frequency. The traffic generator module generates the packet arrivals for each user over the simulation time and queues packets in the buffer. Their test results showed that the system throughput in the case of using the Cross-CC had a slight improvement of 1% in comparison to the case of using an In-CC. Also they found that the cell edge user's throughput in the case of using Cross-CC were much better than in the case where the In-CC was used. In terms of comparing the Cross-CC scheduler with the In-CC scheduler combined with RR, PF, and Max Rate, a similar system throughput resulted for the RR and the Max Rate was found. However, when the PF algorithm was tested, the Cross-CC scheduler had a better performance because it takes into account the average user data rate over multiple CCs while the In-CC scheduler, it does not. In terms of system fairness, the use of Max rate had the worst results, and this was due to unscheduled users that are far away from the eNodeB. In the case of using the RR, both schedulers had similar fairness results. The best fairness was achieved when using the PF algorithms combined with the Cross-CC scheduler.

The authors of [92] compared the QoS performance of two different multi-user scheduling schemes in CA based LTE-A systems; the first one is the Separated Random User Scheduling (SRUS), and the second one is the Joint User Scheduling (JUS). The SRUS is simpler but less efficient while the JUS is optimal but with higher signaling overhead. Moreover, the SRUS needs only one single CC to access for user, while in the JUS all the CCs have to be connected. Furthermore, the SRUS scheme

includes two-level scheduling. The first level is in charge of allocating users to only one of the CCs, its second level scheduler is a Resource Scheduler (RS) that allocates Resource Blocks (RBs) to the authorized waiting users by different strategies such as the RR and PF scheduling algorithms. While the JUS scheme has only one level scheduler which means that it doesn't follow any specific user allocation method as in the case of the SRUS, the RBs of all available CCs in the system are aggregated together as an integrated resource pool managed by one single RS.

The authors of [92] obtained their simulation results by a quasi-dynamic system level simulator that was built in Matlab. In order to obtain their results they applied two traffic buffer models, the full buffer model to represent that the users are continuously receiving and transmitting data all the time, and the Poisson-based finite buffer model which represent the Internet and multimedia applications. Furthermore, the two performance metrics that were considered in their scenarios are; the average user latency and average number of waiting users for trunking efficiency comparison. In the full buffer scenario, the sector throughput of SRUS scheme is the same as the JUS with RR resource scheduling, while in the case of PF, there was only approximately 5%-7% decrease by SRUS in different sector user number configuration. Which meant that the spectral efficiency loss of SRUS scheme is slight. In the Finite buffer scenario, the average user latency of SRUS was larger than JUS by nearly 90%-100% when the arrival rate was small. However, as the traffic increased up to arrival rate of 8, the performance of both schemes were similar. For the blocking status of both schemes by the average number of waiting users in the system, when the arrival rate was below 8, the average waiting user of SRUS was about twice that of JUS. But when the traffic load grew heavier, the waiting users for both schemes became almost the same. Their final conclusion simulation results showed that the SRUS scheme was feasible and only little performance loss in continuous and heavy traffic load scenarios with full or Poisson-based finite buffer traffic input.

1.4.2 Packet Scheduling in LTE: Q-learning Approach

In the literature, the use of machine learning techniques in the field of cognitive radio systems could be classified into supervised and un-supervised learning techniques, each class is proposed for certain learning tasks. In this dissertation we are interested in un-supervised learning techniques such as Reinforcement Learning (RL). RL is recommended for spectrum sensing and Medium Access Control (MAC) protocols, as in [88]. RL plays a key part in the development of a cognitive radio system, and it forms the framework upon which cognitive radio systems are built. This is because the basic and most important characteristic of cognitive learning is its ability to learn in an autonomous way [44].

In [45], the authors proposed an algorithm that uses RL technique to choose a scheduling rule from a pool of scheduling rules, in which the action was defined as what scheduling algorithm to use, and the reward was calculated based on the system throughput, system capacity, and spectral efficiency. The authors modelled their work theoretically without implementing their model in a simulation environment.

In [46], the authors have proposed a scheduling algorithm that is based on using Q-learning technique, in which it is an example of RL. They use Q-learning technique to choose which scheduling algorithm to use for scheduling the resources among users. The authors aimed at their scheduling algorithm to achieve a trade-off between throughput and fairness. In their model, their Q-table's entries consist of two elements, the action and the obtained reward. Their action is what scheduling algorithm to choose, and the reward is based on calculating the average throughput and fairness. They use the LTE-Sim [69] simulator in order to do their simulation. Their results were in terms of the average Jain's fairness, and the average normalized system throughput.

In [56], the authors proposed a Q-learning-based scheduling algorithm, and they implemented, and run experiments to test it using the LTE System level Simulator [54]. The authors proposed two forms of their algorithm. One for a single agent Q-learning platform, in which the eNodeB acts as an agent. And another one for a multi-agent Q-learning platform, in which each eNodeB is an agent, and all these agents coordinate with each other in a harmonized way, and that is why they called their algorithm, the Harmonized Q-learning algorithm. Their results were in terms of user wideband Signal to Noise Ratio (SINR), and the average user spectral Efficiency.

In [83], the authors presented two Q-learning approaches in allocating the unused radio resources by the licensed users to unlicensed users. The two Q-learning approaches were the cooperative Q-learning and non-cooperative Q-learning approach, and they presented these approaches in the form of formulas. The authors also evaluated these approaches by running tests over their model. In their model, they did not use licensed users, but they mimicked their presence by varying the number of unused radio resources. In their evaluation tests, they included four access schemes for unlicensed users to access the unused radio resources. The four access schemes were, the random, non-cooperative, partial cooperation, in which some users cooperate and others don't cooperate, and full cooperative access scheme. Their evaluation test results showed that the full cooperation access scheme had the best results in terms of throughput and fairness, then followed by the partial cooperation, then followed by the non-cooperative, and finally followed by the random access scheme which had the lowest results.

1.5 Dissertation Contribution

This dissertation is important for the following three contributions; the first contribution of this dissertation was published in [79]. The second contribution of this

dissertation was published in [80]. The third contribution of this dissertation was submitted to the International Journal of Computer and Telecommunications Networking, Elsevier, and it is currently under review.

The first contribution of this dissertation lies in modifying the LTE-Sim [69] simulator in-order to support the Intra-band continuous case of Carrier Aggregation, then evaluating the Quality of Service (QoS) performance of the Modified Largest Weighted Delay First (MLWDF), the Exponential Rule (Exp-Rule), and the Logarithmic Rule (Log-Rule) scheduling algorithms over LTE/LTE-A in the Down-Link direction. The QoS performance evaluation is based on the system's average throughput, Packet Loss Rate (PLR), average packet delay, and fairness among users. Simulation results show that the use of CA improved the system's average throughput, and almost doubled the system's maximum throughput. It reduced the PLR values almost by a half. It also reduced the average packet delay by 20-40% that varied according to the video bit-rate and the number of users. The fairness indicator was improved with the use of CA by a factor of 10-20%.

The second contribution of this dissertation lies in modifying the LTE-Sim [69] simulator to support the use of Disjoint Queue Scheduler (DQS) for a HetNet deployment of a macro-cell and a variable number of pico-cells. Then evaluating and comparing the QoS performance of the DQS based MLWDF, with DQS based EXP-Rule, and with a Single Carrier (SC MLWDF). The performance evaluation is based upon the average users' throughput, PLR, and average packet delay. Experiments showed that the use of the DQS can double the pico-cells' users' throughput with a loss of fifth of the macro-cell's users' throughput. The use of the DQS also increased the PLR and the packet delay values for both type of users. The use of both schedulers, the DQS based MLWDF and DQS based EXP-Rule had a similar fluctuating performance in terms of average users' throughput and PLR. However, the use of the DQS based MLWDF had a slightly better performance in terms of packet delay.

The third contribution of this dissertation lies in proposing, implementing, and testing two novel scheduling algorithms that are based on the use of Q-learning formulas for scheduling two types of users. The first type of users are the licensed users which pay for the cost of their service and they are guaranteed a full access to the spectrum, and they are called the Primary Users (PUs). The second type of users are the un-licensed users which don't pay for their service, and they are called the Secondary Users (SUs). The novelty of these algorithms is based on the idea of making a good use of the spectrum holes by scheduling the secondary users over them. The first algorithm combines the use of both the collaborative multi-agent approach for scheduling the primary users, and the competitive multi-agent approach to schedule the secondary users. The second scheduling algorithm uses the competitive multi-agent approach for scheduling the primary users, then the secondary users. Both scheduling algorithms were implemented in Matlab. Then experiments were run on them to measure and compare their performances. The performance measurements were based on the throughput percentages that each user acquired from the total macro-cell bandwidth, and the fairness level of sharing the spectrum among users. Experiments results showed that both scheduling algorithms converged very quickly to 90% utilization of the spectrum, and provided an equal degree of fairness. In regard to the Collaborative Competitive scheduling algorithm, it provided all of this 90% utilization of the spectrum to the primary users, and distributed the resources among them in fair shares by assigning Jains fairness index as the reward function, which will guide the primary user agents in choosing the best joint action, in which executing this joint action will result with the highest spectrum utilization and the least variance between the primary users shares of the spectrum. In regard to the Competitive Competitive scheduling algorithm, it provided 75% of the spectrum utilization to the primary users, which was distributed among them in fair shares, and 15% of the spectrum utilization to the secondary users, which was also distributed among them in fair shares. The Competitive Competitive scheduling

algorithm forced the fairness among the users by creating an upper limit on how much each user can get by controlling the amount of resources that the actions in the actions sets can provide. In conclusion, it is recommended to use the Collaborative Competitive scheduling algorithm when it is needed to provide the primary users with the highest utilization of the spectrum, and with the least variance in distributing the spectrum share.

1.6 Structure of the Dissertation

The remainder of this dissertation is organized as follows: Chapter 2 Provides a detailed explanation of the main features that are included in the evolution process of LTE Release 8/9 to LTE-A Release 10/11, and the road map to 5G cellular network. Chapter 3 Provides a QoS performance evaluation study of Channel-aware/QoS-aware scheduling algorithms, the Modified Largest Weighted Delay First, Log-Rule, and Exp-Rule for video-applications over LTE/LTE-A cellular network that support the use of carrier aggregation, and presents the findings of this study. Chapter 4 Provides another QoS performance evaluation study of a Disjoint Queue Scheduling for video-applications over an LTE-A heterogeneous network with carrier aggregation, and presents the findings of this study. Chapter 5 Provides a detailed explanation of how Q-learning could be used for packet scheduling in LTE cellular networks. Chapter 6 Proposes, implements, and tests two novel multi-agent Q-learning-based scheduling algorithms for LTE Cellular networks, and presents the findings of using these novel algorithms. Finally, Chapter 7 Summaries the dissertation.

Chapter 2

The Evolution from LTE to LTE-Advanced Cellular Networks

2.1 Introduction

In 1998, seven telecommunication standards development organizations united to form the Third Generation Partnership Project (3GPP). These organizations are; the Association of Radio Industries and Businesses (ARIB), American National Standards Institute (ANSI), China Communications Standards Association(CCSA), European Telecommunications Standards Institute (ETSI), Telecommunications Standards Development Society, India (TSDSI), Telecommunications Technology Association (TTA), and Telecommunications Technology Committee (TTC). Now, in regard to the 3GPP, it is a project that covers cellular telecommunications network technologies, including radio access, the core transport network, security, Quality of Service, and thus providing a complete system specifications and providing their members with a stable environment to produce the reports and specifications that define 3GPP technologies. These reports and specifications are grouped and issued

in a form of releases. For example, Releases 8/9 (R-8/9) covers Long Term Evolution (LTE), Releases 10/11 (R10/11) covers LTE-Advanced (LTE-A), Release 12 (R12) covers more features on LTE-A [1] [19] [25].

In this chapter we introduce Long Term Evolution (LTE) cellular network by explaining its architecture in section 2.2, and its radio spectrum basics in section 2.3. Then, in the following sections, we explain the main features that covers the evolution from LTE to LTE-A. This evolution includes enhanced and new features on LTE such as Carrier Aggregation (CA) which is explained in section 2.4, LTE-A Heterogeneous Networks (HetNets) which is explained in section 2.5, Relays and Backhaul which is explained in section 2.6, Coordinated Multi-Point Operation (CoMP) which is explained in section 2.7, Inter-Cell Interference Coordination (ICIC) which is explained in section 2.8, and enhanced ICIC (eICIC) which is explained in section 2.9. LTE-A Release 12 is explained in section 2.10. Then, LTE-Advanced Pro and the road to 5G is briefly introduced in section 2.11. And finally, we provide concluding remarks in the last section.

2.2 LTE Cellular Network Architecture

The LTE cellular network architecture can be divided into two main parts: The Radio Access Network (RAN), and Evolved Packet Core (EPC) as shown in Fig 2.1.

The RAN consists of an Evolved NodeB (eNodeB) and User Equipment (UE). The eNodeB is the connection point for the UE with the core network. It hosts the PHYsical (PHY), Medium Access Control (MAC), Radio Link Control (RLC), and Packet Data Control Protocol (PDCP) layers that include the functionality of user-plane header-compression and encryption. It also offers Radio Resource Control (RRC) functionality that corresponds to the control plane. Scheduling, admission control, and radio resource management are also performed in the eNodeB [53].

The EPC part consists of five main components: The Policy Control and Charging Rules Function (PCRF), Home Subscriber Server (HSS), PDN-Gateway (P-GW), Serving Gateway (S-GW), and Mobility Management Entity (MME) [53].

The PCRF is a logical node responsible for policy control decision-making, and controlling the flow-based charging functionalities in the Policy Control Enforcement Function (PCEF) that is being hosted at the P-GW. It also decides how a certain data flow will be treated in the PCEF by providing the QoS authorization, QoS class identification, and it determine the bit rates in accordance with the user's subscription profile [53].

The HSS is the database of the LTE network, it contains all the users' subscription QoS profile, information about the Packet Data Networks (PDNs) in which the user can connect to, dynamic information that relates the identity of the MME to which the user is currently attached or registered to, and it may also integrate the Authentication Center (AuC) that generates the vectors for authentication and security keys [53].

The P-GW is the gateway which is responsible for QoS enforcement for Guaranteed Bit Rate (GBR) bearers, flow-based charging according to rules from the PCRF, and the allocation of IP addresses to users. In addition, it filters user's IP packets into different QoS-based bearers based on Traffic Flow Templates (TFTs). It also serves as the mobility anchor for inter-working with non-3GPP networks such as WiMAX and WiFi [53].

The S-GW is the gateway that serves as the local mobility anchor for the data bearers while users are moving between eNodeBs, in which all their IP packets are transferred through it. It temporarily buffers user's downlink data when it is in the idle state, while the MME initiates paging of the UE to re-establish the bearers. It performs administrative functions in the visited network such as collecting informa-

tion for charging and legal interception. It also serves as the mobility anchor for inter-working with 3GPP networks such as General Packet Radio Service (GPRS) and Universal Mobile Telecommunication Systems (UMTS) [53].

The MME is the main node in the EPC, it manages the authentication and security, and the subscription profile and service connectivity of users. It is responsible for all the mobility management tasks such as inter eNodeBs handovers, inter MMEs handovers, and keeping track of the location of all users [53].

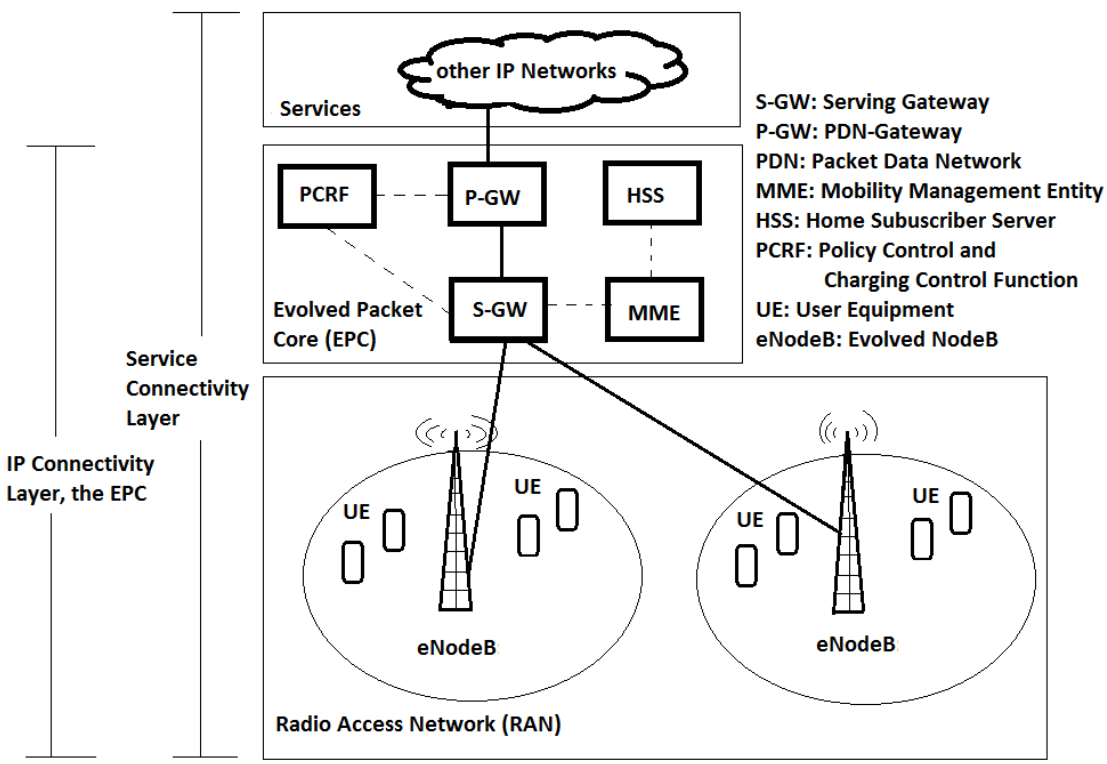

Figure 2.1: LTE Cellular Network Architecture.

2.3 LTE Radio Spectrum

The LTE radio spectrum can be represented in a two dimensional array: one dimension exists in the time domain, and the other one in the frequency domain as shown in Fig 2.2. In the time domain, LTE transmissions are organized into radio frames of 10 ms length period, each frame is equally divided into 10 sub-frames "1 ms each". This sub-frame is the minimum scheduling unit in LTE, each sub-frame consists of two equal time slots "0.5 ms each". There are two types of time slots, one is the normal cyclic prefix which is combined of 7-OFDM symbols, and the other one is the extended cyclic prefix which is combined of 6-OFDM symbols. In LTE, each downlink sub-frame is divided into two regions: the first one is the control region which consists of two or three OFDM symbols, the second region is used for data as shown in Fig 2.3 [48].

In the frequency domain, the bandwidth is divided into sub-carriers, each sub-carrier has a width of 15 KHz, and it is occupied by one OFDM symbol, which is the smallest physical resource in LTE, and it is called resource element, as shown in Fig 2.3. A group of resource elements form a resource block which is extended for one-time slot, consequently the resource block will have a width of 180 KHz "12*15KHz", and it is the minimum scheduling unit for LTE users. Each sub-carrier is being modulated using either Quadrature Phase-Shift Keying (QPSK), 16-Quadrature Amplitude Modulation (16-QAM), or 64-QAM. The number of bits each sub-carrier can occupy at a period of one OFDM symbol time depends on the modulation type [9].

2.4 Carrier Aggregation

Carrier Aggregation (CA) allows the network to aggregate more than one carrier in-order to provide higher bandwidth. Here, each separate carrier which is being

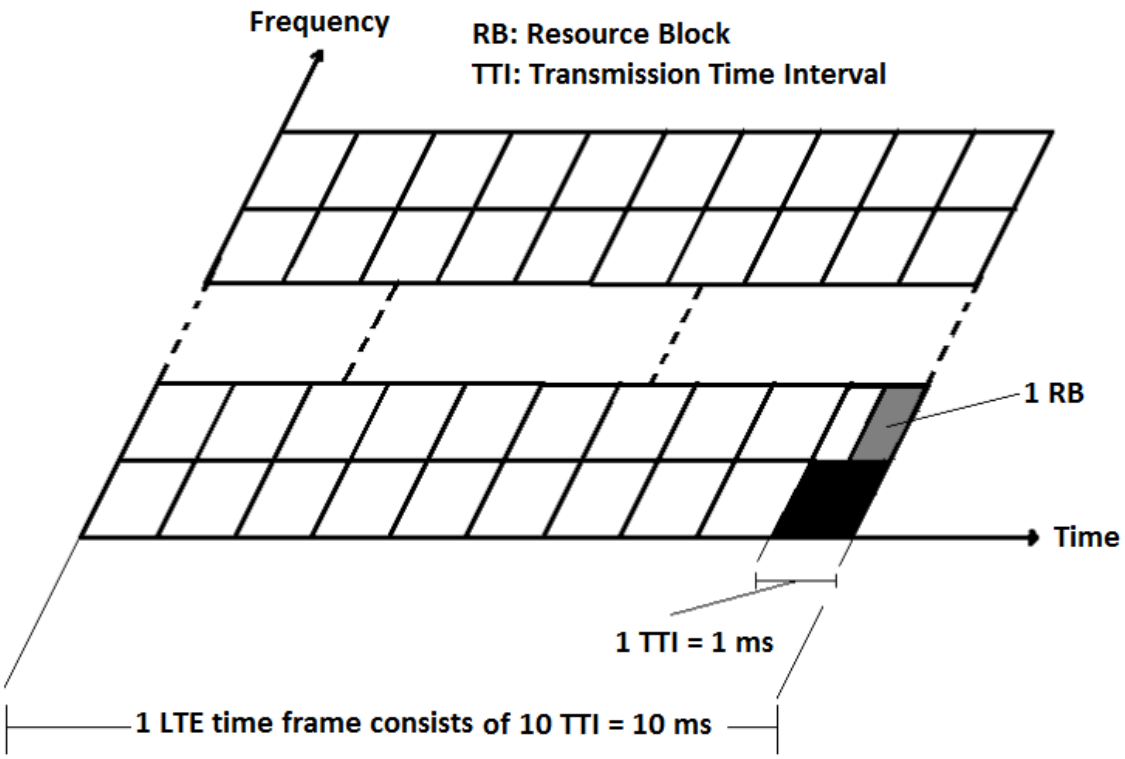

Figure 2.2: LTE radio spectrum.

aggregated is called a Component Carrier (CC). Figure 2.4 shows the principle of carrier aggregation. In 3GPP Release 8/9, User Equipment (UE) can receive at most one Carrier Component (CC) up to 20 MHz of bandwidth. Meanwhile, Release 10/11, UE can receives two CCs up to 40 MHz of bandwidth. In Release 12, a UE can receive three CCs with up to 60 MHz of bandwidth. Carrier aggregation in the uplink and the downlink directions is completely independent as long as the number of uplink carriers cannot exceed the number of downlink carriers [49] [10]. In addition, three types of carrier components allocation were defined by the Third Generation Partnership Project (3GPP) including, intra-band continuous, intra-band non-continuous, and inter-band non-continuous as Figure 2.5 shows [79].

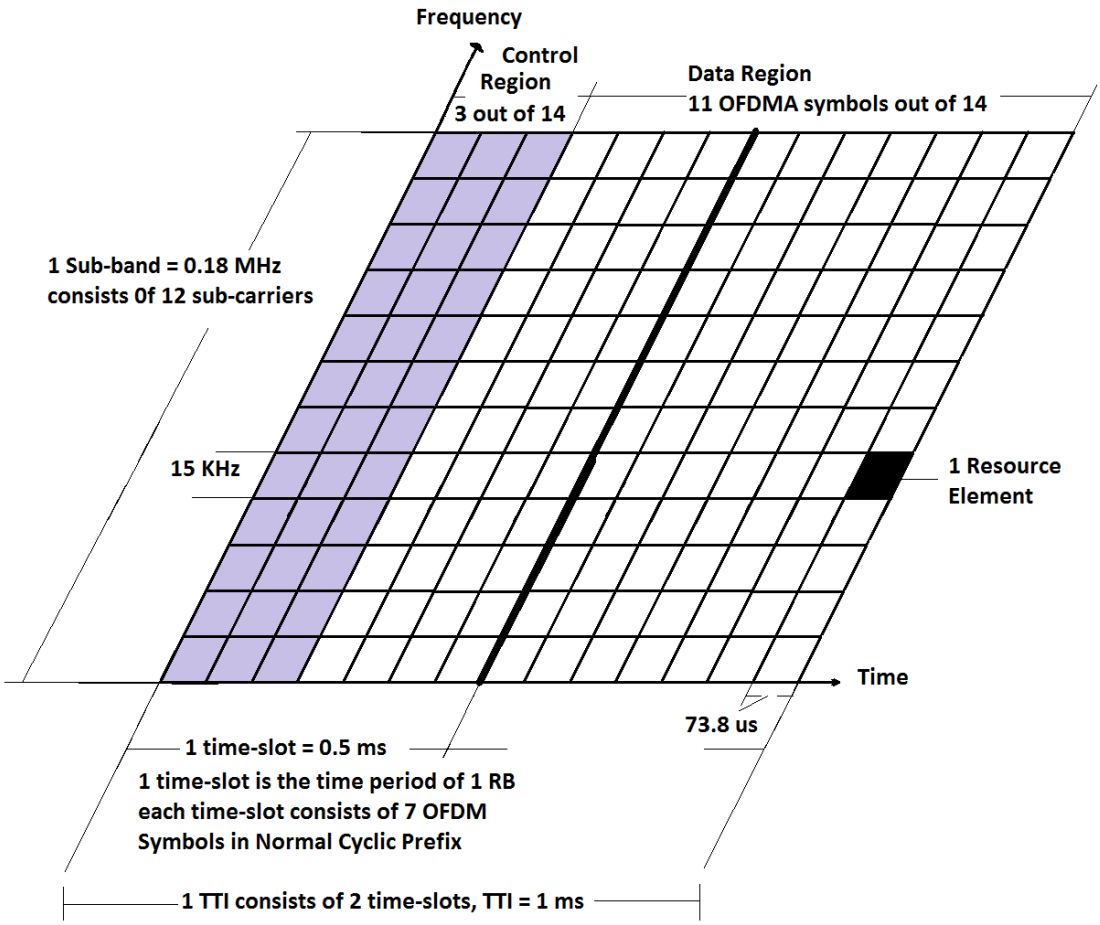

Figure 2.3: The smallest scheduling LTE unit in the time-frequency domain.

2.5 LTE-A Heterogeneous Networks (HetNets)

Heterogeneous Networks (HetNets) consists of a mix of macro-cells, remote radio heads, and low power nodes such as pico-cells, and femto-cells. Macro-cells are basically an eNodeB that provide coverage to few kilo-meters, it provides an open public access and guaranteed minimum data rate under a maximum tolerable delay, it uses a dedicated backhaul, and it emits up to 46 dBm. Remote Radio Head (RRH) are compact-size, high-power and low-weight units, which are mounted outside the

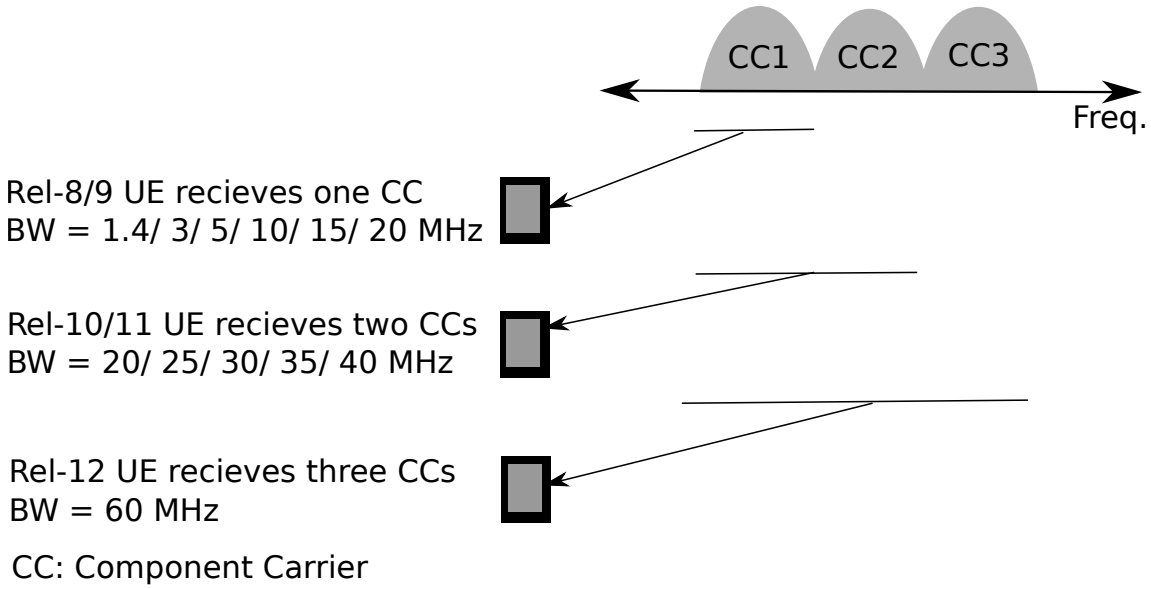

Figure 2.4: The principle of carrier aggregation

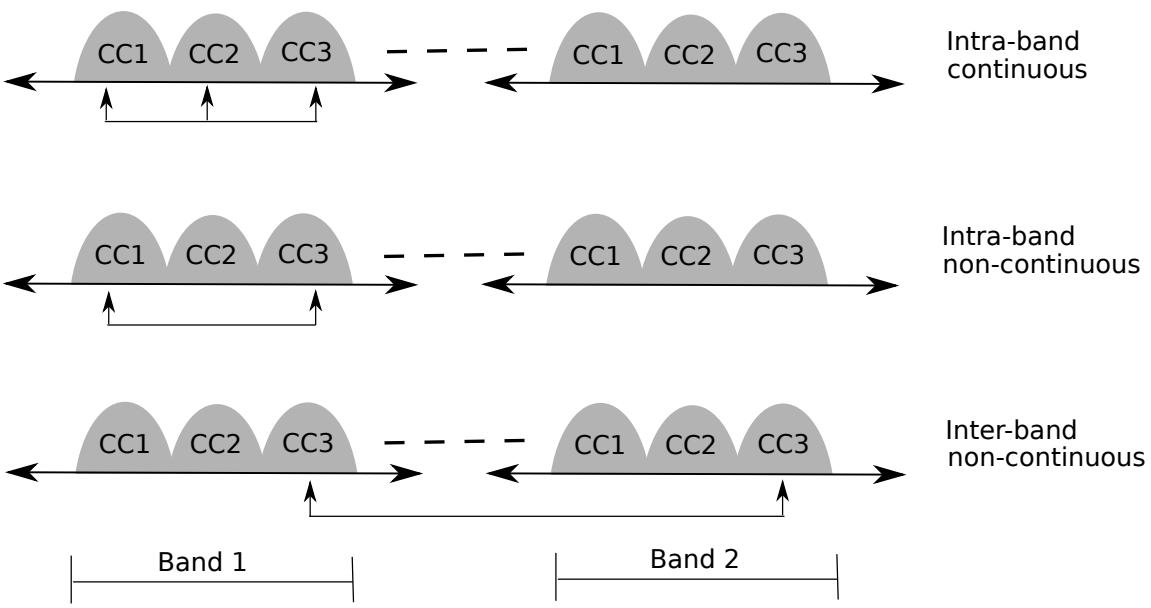

Figure 2.5: Carrier aggregation cases

conventional macro-cell's base station, and connected to it through a fiber optic cable to create a distributed base station, in-which the central macro-cell's base station is

in charge of controlling baseband signal processing, and moving some radio circuitry into the remote antenna. The use of RRHs eliminates the power losses in the antenna cable and reduces the power consumption. Pico-cells are low power eNodeBs that provide coverage up to 300 meters, they are usually deployed in a centralized way with the same backhaul and access features as macro-cells, they are deployed in outdoor or indoor coverage, and they emit power up to 23 to 30 dBm. Femto-cells are also known as home base stations, they are data access point that are installed indoors to get better coverage and capacity gain which makes its deployment an attractive choice [61]. The better coverage is provided due to the short distance between the transmitter and the receiver "about 50 meters at max" which reduces the power consumption. The better capacity gain is obtained from achieving higher Signal to Interference plus Noise Ratio (SINR), and from the dedicated base stations to its users [37]. A basic model that represent the LTE-A HetNets which consists of a macro-cell and a femto-cell, and how they are connected to the LTE core network is shown in Figure 2.6.

2.6 Relays and Backhauls

Relaying is a method of improving the network coverage in difficult conditions, such as to improve urban or indoor throughput, or to extend coverage in rural areas, or to add dead zone coverage [8]. Despite that this coverage improvement could be accomplished by deploying more base stations wired-connected to the rest of the network, the use of relays is more practical due to their shorter time deployment and there is no need to deploy a specific backhaul [48].

Two types of relays are being deployed in 3GPP Release 8, Amplify-and-forward relays, Decode-and-forward relays. In the Amplify-and-forward relays, the signal is simply amplified and forwarded, this type of relays is being used in coverage holes.

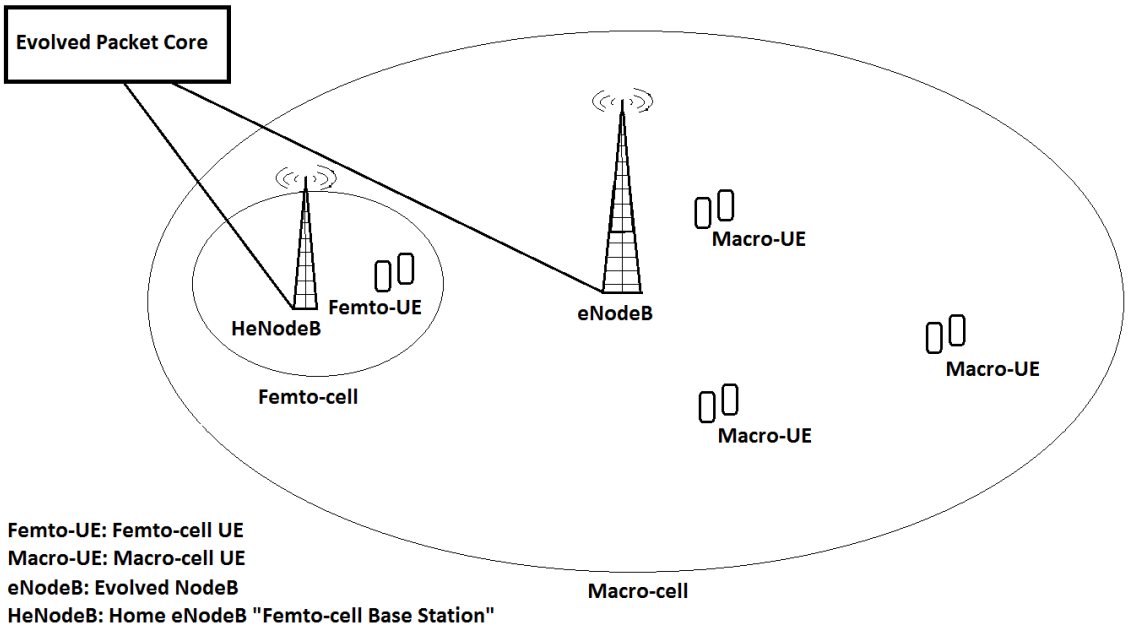

Figure 2.6: LTE-A HetNets.

In the Decode-and-forward relays, the signal is decoded and re-encoded before re-transmission. This type of relays does not amplify the noise which makes it a suitable deployment choice in low-SNR environments [48].

In 3GPP Release 10 the concept of relaying has evolved to a level in which the relay nodes can connect to the eNodeB in two ways: In-band relaying, and out-band relaying. In in-band relaying, the link between the eNodeB and the relay node "Backhaul link" operates at the same channel as the link between the relay node to users' links "Access links". In out-band relaying, the backhaul link and access links operates at different channels [8].

The interference that exists in out-band relaying could be avoided in the frequency domain by sufficiently separating the backhaul link from the access links. Therefore, it could be operated on 3GPP Release 8 air interface without any enhancements. Now, in regard to the interference that exist in in-band relaying, a

proper antenna arrangement is needed to avoid the interference, unless the transmission on the backhaul link and the access link are being separated in the time domain [48].

2.7 Coordinated Multi-Point Operation (CoMP)

CoMP could be described as the art of interference management. If the transmitted signals from different cells are coordinated, the user's performance will be improved especially at cell-edges. An example of CoMP is shown in Fig. 2.7. CoMP primarily can be categorized as Inter-Site or Intra-Site. Intra-site CoMP enables the coordination between sectors of the same eNodeB. The coordination is possible through the use of Multiple Antenna Units (MAUs) that allow the coordination between the sectors. On the other hand, Inter-site CoMP enables the coordination between different eNodeBs [68].

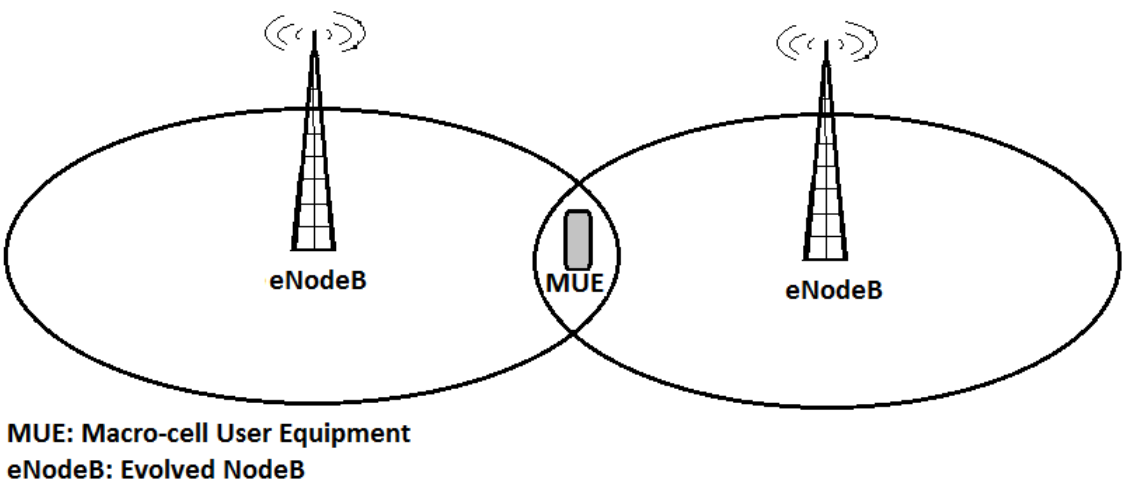

Figure 2.7: The concept of Coordinated Multi-Point Operation (CoMP) in LTE-A.

Two main approaches are being used for the multi-point coordination, centralized and distributed coordination. In centralized coordination, the feedback and Channel

State Information (CSI) data are available and processed at a central unit where it is responsible of handling Inter-Cell Interference (ICI) and radio resource scheduling, processed data are sent to the coordinated cells over a star network. The main issue that rises in the use of this architecture is the high backhaul overhead and the stringent latency requirements. In distributed coordination, the feedback and CSI data are being exchanged between the coordinated cells over a fully meshed signaling Network using X2 interface, one of the coordinated cells can operate as a master cell while the other nodes as slaves, the master cell perform a central scheduling that manages resource allocation and retransmission in a coordinated manner [68].

CoMP in downlink could be classified into two schemes, the Coordinated Scheduling and/or Beam-Forming (CS/CB) and Joint Processing (JP). Both of these downlink schemes are good solutions to mitigate ICI in the downlink of MIMO OFDM systems [68].

CS/CB is characterized as a combination of multiple joint eNodeB coordination and Dynamic Inter Cell Interference Coordination (D-ICIC) schemes. CS/CB uses the MIMO antenna capabilities through beam-forming in a coordinated manner. While using beam-forming scheme, beams of different cells might collide. Therefore, neighboring cells have to guess the interference that will be experienced. In order to face this problem, the Coordinated Beam-Switching CoMP (CBS-CoMP), and the Coordinated Scheduling CoMP (CS-CoMP) were proposed. In the case of the CBS-CoMP, each cell determines a sequence of beams over which it continuously cycles. Coordination could be distributed between cell sites, or it could be centralized through a centralized scheduler. In the case of the CS-CoMP, ICI is being mitigated by enabling the collaboration of multiple eNodBs. The most famous CS-CoMP schemes enable the coordination of multi-cell Pre-Coding Matrix Index (PMI) between cooperating eNodeBs, which allows the option of not using a centralized scheduler [68].

In JP, a CoMP set consists of a number of cell-sites that coordinate to optimize the cell-edge performance by jointly processing cell-edge users' data as a unique entity. JP is classified into Joint Transmission (JT) and Dynamic Cell Selection (DCS). In JT, the same resource block of the PDSCH is transmitted from multiple cells associated with a UE-specific demodulation Reference Signal (UE-RS) among coordinated cells [68]. If the cells' joint transmission was time synchronized it is called coherent JT, if it is not synchronized it is called non-coherent JT. Also in Dynamic Cell Selection the PDSCH data has to be available at many cells. However, it is only sent from one cell at a given time in order to reduce interference [22].

In CoMP reception in the uplink, the Physical Uplink Shared Channel (PUSCH) is received at multiple cells where Maximal Ratio Combining (MRC) is used. Two main schemes could be used, multi-point reception with Interference Rejection Combining (IRC) and the multi-point reception with coordinated scheduling. In the IRC, multiple UEs transmit the PUSCH simultaneously using the same resource block. However, received weights are generated so that the received SINR or signal power after combining at the central eNodeB is maximized in CoMP reception with IRC. In the multi-point reception with coordinated scheduling, the received PUSCHs at multiple cell sites are combined by the use of Minimum Mean Squared Error (MMSE) or Zero Factoring algorithm. Both schemes improve the cell-edge user experience due to the increase of signal power [68].

In 3GPP Release 8 the generation of the Demodulation Reference Signal (DMRS), in which it is embedded in two defined SC-FDMA symbols in an uplink sub-frame, depends on the physical cell identity (PCI), in which it is derived from the downlink. A fundamental change to CoMP in the LTE uplink is the introduction of virtual cell ID's, which will allow the macro cell and small cells to use the same cell identities in the case of heterogeneous network deployments [22].

There are further enhancements to the CoMP in 3GPP Release 12/13 in both

ideal and non-ideal backhaul scenarios. In ideal backhaul scenarios, the introduction of Channel Status Information-Reference Signals (CSI-RS) based Reference Signal Received Power (RSRP) measurements, uplink sounding, and power control enhancement. While in the non-ideal backhaul scenarios, schemes will be developed to deal with the limitation of backhaul when using CoMP in order to get higher cell edge throughput and more efficient mobility management [16].

2.8 Inter-Cell Interference Coordination (ICIC)

One of the main features of LTE that maximizes the spectrum efficiency is frequency reuse. It allows cells to use the same frequency channels, which will lead to an interference among the cells, especially at the cell edges. At the cell edges, the probability for a cell-edge user to be scheduled on a resource block which is being transmitted by the neighboring cell is high; consequently, the interference is high. In-order to deal with cell-edge interference, 3GPP Release 8/9 (Rel-8/9) introduced Inter-Cell Interference Coordination (ICIC). ICIC reduces cell-edge interference on traffic channels e.g. Physical Downlink Shared Channel (PDSCH) from neighboring cells, and this is done by the use of three interference reduction schemes that works in the power and frequency domain. These schemes are based on reducing the chance of frequency overlap. The first scheme, is by instructing the two neighboring eNodeBs to use completely different sets of resource blocks throughout the cell at a given time. This scheme will significantly reduce interference, but it comes with a cost of not fully utilizing the whole set of resource blocks. In the second scheme, the eNodeBs distinguishes between centrally and edge located users, in this way eNodeBs can utilize the whole set of resource blocks for centrally located users, but for the edge users it uses completely different set of resource blocks. The third scheme is an enhanced version of the second one. The resource blocks are used in the same exact

way, but all neighboring eNodeBs uses different power schemes for their edge located users [7].

The flexibility nature of the PDSCH in the in LTE frame allows the ICIC schemes to directly work on scheduling them. However, in the case of the Physical Downlink Control Channel (PDCCH), ICIC schemes can't work directly on them, because they have a very different channel structure and they are much less flexible than the PDSCH. Hence, ICIC Interference reduction schemes can be applied only on traffic channels, and they can't be applied on control channels [15].

2.9 enhanced ICIC (eICIC)

Since Rel-8/9 supports only non-overlapping transmissions in the frequency domain, ICIC works will in a homogeneous networks environment, but fails in a HetNets environment. In 3GPP Release 10/11 (Rel-10/11), the enhanced Inter-Cell Interference Coordination (eICIC) was introduced in-order to manage the interference issues in HetNets. eICIC reduces the interference on both the traffic and control channels. It uses power, frequency and also time domain to mitigate intra-frequency interference in HetNets [7]. eICIC has two main features: Cell Rang Expansion (CRE), which was introduced in 3GPP Release 8, and then enhanced in 3GPP Release 10/11. And the other feature is the Almost Blank Sub-frame (ABS), which was introduced in 3GPP Release 10.

CRE allows the coverage of a pico-cell or femto-cell to expand in-order to include more users which exists at its edges. In 3GPP Release 8, the process of selecting the cell in which its range will be expanded is based on the received signal strength, but this approach is limited to the order of up to 9 dB gain. In 3GPP Release 10, the process of selecting the cell is based on minimum path loss and the interference levels [11].

ABS is a time-domain-based eICIC, it is a Time Domain Multiplexing (TDM) technique, it allows both the macro-cell and the small-cell, whether it is a pico-cell or femto-cell to use the same radio resources, but at a different time slots. This is done by muting certain sub-frames of one layer of cells in-order to lower the interference in the other layer as shown in Fig 2.8 [17] [11].

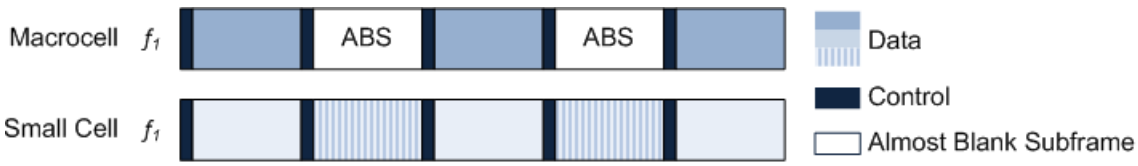

Figure 2.8: The concept of Almost Blank Sub-frame (ABS) [11]

2.10 LTE-A Release 12

3GPP Release 12 comes with more features for LTE-A that will benefit and boost the overall network performance. These features focuses on enhancing the capacity, coverage, and the coordination between cells. These features have helped in enhancing the deployment of small-cells, macro-cells, and carrier aggregation. One of these features is the small-cell enhancement based on Inter-site Carrier Aggregation (Inter-site CA), which optimizes small-cell mobility by reducing RAN to CN signaling, and improves data rates by using macro-cell and small-cell together "dual connectivity", and by allowing for more Time Division Duplex (TDD) spectrum use. In carrier aggregation, it supported the aggregation between sites "Inter-site CA", and the support of aggregating three downlink carriers up to 60 MHz of total spectrum. In macro-cell, many enhanced features are combined such as, the increased number of transmit and receive antennas at the base stations up to eight, the use of Active Antenna Systems (AAS) with vertical sectorization, and user specific elevation beamforming/3D-MIMO which enhanced the macro-cell's capacity and coverage [19].

2.11 LTE-Advanced Pro and the road to 5G

LTE-Advanced Pro is covered by what has been achieved with the completion of 3GPP Release 13 (R13) standards on March 2016. The use of LTE-Advanced Pro extends the telecommunication sectors to critical communications such as blue light services. It is not for telecommunication sectors only, but it is also set to be used for other sectors such as, critical communications (blue light services), machine-to-machine communications, Internet of Things (IoT), and other areas. LTE-Advanced Pro is considered the 3GPP step stone to 5G systems [1]. The main achievements that were completed by Release 13 in which the work on them started in previous releases include: Massive Machine-Type Communications (MTC) enhancements, public safety features such as Device to Device (D2D) communications, small cell dual-connectivity and architecture, carrier aggregation enhancements, interworking with Wi-Fi, licensed assisted access (at 5 GHz), 3D/FD-MIMO, indoor positioning, single cell-point to multi-point and work on latency reduction [6].

The completed achievements in R13 will have a continuous evolution in 3GPP Release 14 (R14) to further enhance them. The main technologies that are included in this continuous evolution are: latency reduction, unlicensed spectrum, new use cases, massive machine-type communication, massive Multi-Input Multi-Output (MIMO) [23].

The most LTE evolved features and the new radio access technologies will together lay down the ground of the development of the next-generation wireless access, which is referred to with 5G. The development of 5G will be accomplished into two phases. The first phase will be covered by 3GPP Release 15 (R15) and it is scheduled to be completed by late 2018. The second phase will be covered by 3GPP Release 16 (R16) and it is scheduled to be completed in 2020 [4].

2.12 Conclusions

This chapter has provided a detailed explanation of the main features that are included in the evolution process of LTE to LTE-A. Then, it briefly explains the road map beyond LTE-A. This road map starts by LTE-A Release 12 evolving to LTE-A pro, then eventually to 5G, in which it is expected to be completed by 2020. The importance of this chapter to be part of this dissertation is in laying the foundation of understanding the technologies which will be further studied and modelled as a part of performance measurement experiments in the following chapters.

Chapter 3

QoS Evaluation of Scheduling Algorithms over LTE/LTE-A

3.1 Introduction

The LTE was introduced as an evolution to the Universal Mobile Telecommunication Systems (UMTS) to provide cellular network users with high data rates in both the uplink and downlink direction, decreased latency, and good spectrum utilization [3]. The spectrum utilization could be achieved by the use of the right scheduling algorithm that meets with the environment's conditions and the users' requirements demands. There are many scheduling algorithms that exist in the literature that are used in the LTE scheduling process. These algorithms can be classified in five main groups: channel-unaware, channel-aware/QoS-unaware, channel-aware/QoS-aware, semi-persistent for VoIP support, and energy-aware [36]. When the number of users and their applications increases, such as video-streaming and video-conferencing, this requires higher data rates and decreased latency, which declines the service that the LTE provides to its users. This challenge of providing a reliable service

up to the users' requirements demands can not be solved entirely by choosing the right scheduling algorithm, because the performance of these scheduling algorithms is bounded by the existing LTE capabilities, such as the system's bandwidth. The LTE supports at max 20 MHz channel bandwidth. However, the LTE-A can support more channel bandwidth according to the release as specified in the 3GPP's technical specifications. In Release 10 (R10), the maximum aggregated bandwidth is 40MHz. And it is also 40MHz in Release 11 (R11), but with much more CA configurations. In Release 12 (R12), the maximum aggregated bandwidth is 60MHz [2]. This lead to the motivation of this chapter, which is evaluating the QoS performance of three Channel-aware/QoS-aware scheduling algorithms for video-applications over the LTE Release 8/9 and LTE-A Release 10/11. The LTE-Sim can only simulate the LTE network without the use of CA, so the performance of these algorithms over LTE-A could not be evaluated without making these modifications to the LTE-Sim, which also motivated us to modify it in order to make these evaluations.

This chapter is structured as follows: in section 3.2, the related work which exists in the literature is briefly introduced. In section 3.3, the Channel-aware/QoS-aware LTE scheduling algorithms which were evaluated in this chapter are explained. In section 3.4, the experiments' set-up is explained and its parameters are listed. In section 3.5, the experiments' results are used to measure the QoS parameters which are displayed in line charts and then analysed. And finally, concluding remarks are provided in the last section.

3.2 Related work

Similar comparison-based studies have been published in the literature that uses the same LTE-Sim simulator which was developed by [69]. These studies differs from each other by the class and type of the compared LTE scheduling algorithms, the set-

tings of their experiments, and the parameters which were used in their comparisons. For example, in [30], the authors evaluated and compared the performance of six LTE scheduling algorithms which included: the Round Robin (RR), Best CQI (BCQI), Kwan Maximum Throughput (KMT), Proportional Fairness (PF), Max Min, and Resource Fair (RF). Their evaluation was in terms of user's throughput and fairness. Another example is found in the work of [71], in which the authors evaluated three LTE scheduling algorithms which included Modified Largest Weighted Delay First (M-LWDF), Exponential/Proportional Fairness (EXP/PF), and the Maximum Rate. Their evaluation was in terms of system throughput, packet loss, and fairness. Another example that is about comparing the performance of LTE scheduling algorithms is also found in [29], in which the authors made their comparison study based in terms of Quality of Experience (QoE) focusing on the MOS score, which is linked with end user perceived quality. The algorithms that were included in their Evaluation study included the PF, EXP-PF, and MLWDF. In all the these three examples, LTE-Sim was used to obtain the experiments' results.

3.3 Channel-aware/QoS-aware LTE Scheduling Algorithms

The LTE scheduling algorithms that were studied in this chapter are: the Modified Largest Weighted Delay First (MLWDF), the Logarithmic Rule Algorithm (Log-Rule), and the Exponential Rule Algorithm (Exp-Rule). In all these algorithms the Proportional Fairness (PF) scheduler is used in-order to achieve channel awareness, which makes a trade-off between users' fairness and spectrum efficiency [36]. It schedule users in a fair way by taking into account both the experienced channel state and the past data rate when assigning radio resources. It aims to obtain satisfying throughput and at the same time, guarantee fairness among flows. The

equation that users are selected based on formula 3.1 [60]:

$$k = argmax \frac{r_i(t)}{R_i(t)} \tag{3.1}$$

Where $r_i(t)$ is the achievable data rate according to the instantaneous channel quality of user i at *t-th* TTI, and $R_i(t)$ is the average data rate of user i over a time window, and it is calculated based on formula 3.2 [60]:

$$R_i(t) = (1 - \beta) * R_i(t-1) + \beta * r_i(t-1) \tag{3.2}$$

Where β is a variable ranging from 0 to 1.

Modified Largest Weighted Delay First (MLWDF)

The MLWDF scheduling algorithm is designed to support multiple real time data users by taking into account their different QoS requirements. For example, in the case of video services, the instantaneous channel variations and delays are taken into account. It tries to balance the weighted delays of packets and to utilize the knowledge about the channel state efficiently. It chooses user j at time t based on formula 3.3 [55]:

$$j = max_i \alpha_i \frac{\mu_i(t)}{\bar{\mu}} W_i(t) \tag{3.3}$$

Where $\mu_i(t)$ is the data rate corresponding to user i's channel state at time t, $\mu_i(t)$ is the mean data rate supported by the channel, $W_i(t)$ is the HOL packet delay and $\alpha_i > 0$, $i = 1, ... , N$ are weights that represent the required level of QoS.

The MLWDF's delay is bounded by the Largest Weighted Delay First (LWDF) scheduler. The LWDF metric is based on the system parameter, representing the acceptable probability for the *i-th* user, in which a packet is dropped due to deadline expiration, and this metric is calculated based on formula 3.4 [36]:

$$m_{i,k}^{LWDF} = \alpha_i . D_{HOL,i} \tag{3.4}$$

Where α_i is calculated based on formula 3.5:

$$\alpha_i = -\frac{log\delta_i}{\tau_i} \tag{3.5}$$

The MLWDF is also expressed in terms of the PF scheduler as in formula 3.6:

$$m_{i,k}^{MLWDF} = \alpha_i D_{HOL,i} . m_{i,k}^{PF} = \alpha_i D_{HOL,i} . \frac{d_k^i(t)}{\bar{R}^i(t-1)} \tag{3.6}$$

Logarithmic Rule Algorithm (LOG-Rule)

The delay of this scheduling algorithm is bounded by the following logarithmic formula [36]:

$$m_{i,k}^{LOGrule} = b_i log(c + \alpha_i D_{HOL,i}) . \Gamma_k^i \tag{3.7}$$

Where α_i , b_i , c are tunable parameters, and Γ_k^i represents the spectral efficiency for the $i-th$ user on the $k-th$ sub-channel.

Exponential Rule Algorithm (EXP-Rule)

The delay of this scheduling algorithm is bounded by the following Exponential formula [36]:

$$m_{i,k}^{EXPrule} = b_i exp(\frac{\alpha_i D_{HOL,i}}{c + \sqrt{(1/N_{rt}) \sum_j D_{HOL,j}}}).\Gamma_k^i \tag{3.8}$$

3.4 Experiments

The work of the following experiments was part of a published conference paper in [79].

3.4.1 Experiments set-up

The experiments set-up consists of one Macro cell that is served by one transmitter "eNodeB". The bandwidth was varied from 20MHz "to represent the LTE maximum bandwidth – the case in which CA was not used" to 40MHz "to represent the LTE-A bandwidth – the case in which the CA was used", the number of users was varied from 15, 30, 60, 90, 120, 150, 180, 210 and the video bit-rate was varied from 128Kbps, 242Kbps, and 440Kbps. Detailed parameters of these experiments are listed in Table 3.1.

3.4.2 Experiments results

The LTE-Sim [69] was used in this paper after modifying it to support the first case of the CA. While the LTE-Sim simulator is in the process of simulating a scenario with a pre-defined conditions, it takes into account both the signalling and data traffic. However, it only displays the data traffic in its traces. These data traffic traces are

Table 3.1: Experiments set-up Parameters

Parameter	**Value**
Simulator	LTE-Sim
experiments time	20 sec
Scheduling Algorithms	Exp-Rule, Log-Rule, MLWDF
Network Layout	1 Macro cell “Urban environment"
Transmitter	1 eNodeB
Cell Radius	1 Km
Carrier frequency	2120, 2130 MHz
Bandwidth	2130-2110=20, 2150-2110=40 MHz
Carrier Aggregation case	Inter-band contiguous
Frame structure	FDD
Number of users	15, 30, 60, 90, 120, 150, 180, 210
Users’ Distribution	Random
User speed	3 Km / h
Traffic type	Video
Bit rate	128, 242, 440 kbps
Maximum delay	0.1 sec
Buffer type	Infinite buffer
Propagation model	Macro urban channel realization

used to measure the QoS parameters, the system’s average throughput, Packet Loss Rate (PLR), average packet delay, and fairness among users. These measurements are displayed in all the following figures by taking the number of users as its X-axis factor and the QoS parameter as the Y-axis factor.

System’s Average Throughput

System’s average throughput is defined as the amount of the total received packets for all users per second. The system’s average throughput with and without the use of carrier aggregation for the three scheduling algorithms at different video bit-rates are displayed in the following figures “Fig. 3.1, 3.2, and 3.3”.

According to the obtained results that are displayed in figures “Fig. 3.1, 3.2, and

3.3", increasing the number of users will increase the system's average throughput until it reaches its maximum value. This increase is due to transmitting more data from the eNodeB to the new added users. The maximum value of the system's average throughput differs based on the system's capabilities.

The use of CA will increase the bandwidth which will decrease the values of the spectral efficiency. This is defined in the literature as "the number of successfully transmitted bits normalized by the consumed resources in time and in bandwidth" [39]. This will prompt the eNodeB to transmit more data to users leading to higher system's average throughput which will in turn lead to increasing the spectral efficiency. This is shown in figures "Fig. 3.1, and 3.2" in which the use of CA has slightly increased the system's average throughput even before reaching the maximum value of the system's average throughput in the case where the CA was not used.

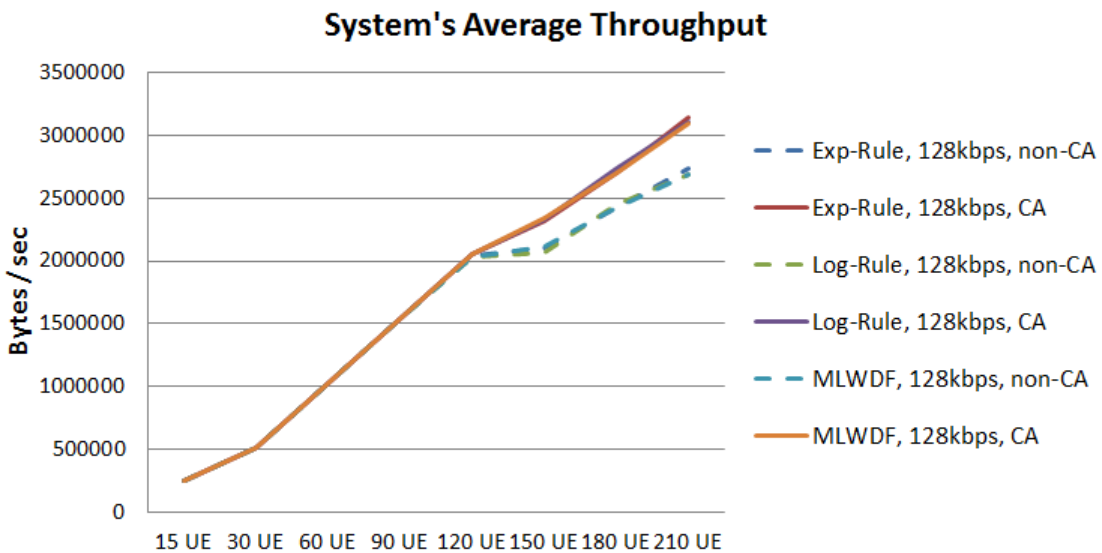

Figure 3.1: System's average throughput at video bit-rate 128kbps, with and without the use of CA.

According to the obtained results that are displayed in Fig. 3.1, it is shown that

at this scenario's conditions, the three algorithms showed similar performance in both cases.

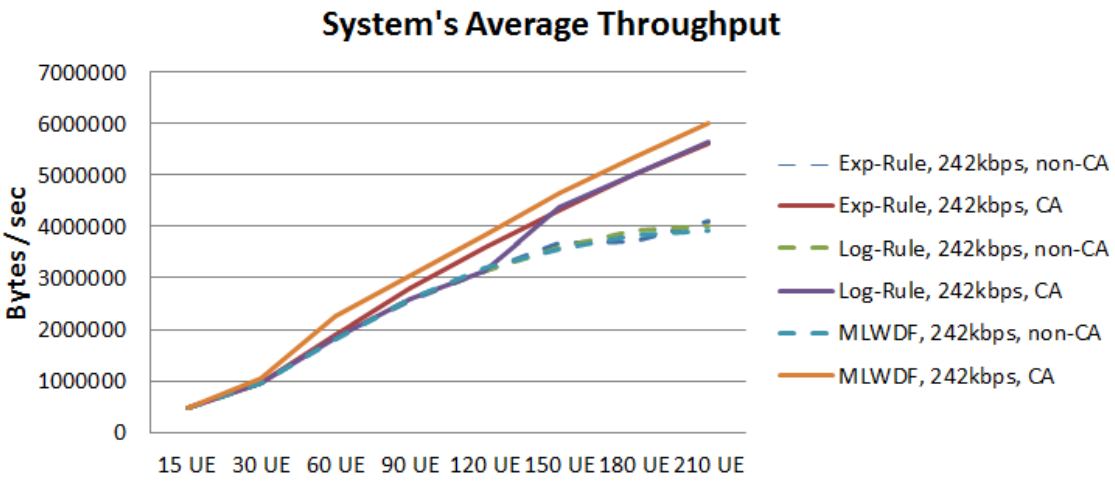

Figure 3.2: System's average throughput at video bit-rate 242kbps, with and without the use of CA.

According to the obtained results that are displayed in Fig. 3.2, in both cases when the CA was and was not used, it is shown that the system's average throughput increased gradually by increasing the number of users. However, in the case in which the CA was not used and the increase of the system's average throughput started to reach its maximum value of between (4 and 4.5) MBps, this increase almost stopped. At this scenario's conditions, when the CA was not used, the three algorithms showed similar fluctuating performance. However, when the CA was used, the use of the MLWDF led to a slightly higher system's average throughput than the Exp-Rule, and the Log-Rule.

According to the obtained results that are displayed in Fig. 3.3, it is shown that the maximum value of the system's average throughput was almost doubled by the use of CA. At this scenario's conditions, the three algorithms showed a similar fluctuating performance in both cases.

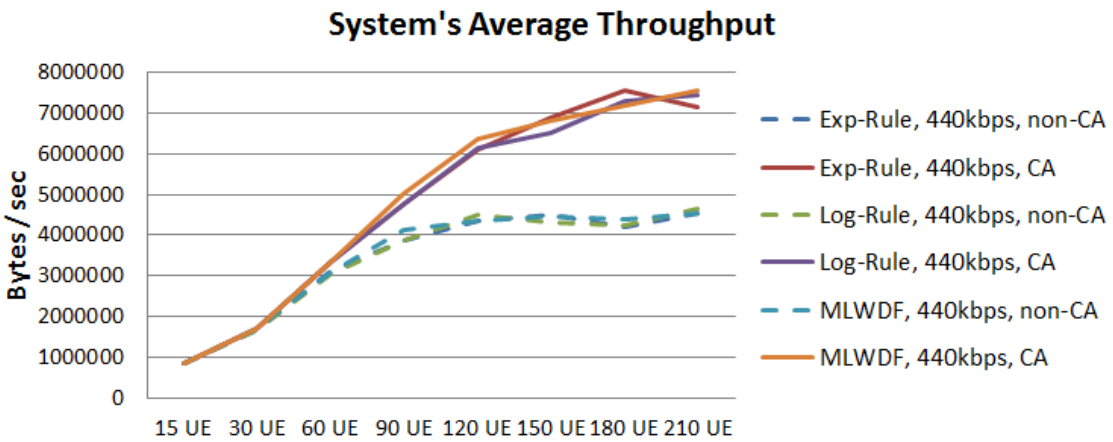

Figure 3.3: System's average throughput at video bit-rate 440kbps, with and without the use of CA.

Packet Loss Rate (PLR)

Packet Loss Rate (PLR) is measured by dividing the difference between the total transmitted and received packets for all users over the total transmitted packets. The greater the system's load the higher the value of the PLR. The system's load could be increased by increasing the number of users in the same cell, or by increasing the video bit-rates. The increase in the PLR values with the increase of the system's load is due to the increasing number of packets in the waiting queues that are competing for the same resource blocks. This will lead to a higher rate of dropped packets from these queues. Since both factors, the number of users and the video bit-rates, are proportionally related to increasing the PLR values, increasing one will limit the increase of the other in a limited resources system. For example, the significant increase of the PLR values started to take place when the number of users exceeded 120 users at a video bit-rate of 128kbps, and when it exceeded 60 users at a video bit-rate of 242kbps, and when it exceeded 30 users at a video bit-rate of 440kbps. The increases of the PLR values with the increase of the number of users and the video bit-rates are shown in figures "Fig. 3.4, 3.5, and 3.6". The results in these three

figures, shows a decrease of the PLR values with the use of CA. This is because using the CA will increase the available resources and decrease the values of the spectral efficiency. This will prompt the eNodeB to allocate more resource blocks to the same user, which will reduce the amount of packets in the waiting queues, allowing more packets to be served and fewer packets to be dropped. This causes a decrease in the values of the PLR as shown in figures "Fig. 3.4, 3.5, and 3.6".

The PLR with and without the use of carrier aggregation for the three scheduling algorithms at different video bit-rates are displayed in the following figures "Fig. 3.4, 3.5, and 3.6".

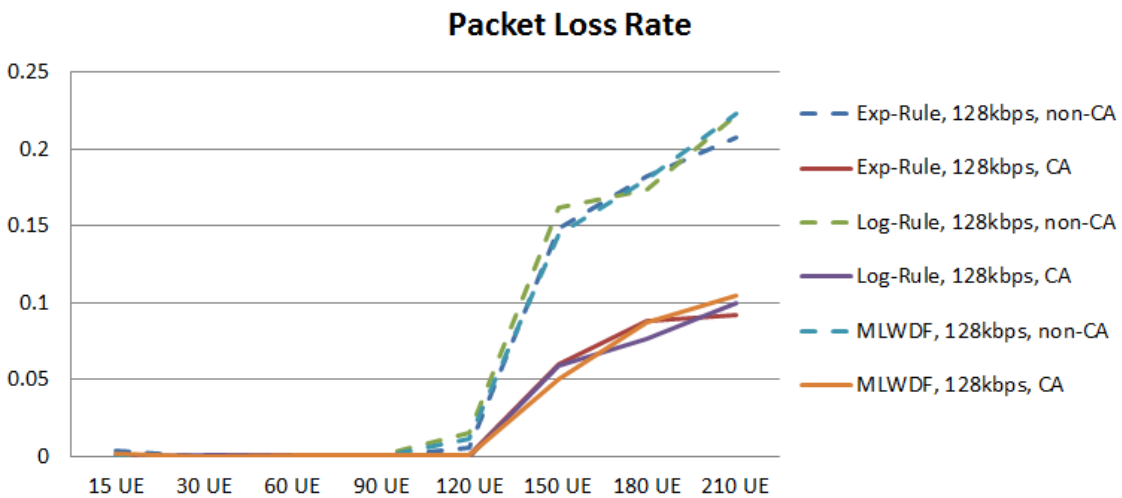

Figure 3.4: Packet Loss Rate (PLR) at video bit-rate 128kbps, with and without the use of CA.

According to the obtained results that are displayed in Fig. 3.4, it is shown that the number of lost packet started to increase significantly when the number of users exceeded 120 UEs. However, when the CA was not used, this increase was twice what it was when the CA was used. At this scenario's conditions, the three algorithms showed similar fluctuating performance in both cases.

According to the obtained results that are displayed in Fig. 3.5, the number

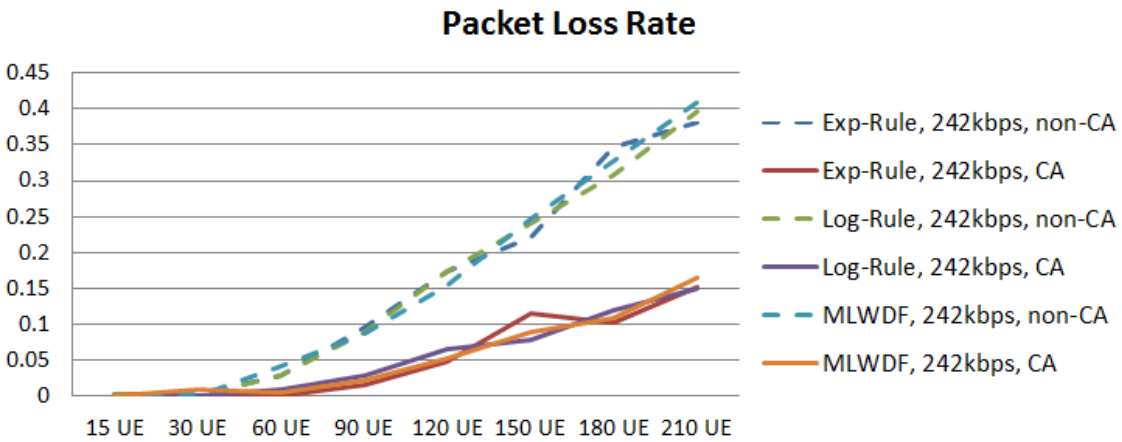

Figure 3.5: Packet Loss Rate (PLR) at video bit-rate 242kbps, with and without the use of CA.

of lost packets started to increase significantly after the number of users exceeded 60 UEs. However, when the CA was not used, the PLR was about two to three times what it was when the CA was used. At this scenario's conditions, the three algorithms showed similar fluctuating performance in both cases.

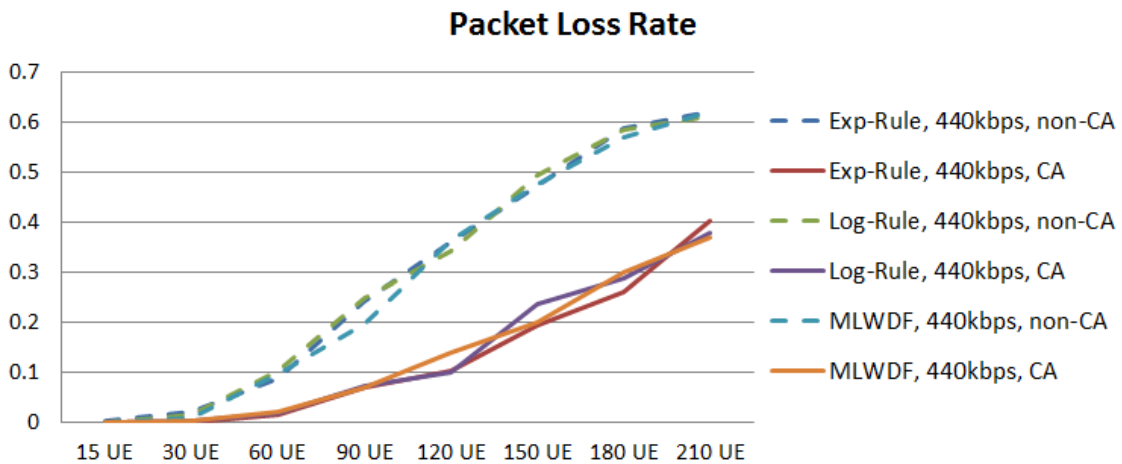

Figure 3.6: Packet Loss Rate (PLR) at video bit-rate 440kbps, with and without the use of CA.

According to the obtained results that are displayed in Fig. 3.6, the number of

lost packets started to increase critically after the number of users exceeded 30 UEs. However, when the CA was not used, the differences between the values of the PLR in both cases were on an average of twice what it was when the CA was used. At this scenario's conditions, the three algorithms showed similar fluctuating performance in both cases.

Average Packet Delay

The packet delay is the time that it takes a packet to travel from the source to its destination. It includes the propagation and waiting time of the packet. The Average Packet Delay is measured by dividing the sum of the total packet delays that were successfully received over the number of total packets. The use of the CA causes a significant beneficial reduction of the average packet delay. This is because it reduces the propagation time which is found by dividing the packet length by the link bandwidth. Also, it reduces the waiting time for the packets in the waiting queues at the eNodeB.

The average packet delay with and without the use of carrier aggregation for the three scheduling algorithms at different video bit-rates are displayed in the following figures "Fig. 3.7, 3.8, and 3.9".

According to the obtained results that are displayed in Fig. 3.7, when the CA was not used, the average packet delay kept significantly increasing with the increase of the number of users into the the cell. While this was occurring, the PLR values remained almost negligible at this scenario's conditions, as seen in Fig. 3.6. This led to a high queueing delay which peaked at 120 UE. However, when the number of users exceeded 120 UE, the waiting time for some of the packets in the waiting queues started to exceed the threshold defined as 0.1 sec, resulting in a higher rate of dropped packets. Consequently, the PLR values started to increase significantly.

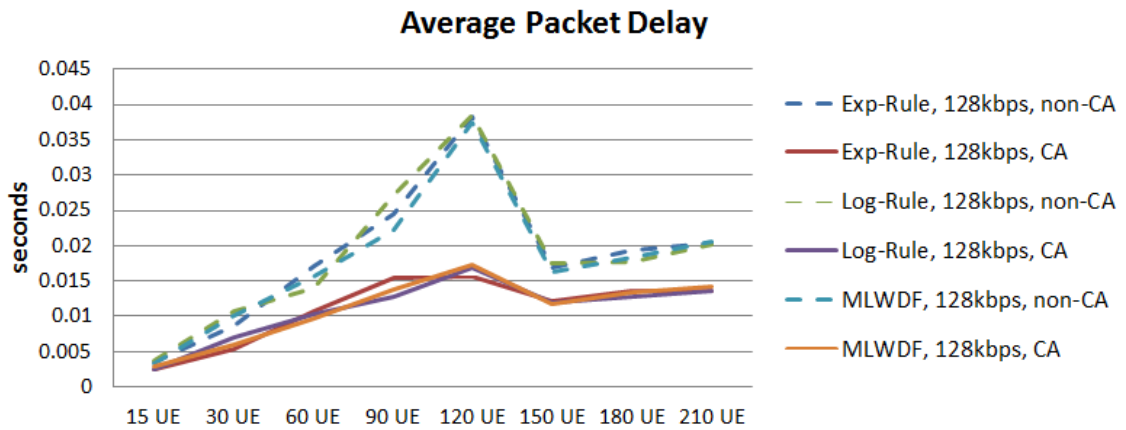

Figure 3.7: Average Packet delay at video bit-rate 128kbps, with and without the use of CA.

And since the average packet delay does not include in its calculations the dropped and lost packets, the values of it reduced significantly. This problem did not occur when the CA was used, because the available resources were almost doubled and the packets at the waiting queues were able to be served more quickly. At this scenario's conditions, the three algorithms showed similar fluctuating performance in both cases.

According to the obtained results that are displayed in Fig. 3.8, it is shown that the use of CA reduced the average packet delay to 60% of what it was when the CA was not used. The three algorithms showed similar fluctuating performance in both cases. However, the MLWDF results indicate that this algorithm has a more reliable performance in terms of increasing the average packet delay with increasing the number of users.

According to the obtained results that are displayed in Fig. 3.9, it is shown that the use of CA reduced the average packet delay to 50-60% of what it was when the CA was not used. This effect of the reduction continued until the number of UEs exceeded 90. After adding more users to the Macro-cell, this reduction started to

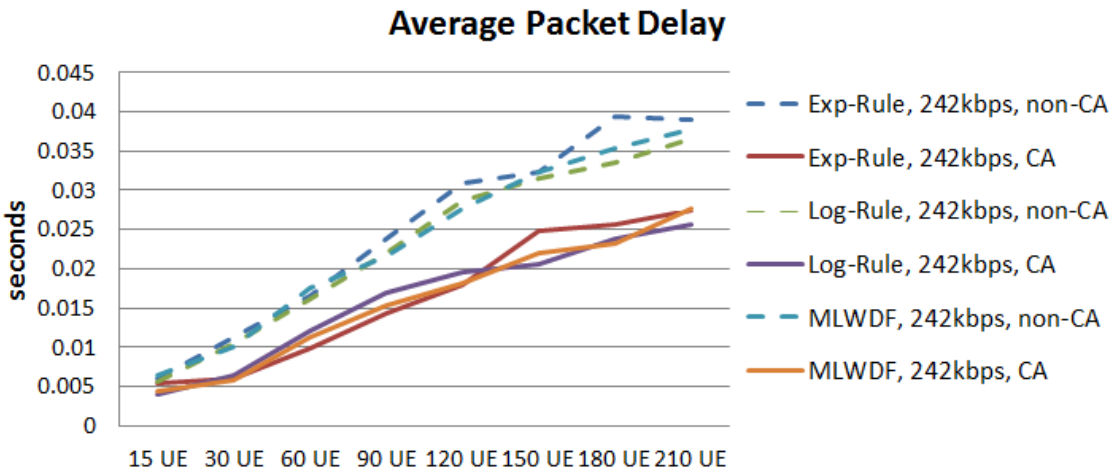

Figure 3.8: Average Packet delay at video bit-rate 242kbps, with and without the use of CA.

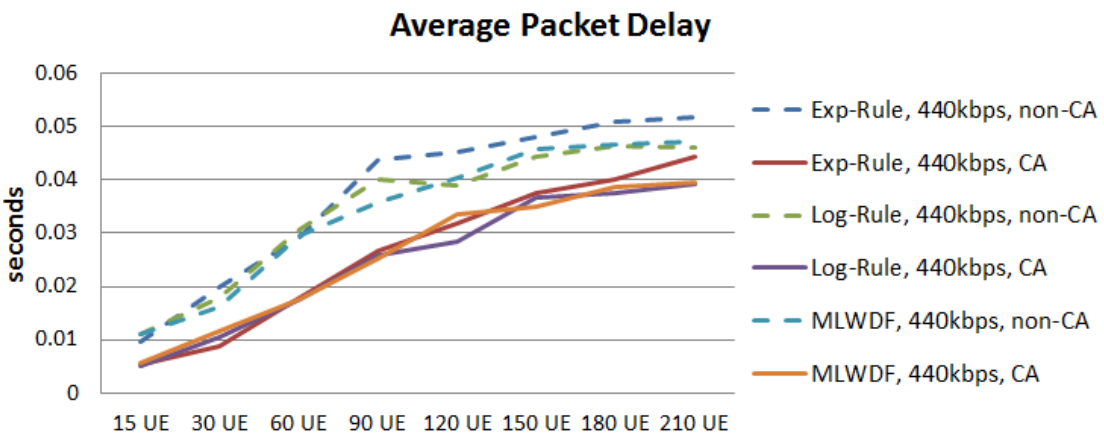

Figure 3.9: Average Packet delay at video bit-rate 440kbps, with and without the use of CA.

decrease until the value of the average packet delay was almost 80% of what it was when the CA was not used. At this scenario's conditions, the three algorithms showed similar fluctuating performance in both cases with more performance stability to the MLWDF. The Exp-Rule had a slightly higher average packet delay than the other two algorithms.

Fairness

Jain's fairness index is used in this paper to determine if the scheduling algorithms are distributing fair portions of the spectrum to the users. It is measured by the following formula [33]:

$$R = ((\sum_{i=1}^{N} T_i)^2)/(N \sum_{i=1}^{N} T_i^2) \tag{3.9}$$

T_i denotes the throughput obtained by user i. N is the number users.

The Jain's fairness index for the three scheduling algorithms at different video bit-rates, with and without the use of carrier aggregation, are displayed in the following figures "Fig. 3.10, 3.11, and 3.12".

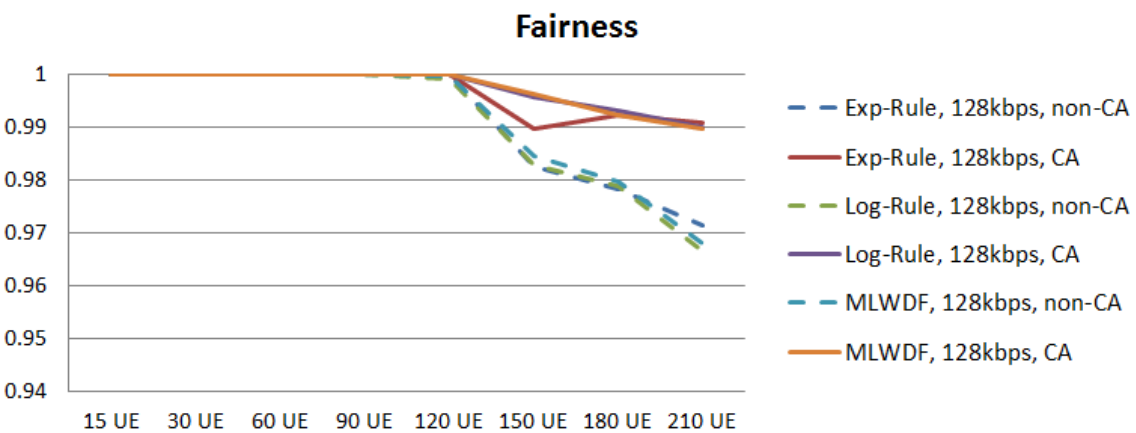

Figure 3.10: Fairness index for the three algorithms at video bit-rate 128kbps, with and without the use of CA.

According to the obtained results that are displayed in Fig. 3.10, at this scenario's conditions, the three algorithms showed similar fluctuating fairness in both cases. An excellent fairness took place among users for the three algorithms when the CA was

used. However, when the CA was not used, the fairness indicator dropped slightly after the number of users exceeded 120 UEs.

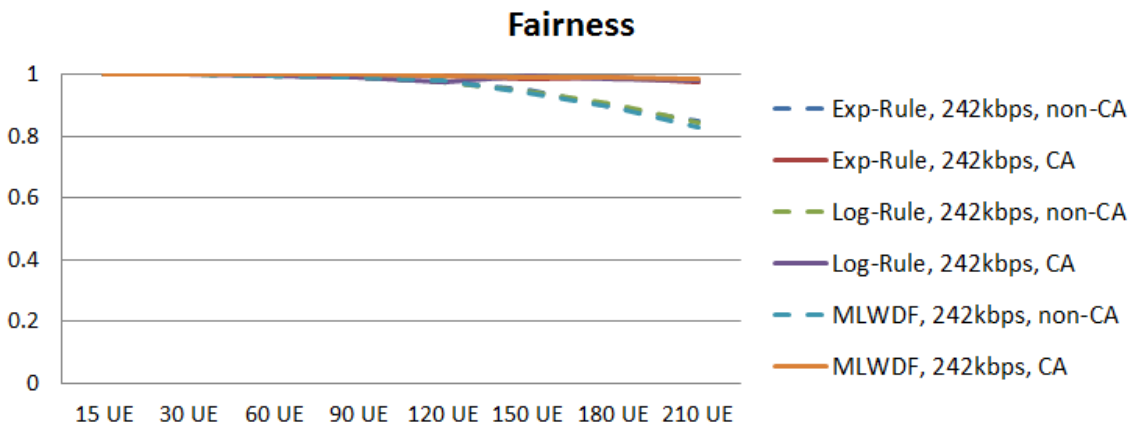

Figure 3.11: Fairness index for the three algorithms at video bit-rate 242kbps, with and without the use of CA.

According to the obtained results that are displayed in Fig. 3.11, at this scenario's conditions, the three algorithms showed similar fluctuating fairness in both cases. An excellent fairness was forced among users for the three algorithms when the CA was used. However, when the CA was not used, the fairness indicator dropped 5-20% from what it was when the CA was used, this drop started to take place after the number of users exceeded 120 UEs.

According to the obtained results that are displayed in Fig. 3.12, at this scenario's conditions, the three algorithms showed similar fluctuating fairness in both cases. When the CA was used, and when the number of users started to exceed 90 UE, the fairness indicator started to drop until it reached a value of 0.8 when the number of users was 210 UE. When the CA was not used the drop of the fairness indicator was more significant, it reached to a value of 0.6 when the number of users was 210 UE.

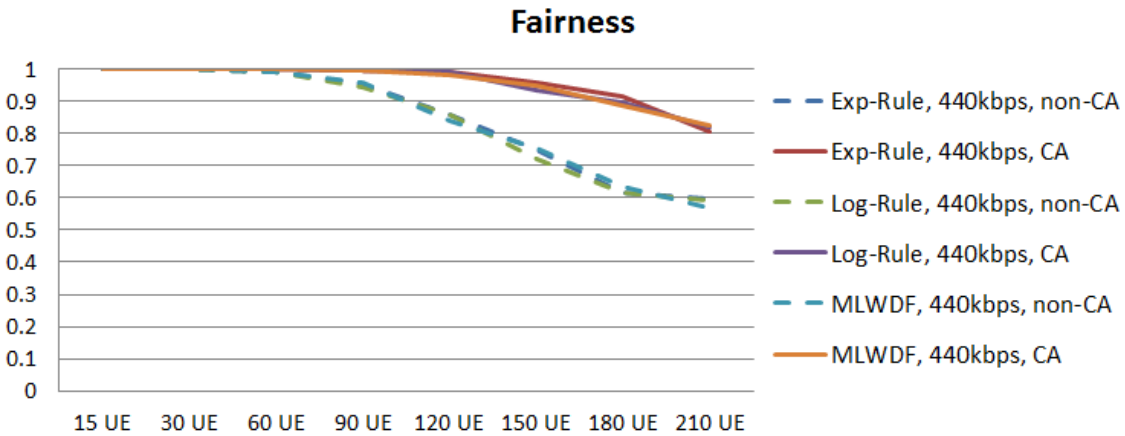

Figure 3.12: Fairness index for the three algorithms at video bit-rate 440kbps, with and without the use of CA.

3.5 Conclusion

This chapter has provided a comparative study on three Channel-aware/QoS-aware scheduling algorithms over LTE/LTE-A for video-applications. The comparison aimed to study the behaviour of the selected algorithms when the network load reaches the capacity limitations of the LTE macro-cell and to compare it when the network is supported by the CA feature to operate as LTE-A. In addition, there was a comparison among the scheduling algorithms in both cases. The evaluation process was based on simulating different scenarios by varying the number of users, the video bit-rates, and the system's bandwidth. The LTE-Sim was used in the experiments process both with and without modifications. The QoS performance evaluation was in terms of the QoS parameters, the system's average throughput, Packet Loss Rate (PLR), average packet delay, and fairness among users. Experiments results show that the system's average throughput was significantly improved by the use of CA. The capacity limitation boundaries were also doubled. The use of the MLWDF slightly improved the system's average throughput while the CA was used. The PLR was significantly reduced almost 50% by the use of CA at a video

bit-rate of 128kbps, by 50-70% at a video bit-rate of 242kbps, and by 40-60% at a video bit-rate of 440kbps. The average packet delay was reduced by the use of CA at a video bit-rate of 128kbps, and at a video bit-rate of 242Kbps by 30-40%, and at a video bit-rate of 440kbps by 20-30%. The MLWDF showed more performance stability in terms of increasing the average packet delay with increasing the number of users. The Exp-Rule had a slightly higher delay than the LOG-rule and the ML-WDF. The fairness indicator was improved with the use of CA by a factor of 10-20%. These results show that the use of CA is worth being investigated by researchers, implemented by the manufacturers, and deployed by the service providers.

Chapter 4

QoS Evaluation of DQS Scheduler over LTE-A HetNets

4.1 Introduction

Heterogeneous Networks (HetNets) are networks which consists of macro-cells, and low power nodes such as pico-cells or femto-cells. HetNets allow cellular network operators to support higher data traffic by offloading it to a smaller cells such as pico-cells [78].

As explained in section 2.4 of this dissertation, carrier aggregation allows the network to aggregate more than one carrier in-order to provide higher bandwidth. Carrier aggregation has four main deployment scenarios. Some of them are recommended for homogeneous network deployments, whereas others are recommended for HetNets deployments. The four main deployment scenarios are shown in Figure 4.1 [57]. In Figure 4.1, the macro-cell has three sectors. The coverage areas in blue "light shading" refers to Frequency 1 (f_1), and it is called the primary frequency. The coverage areas in purple "dark shading" refers to Frequency 2 (f_2), and it is called

the secondary frequency. (f_1) is greater than (f_2).

In Scenario 1, both the (f_1) and (f_2) carrier components are operating at the same band or the frequency separation is small. This leads to similar coverage. In Scenario 2, the (f_1) and (f_2) carrier components are operating at different bands or the frequency separation is large, and this leads to a different coverage. Hence (f_1) will be used to provide sufficient coverage, and (f_2) will be used to provide extra throughput. Next in Scenario 3, both (f_1) and (f_2) are operating at different bands, but (f_2) is used to increase the cell-edge throughput by directing (f_2) antennas to (f_1) cell boundaries. These three scenarios are best suited for homogeneous networks layout. However, for a heterogeneous networks layout, it is best to use Scenario 4, in which (f_1) is used by the macro-cell, and (f_2) is used by the pico-cell. In this scenario, the carrier component that is provided by the macro-cell, has a lower frequency which will result in a higher coverage. Meanwhile the carrier component that is provided by the pico-cell have a higher frequency and lower coverage [57]. A larger view of Scenario 4 is shown in Figure 4.2 [67].

There are two main deployment approaches for LTE-A HetNets using CA "Scenario 4". One approach uses a centralized architecture, and the other one does not use a centralized architecture. Both approaches consider the macro-cell to be the Primary Cell (PCell) in each sector, and the pico-cells to be the Secondary cells (SCells). More detailed differences of these two approaches are listed in Table 4.1 [67].

4.1.1 Contribution

The first contribution of this chapter, is in modifying the LTE-Sim simulator to support the use of Disjoint Queue Scheduler (DQS) for a HetNet deployment of a macro-cell and a variable number of pico-cells. The use of the DQS will allow the user to be scheduled on multiple carrier components, e.g. the carrier components of

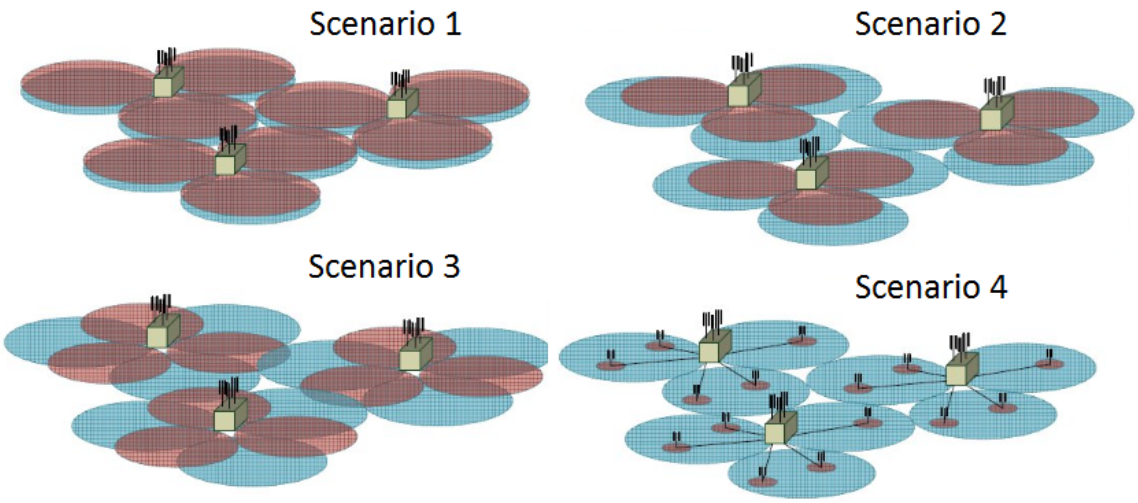

Figure 4.1: The four main deployment scenarios for CA [57]

both the macro-cell and the pico-cell at the same time.

Then, the second contribution, is in comparing the QoS performance of a three cross carrier aggregation scenarios. The first aggregation scenario included the use of the DQS that is based on the MLWDF algorithm, and it was called "DQS MLWDF".

Table 4.1: centralized vs. non-centralized architecture approach

Centralized architecture	**Non-centralized architecture**
The same spectrum deployment is used for the three sectors of the 3-sectored macro-cell.	Different spectrum deployment will be used in each sector of the 3-sectored macro-cell.
Higher spectral efficiency will be achieved because all the spectrum frequencies are available in each sector.	Multiple frequency bands might not be used most efficiently.
Very challenging to limit inter-cell interference.	Inter-cell interference is minimized.
Centralized processing for synchronization and tight coordination is needed.	Such synchronization and tight coordination is not necessary.
Very challenging to provide mobility between cells using the same frequency.	Providing mobility is not a challenge.

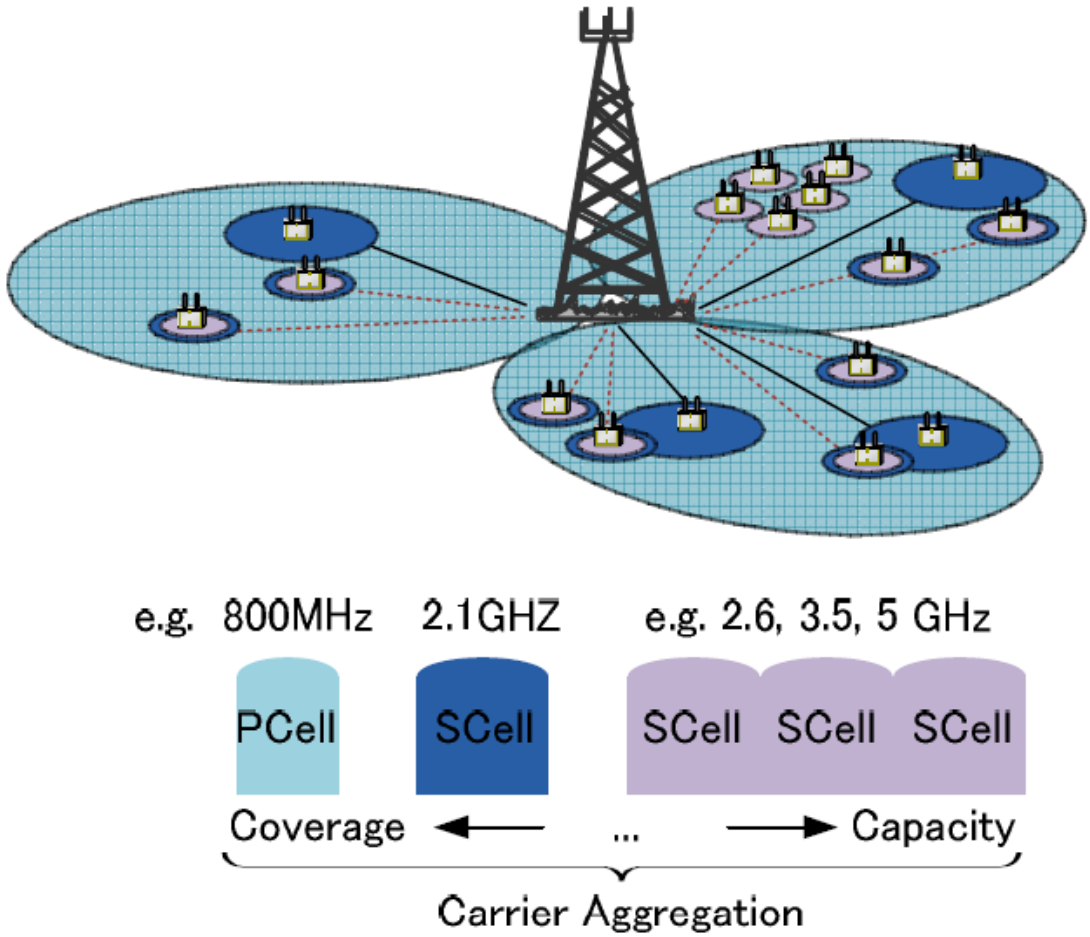

Figure 4.2: The deployment of HetNets "3-sectored macro-cell, and pico-cells" using carrier aggregation [67]

The second aggregation scenario included the use of the DQS that is based on the EXP-Rule algorithm, and it was called "DQS EXP-Rule". The third aggregation scenario included the use of the MLWDF and the use of a single carrier only, i.e, users are scheduled to a single carrier, either the macro-cell carrier or the pico-cell carrier, and it was called "SC MLWDF".

4.2 Related Work

The main difference between scheduling in LTE and LTE-A with CA is in the ability of scheduling the same user to different Carrier components as long as the user exists in the coverage of both carriers. If we take a quick look at the recent literature on Radio Resource Management (RRM) techniques for LTE-A with CA, we can see that the general structure of these schedulers could be classified into two main structures, the Joint Queue Scheduler (JQS) as shown in Figure 4.3 and the Disjoint Queue Scheduler (DQS) as shown in Figure 4.4 [57].

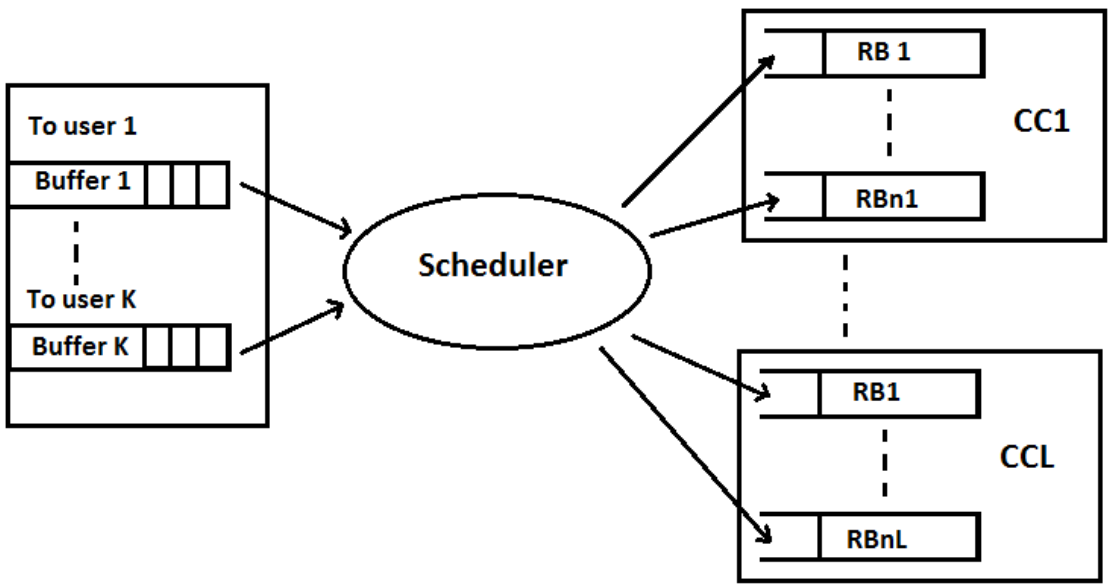

Figure 4.3: Joint Queue Scheduler (JQS).

In both scheduling structure, the scheduling process is divided into two stages; the first stage is performed at the carrier level and it is called the Component Carrier (CC) selection and management, and the second one, which comes after is performed at the sub-carrier level and it is related to the packet scheduling. In the DQS, there is a separate algorithm for each stage, and it is used to reduce the complexity as in [93] [86]. However, in the JQS, the two stages scheduling process is performed by

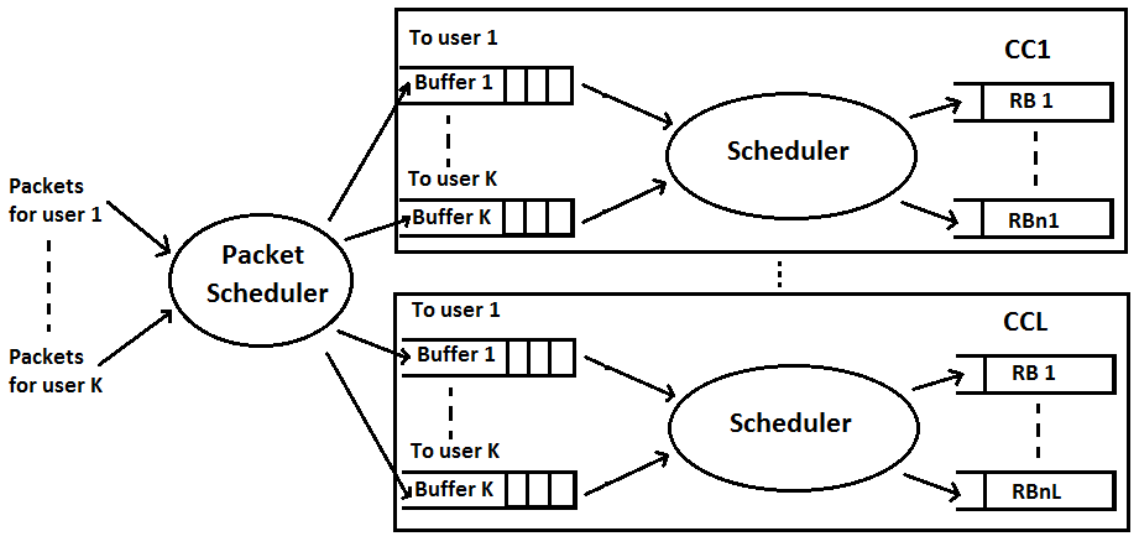

Figure 4.4: Disjoint Queue Scheduler (DQS).

one algorithm, and it is used to improve the performance as in [93] [92]. In the DQS, each user has one traffic queue on each CC. However, in the JQS, each user has only one joint queue for all the CCs, and this queue is shared by all the CCs. This pool of CCs is considered by the JQS scheduler as one carrier when it maps users' traffic to all the RBs in all the CC [57].

In regards to the CC selection and management algorithms, the most used algorithms in terms of load balancing are; the random selection, circular selection, least load, and modified least load. The benefit of using the Random selection as in [82] [84] of carrier components for users, is that it allows for an effective load balancing over the long term. However, it leads to an unbalanced loading in the short term. The use of the circular selection as in [93] [91] provides better performance than the Random selection. However, it is inefficient when the users packet sizes are significantly different. The use of the Least Load algorithm as in [38] [85] result in choosing the carrier component with the least traffic load. Hence, a better performance is achieved if compared with another schemes that don't consider the traffic

load. The use of the Modified least load (M-LL) as in [93] perform load balancing while taking into consideration the varying channel gain. However, it requires an accurate estimation of future average user rates.

In regards to the packet scheduling, there are lots of packet scheduling algorithms, each has its own unique utility function, whether to increase the throughput, or to decrease the delay, or to improve the fairness. A good classification of these algorithms that is based on their characteristics is found in [36]. One of these algorithms classes that is related to this work is the QoS-aware/channel-aware algorithms' class. The Modified Largest Weighted Delay First (MLWDF) [32] and Exponential Rule (EXP-Rule) [75] algorithms are an example of the QoS-aware/channel-aware class. The MLWDF scheduling algorithm is designed to support multiple real time data users by taking into account their different QoS requirements. And its delay function is bounded by the Largest Weighted Delay First (LWDF) scheduler. The LWDF metric is based on the system parameter, representing the acceptable probability for the $i-th$ user, in which a packet is dropped due to deadline expiration [32]. In regard to the EXP-Rule scheduling algorithm, its delay function is bounded by an exponential equation [75]. Both the MLWDF and the EXP-Rule uses the Proportional Fairness (PF) [34] scheduler to achieve channel awareness. The PF scheduler makes a trade-off between users' fairness and spectrum efficiency. It schedule users in a fair way by taking into account both the experienced channel state and the past data rate when assigning radio resources. And its objective function aims to obtain satisfying throughput and at the same time, guarantee fairness among flows [79] [36].

4.3 Experiments

The work of the following experiments was part of a published conference paper in [80].

4.3.1 Experiments Set-up

In these experiments, the network deployment which was used consisted of one macro-cell that is served by one transmitter with a power of 43 dB, and 10 pico-cells. All the pico-cells lie inside the coverage of the macro-cell, and each pico-cell is served by one transmitter with a power of 30 dB. The bandwidth of the macro-cell and of each pico-cell was fixed to 20 MHz. The three cross carrier aggregation scenarios were tested on this network deployment.

Also, in this paper, users which were in the coverage of the macro-cell coverage area only were called Macro-cell User Equipments "MUEs", and users which where in the coverage of the macro-cell in addition to one of the pico-cells were called Pico-cell User Equipments "PUEs". In all scheduling scenarios, the percentage of MUEs to PUEs (MUE:PUE) was varied over nine different percentages in-order to study the optimal percentage of macro-cell users to pico-cell users.

In regards to the total number of users, it is chosen to be 200 in all experiments, and this number choice was based on researching the related work that exists in the literature which uses the LTE-Sim simulator as its simulation framework, i.e. [57] [72] [79] [78] [87] [30] [66], we can see that they all consider the maximum number of users to be 200 users or less, and this is due to the simulator performance limitations.

In regards to the total experiments running time, for each percentage in each scenario in each network deployment, the running time was 50 sec "which is equal to 50,000 Transmission Time Intervals (TTI), in which the scheduling process is repeated every TTI", and each experiment was repeated three times and the final results were averaged, then the final results were used in the plots that are shown in Figures "Fig 4.5, 4.6, and 4.7", so the total number of experiments that was done is equal to 162 experiments, resulting in a total running time of 8,100 seconds. More detailed parameters of these experiments are also listed in Table 4.2.

Table 4.2: Experimental Parameters

Parameter	**Value**
Macro-cell transmission range "cell radius"	500 m
Macro-cell's sector numbers	one sector
Macro-cell's antenna type	Omni-directional
Pico-cell transmission range "cell radius"	50 m
Macro-Cell frequency band and bandwidth	Band-20, 20MHz
Pico-Cell frequency band and bandwidth	Band-7, 20MHz
MUE to PUE "MUE:PUE" percentages	9:1, 8:2, 7:3, 6:4, 5:5, 4:6, 3:7, 2:8, 1:9
Users' distribution in each cell	Random
Users' movement's speed and direction	3Km/h, random
Traffic type	Video
Video Bit-rate	440 Kbps
maximum delay	0.1 sec
Frame structure	FDD

4.3.2 Experiments Results

The LTE-Sim simulator takes into account both signalling and data traffic. However, in its traces, it only displays data traffic. Overall, the generated data traffic traces were used to measure key QoS parameters such as the average user throughput, Packet Loss Rate (PLR), and average packet delay. These measured QoS values were then plotted by using the MUE:PUE ratio for the x-axis, i.e, see plots in Figures "Fig 4.5, 4.6, and 4.7".

Average User's Throughput

it is defined as the average amount of received packets for each user per second. These values are measured per macro-users, and pico-users separately. Now according to Figure 4.5, the use of the "DQS MLWDF" and "DQS EXP-Rule" aggregation

scenarios has a similar fluctuating performance. However, this performance differed from the use of the "SC MLWDF" aggregation scenario. With regard to the PUEs, the average user's throughput values increased significantly from 17_KBps "in what it was in the "SC MLWDF" aggregation scenario" to 30_KBps. This is because the PUEs were scheduled to both radio bands, i.e, the macro-cell's band and the pico-cell's band. Meanwhile, for the MUEs, their average throughput values dropped from 17_KBps "in what it was in the "SC MLWDF" aggregation scenario" to 13_KBps. This occurs since the macro-cell's radio band was shared by both the MUEs and the PUEs. Finally, in terms of (MUE:PUE) percentages, the average throughput per MUE and PUE remained constant except at 9:1 and 1:9 it dropped 4_KBps. The optimal MUE:PUE percentage could be considered as any percentage of the nine tested percentages. This is because the network did not reach its maximum value of throughput per user.

Packet Loss Rate (PLR)

it is measured by dividing the difference between the total transmitted and received packets for all users over the total transmitted packets. These values were measured per macro-users and per pico-users separately. According to Figure 4.6, when the "SC MLWDF" aggregation scenario was used, the PLR values for the PUEs and MUEs showed almost a symmetric reverse results. This is due to the fact that traffic was offloaded in an equal gradual amount from the macro-cell to the pico-cells. The decrease in PLR values for an increase in the amount of offloaded traffic is due to the decreasing number of packets in the waiting queues that are competing for the same resource blocks. In general, this will lead to a lower rate of dropped packets from these queues. The optimal MUE:PUE percentage regarding the minimal PLR values in this aggregation scenario was seen to be 5:5. Namely, at this percentage value the PLR value dropped to almost zero for both the MUEs and PUEs.

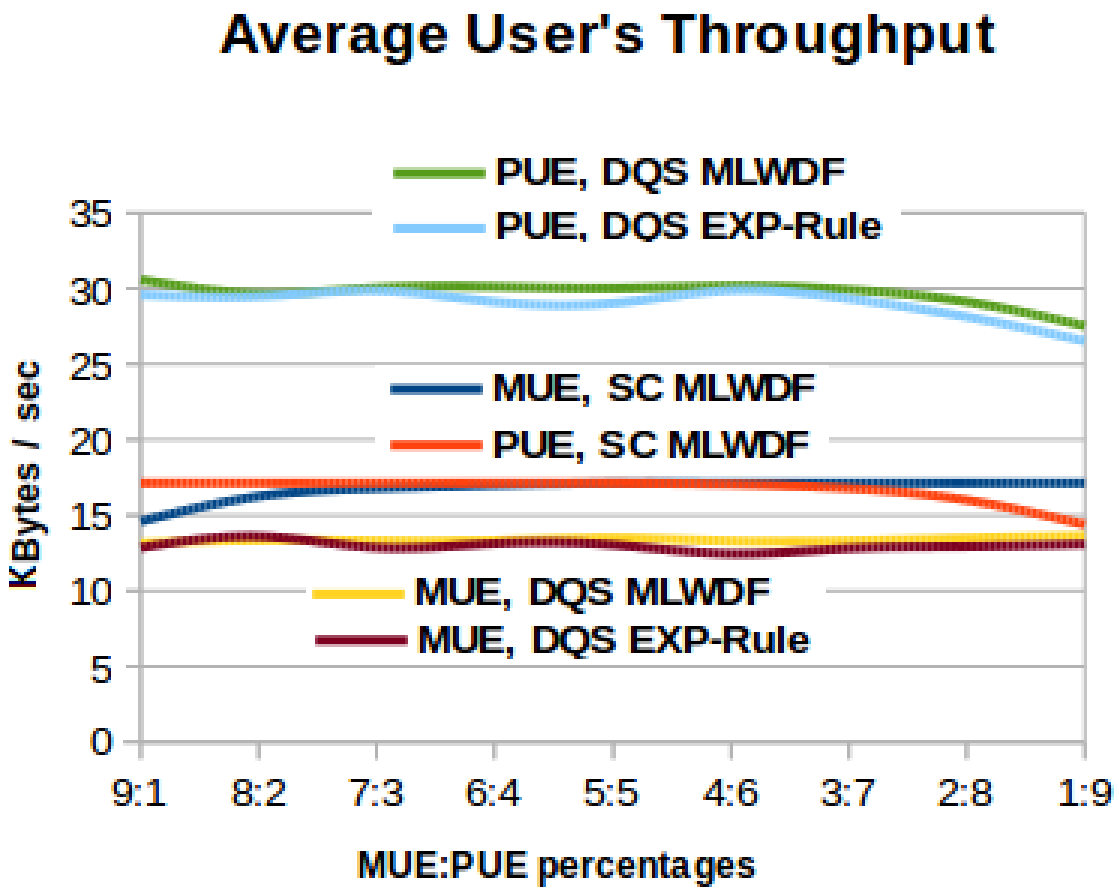

Figure 4.5: The experimental results in regards to the average user's throughput.

Now with regard to both aggregation scenarios, the "DQS MLWDF" and "DQS EXP-Rule", they showed a similar fluctuating performance in terms of PLR also. The PLR values in regards to the MUEs increased to 0.22, and it remained close to this value despite the decrease in their percentages. Regarding the PUEs, the PLR values increased to 0.13, and it remained mostly around this value despite the increase in their percentages until the number of MUEs and PUEs was equal. Then, the PLR values started to increase with an increase in their percentages. All this is likely because the users which were being offloaded from the macro-cell to the pico-cells were still competing with the MUEs, and they were still sharing macro-cell's

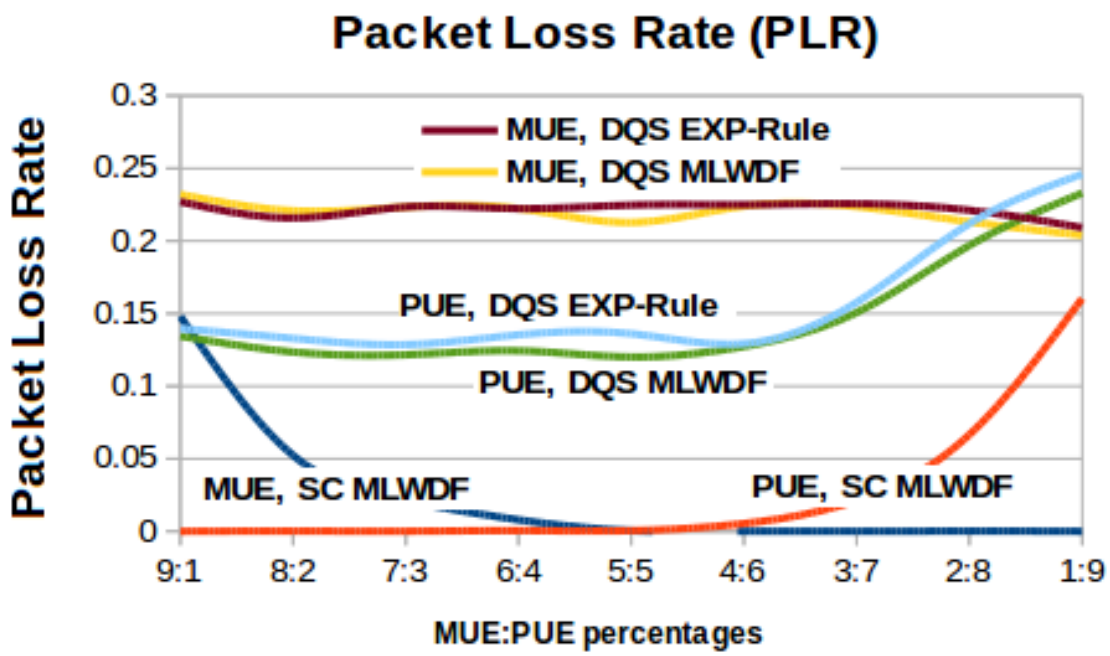

Figure 4.6: The experimental results in regards to the packet loss rate.

resources, e.g., radio bands and waiting queues. The optimal MUE:PUE percentage for the minimal PLR values in both aggregation scenarios was found to be about 5:5.

Average Packet Delay

it is measured as the time which a packet takes to travel from the source to destination. It includes the propagation and waiting time of the packet. Meanwhile, The average packet delay is measured by dividing the sum of a total packet delays that were successfully received over the total number of packets. These averaged values were measured per macro-users and per pico-users separately.

Now according to Figure 4.7, when the "SC MLWDF" aggregation scenario was used, the average packet delay values started to decrease for the MUE with a decrease in their percentages. This occurs since traffic was being offloaded gradually to pico-

cells, which resulted in a gradual release of the available resources, e.g., the waiting queues. This allowed the packets to be outputted for transmission quicker.

Also in both aggregation scenarios, the "DQS MLWDF" and "DQS EXP-Rule", the average packet delay remained almost the same for the MUEs with a decrease in their percentages, but with a slightly better performance to the use of the "DQS MLWDF" aggregation scenario. This is due to the fact that the users which were being offloaded from the macro-cell to pico-cells were still sharing the macro-cell band. Also the macro-cell's transmitter was still generating packets for those users, so its waiting queue has almost the same number of packets.

Now with regard to PUEs, the average packet delay values are also shown in Figure 4.7. These values started to increase for the PUEs with an increase in their percentages. However, the minimum delay value was 0.01 sec when the "SC ML-WDF" aggregation scenario was used, but it was 0.03 sec when the "DQS MLWDF" aggregation scenario was used, and it was 0.032 sec when the "DQS EXP-Rule" aggregation scenario was used. The increase in all the aggregation scenarios is due to gradual traffic offloading from the macro-cell to the pico-cells which gradually fills the waiting queues of the pico-cells transmitters with packets. In addition to this, the PUEs receive packets from the macro-cell's transmitter, and it is much further than the pico-cell transmitter yielding a higher transmission time which leads to a higher delay values. The optimal MUE:PUE percentage for the least equal delay was observed to be 5:5.

4.4 Conclusion

This chapter has provided a comparative study on the effects of using the disjoint queue scheduler for video applications in a HetNet deployment with a one macro-cell and a variable number of pico-cells on the users' QoS. Users where classified into

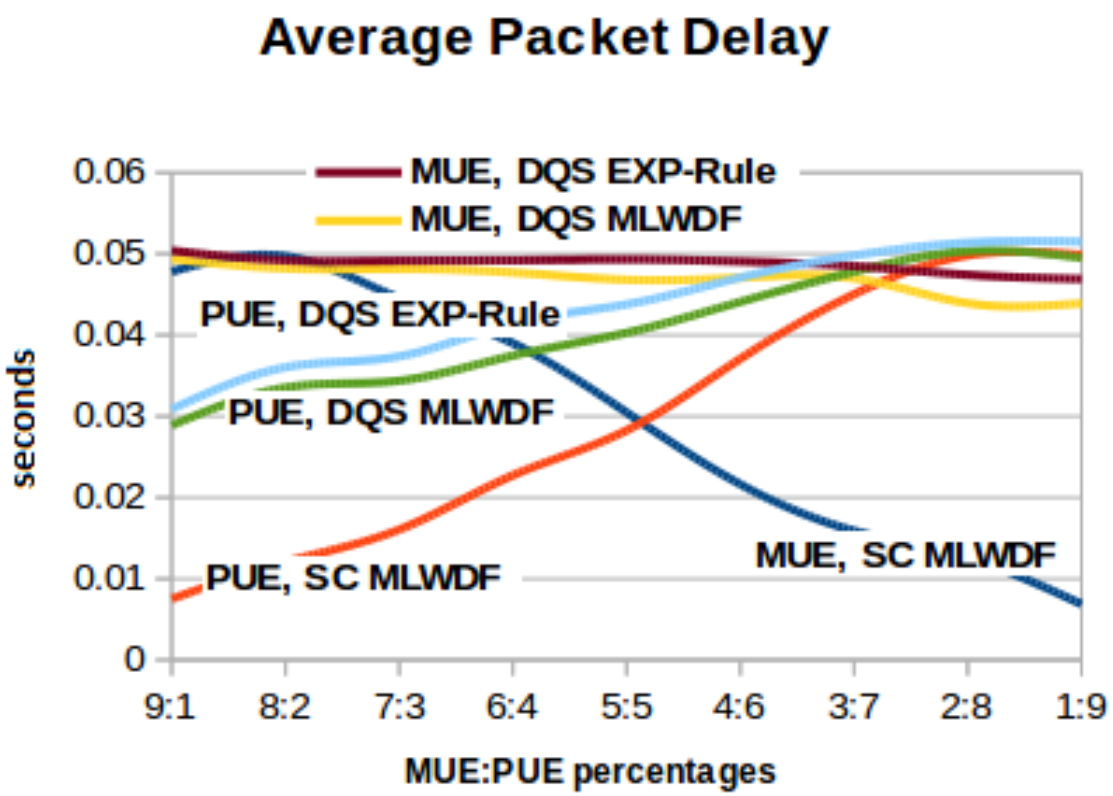

Figure 4.7: The experimental results in regards to the average packet delay.

macro-cell users or pico-cell users based on their location and service coverage. And the QoS parameters which were studied include user average throughput, packet loss rate, and average packet delay. In-order to test this, the LTE-Sim was modified to support the use of disjoint queue scheduler in a HetNet deployment with a one macro-cell and a variable number of pico-cells. Experiments' results show that the average pico-cells user throughput almost doubled when disjoint queue scheduler was used. However, this increase came with a cost of decreasing the average macro-cell user throughput by a factor of about 0.2. Also, the Packet Loss Rate (PLR) values increased with the use of the disjoint queue scheduler, increasing on an average of almost three to four times for pico-cells users, and five to six times for macro-cell

users. The use of both DQS schedulers types, the DQS based MLWDF and DQS based EXP-Rule had a similar fluctuating performance in terms of average users' throughput and PLR. The average packet delay values also fluctuated between minimum and maximum values depending upon the percentage of macro-cell to pico-cells users. However, the maximum value did not change with the use of the disjoint queue scheduler. Nevertheless, the minimum values increased five times for the macro-cell users and three times for the pico-cells users. The optimal users percentages for minimal PLR and average packet delay were at an equal number of users from different types. The use of the DQS based MLWDF had a slightly better performance than the DQS based EXP-Rule in terms of packet delay. Upon the experimental results, it is recommended to use the disjoint queue scheduler for for non-real time video traffic.

Chapter 5

The use of Multi-agent Q-Learning in LTE Packet Scheduling

5.1 Introduction

In section 5.2 of this chapter, we explain the concept of spectrum underutilisation, and why it occurs. Then, in section 5.3, we explain the concept of Cognitive Radio (CR). Then, in section 5.4, we explain the concept of Reinforcement Learning (RL). Then, in section 5.5 and 5.6, we move into explaining Q-learning in more details, and we explain how this technique is suitable to be used as a scheduling algorithm for LTE cellular networks. Finally, in section 5.7, we make some concluding remarks.

5.2 Spectrum Underutilisation

According to the Federal Communication Commission (FCC) in [14], the fixed assignment of spectrum resources can lead to spectrum underutilisation "as shown in

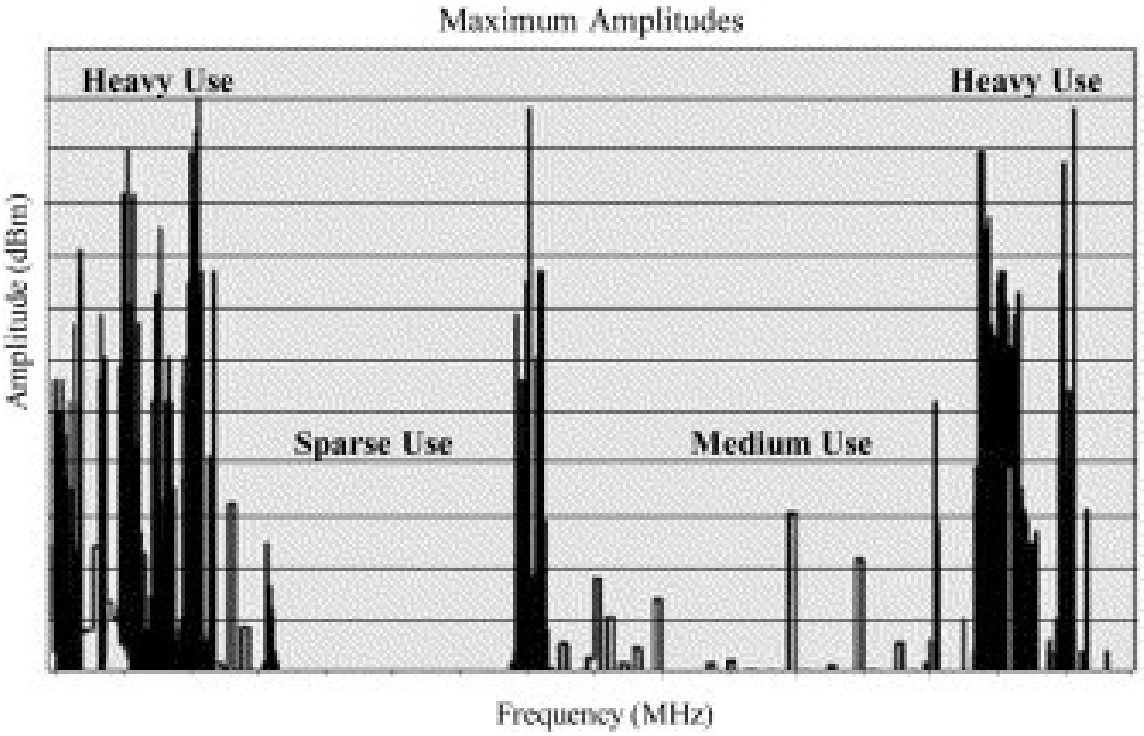

Figure 5.1: Spectrum utilisation [27]

Fig. 5.1", and this is because of the irregular usage demands by licensed users, in which this demand varies depending on time and geographical area. In other words, Spectrum underutilisation can occur when some resource blocks that are assigned to licensed users at some particular times are not being used. These un-used resource blocks are called white spaces or spectrum holes. In order to solve this underutilisation problem and make the most out of a spectrum, Dynamic Spectrum Sharing (DSS) that is based on dynamic spectrum assignment has to be deployed instead of the fixed spectrum assignment. This made a lot of scientists to conduct research on the different implications of communication and signal processing that is needed for Dynamic Spectrum Access (DSA) networks. DSA is a set of techniques that aims to better utilize the use of the licensed spectrum by detecting the spectrum holes due to underutilizing the use of it, and allow unlicensed users to use it as well [27] [94].

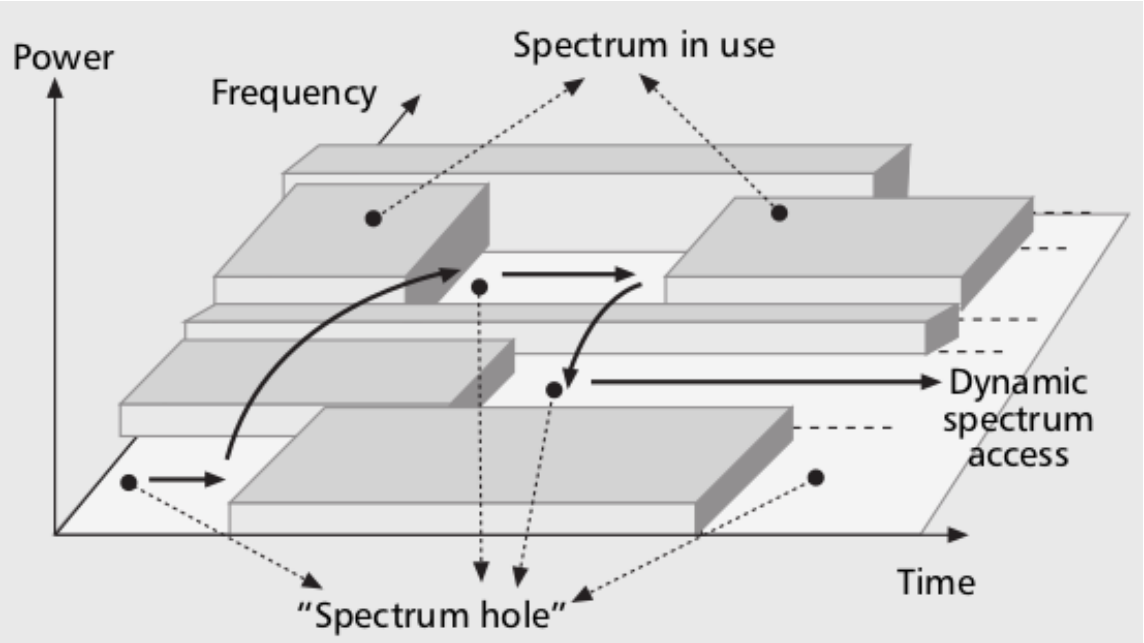

Figure 5.2: The concept of spectrum holes and dynamic spectrum access [28]

The concepts of spectrum holes and dynamic spectrum access are shown in Fig. 5.2.

5.3 Cognitive Radio (CR)

Cognitive Radio (CR) is defined by Mitola in [63] as a form of wireless communication in which a transceiver can intelligently detect which communication channels are in use and which are not, and can be dynamically configured to move into a vacant channels while avoiding occupied ones.

Cognitive radio systems were designed to optimally use the electromagnetic spectrum through their ability to detect vacant channels and moving into them. This goal is achieved through a learning cycle that cognitive radio systems go through. This learning cycle consist of three main stages, the perception, learning, and reasoning, and it is shown in Fig. 5.1. Perception is the first stage of the learning cycle,

and it starts by sensing the spectrum in order to collect data about the surrounding radio environment, e.g., the channels' conditions and their availabilities. CR systems should not only sense and be aware of the medium, but it should also have the ability to learn and reason. Learning is the second stage and most important stage, and this is because it includes transforming the obtained information about the radio environment into knowledge through the use of classification methodologies. Reasoning is the final stage in this cycle, in which the obtained knowledge is used to make decisions that meet with the cognitive radio objectives, e.g., optimizing the usage of the spectrum to maximise the system's throughput [63] [81].

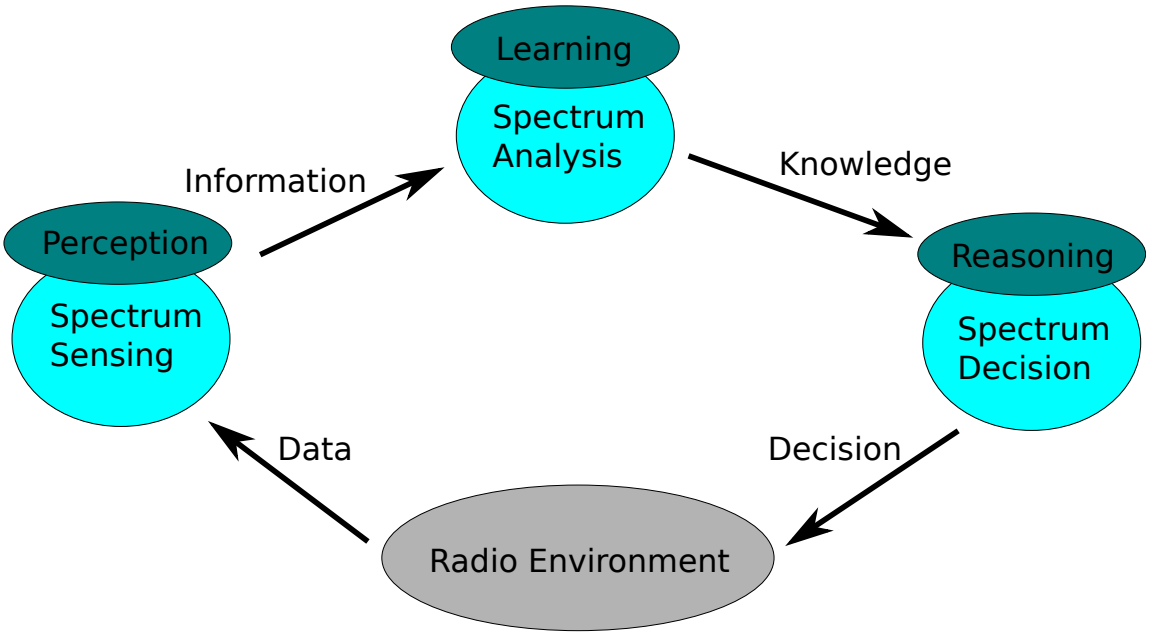

Figure 5.3: Cognitive radio learning cycle

5.4 Reinforcement Learning (RL)

In machine learning, learning can be either supervised or unsupervised. In the case of supervised learning approach, the learning agent learns by instruction. In the case of

unsupervised learning approach, the learning agent can learn by reinforcement [81].

Reinforcement Learning (RL) could be explained in its most simplistic terms, it implies a situation in which a learning agent is left alone and not told what to do, and it has to form a basic understanding of its environment. RL offers a powerful set of tools for sequential decision making under uncertainty. In RL, there are five main elements, the learning agents, actions, policy rules, rewards, and the system model. The learning agent learns what to do "what action to perform" in an environment by trying the action despite significant uncertainty about the environment it faces and the action's effect on the environment. Then, the learner maps the effect of this action in that situation to the environment with the performed action in-order to maximise a numerical reward signal. This mapping between the actions and rewards is called the policy rules which defines the behaviour of the learning agent [81] [64] [18].

An agent was defined by [74] as autonomous to the extent that its behaviour is determined by its own experience. A more precise definition of a learning agent is found in [52], in which a learning agent is an agent that develops through own experience and with the help of some built-in knowledge an action policy directly mapped from its observations and internal conditions.

5.5 Q-Learning and its use in LTE scheduling

Q-learning is a model free reinforcement learning techniques, it could be used even if the channels or the sub-bands Markov model are not known. In Q-learning based system models, learning agent is deployed in an environment which have a set of states S. The learning agent can sense it's current state s_t at time t, in which $s_t \in S$. Based on this current state, the learning agent will choose an action a from a set of actions A to be executed in time $t+1$. Based on this executed action and its effect on the environment, a reward function $r_{t+1}(s_t, a)$ will be calculated, the higher the

reward the higher the probability of choosing this performed action [81] [59] [20]. In each Q-learning-based model, a Q-table $Q(s, a)$ is constructed and updated, as in Table 5.1.

Table 5.1: An example of a Q-table structure for a single-agent

	s_0	s_1	...	s_{t-1}	s_t	s_{t+1}	...
a_1							
a_2							
$\vdots$							
a_n					$Q(s_t, a_n)$		

The general formula of Q-Learning that is used to update an entry in the Q-table is shown in formula 5.1, as proposed by [81].

$$Q(s_t, a_n) \leftarrow (1 - \alpha)Q(s_t, a_n) + \alpha[(r_{t+1}(s_t, a_n) + \gamma \underset{a_i}{max} Q(s_{t+1}, a_i)] \tag{5.1}$$

In cognitive radio, the environment is the radio channels and their states, $s_t \in S$, s_t will represent the availability of these channels at time t, and S will be the set of all the radio channels' states at all time. Each radio channel will have two states, either Idle (I), or Busy (B).

The action a of selecting radio channels belong to the actions set A, $a \in A = \{a_1, ..., a_n\}$. The decision policy of choosing an action a in time period t, to be executed in time period $t + 1$ is based on a maximum argument, $\underset{a_i}{max} Q(s_{t+1}, a_i)$, where i = {1, ..., n}, a_i representing all the actions in the action set at state s_{t+1}.

The reward r_{t+1}, is the immediate reward that is obtained after executing action a in state s_{t+1}. $r_{t+1} \in r$, where r is the set of rewards. r_t is defined by the system designer, it could be defined as the actual achieved user's communication throughput, or it could be defined as the Jain's fairness index, as in formula 3.9 in this dissertation.

The learning rate is denoted by $\alpha \in (0,1)$. The discount factor is denoted by $\gamma \in [0,1)$, and it determines the importance of future reward.

5.6 Multi-agent Q-Learning in LTE scheduling

In Multi-agent Q-learning algorithms, learning agents either collaborate or compete among each other. In the case of collaborative learning agents, the system is called as a collaborative multi-agent system, and in the case of competitive learning agents, the system is called as a competitive multi-agent system. The main difference between these two systems is that the collaborative learning agents' decision making policies are based on maximizing the joint reward. While, the competitive learning agent's decision making policies are based on maximizing its individual reward [70].

In the Q-learning-based scheduling algorithms, each user is considered a learning agent, and since we are scheduling more than one user, a Multi-Agent Reinforcement Learning (MARL) approach will be applied. Multi-agent systems that are found in literature could follow the collaborative approach as in [40] [44] [83] [90], or the competitive approach as in [83] [58]. In the case of the collaborative approach, part of the channel has to be reserved for information sharing. However, in the case of competitive approach, there is no need for information sharing. In addition to this, in the collaborative approach, there is one centralised node that contains one Q-table for all the agents, in which they cooperate by sharing their sensing information in order to update the centralised shared policies. However, in the competitive approach, each agent senses the medium by considering other agents part of the Radio Frequency (RF) environment, and each agent updates its own Q-table [81] [35] [40].

5.7 Conclusion

This chapter has provided a detailed explanation of how Q-learning is a suitable technique for packet scheduling in LTE cellular networks. The importance of this chapter to be part of this dissertation is in laying the foundation of understanding this techniques, in which it will be used in the implementation of the two novel scheduling algorithms that are proposed in the next chapter of this dissertation.

Chapter 6

Proposed Multi-agent Q-learning LTE Scheduling Algorithms

6.1 Introduction

In this chapter we propose, implement, and test two novel Q-learning-based LTE packet scheduling algorithms. The implementation and testing of these algorithms was in Matlab, and they are based on the use of Reinforcement Learning (RL) approach, more specifically, the Q-learning technique for scheduling two types of users. The first scheduling algorithm is called Collaborative Competitive scheduling algorithm, and the second algorithm is called Competitive Competitive scheduling algorithm. The first type of the scheduled users is the Primary users (PUs), and they are the licensed subscribers that pay for their service. The second type of the scheduled users is the Secondary Users (SUs), and they are un-licensed subscribers that don't pay for their service. Each user whether its a primary or secondary is considered as an agent. Hence, it is a Multi-Agent Reinforcement Learning (MARL) system. In the Collaborative Competitive scheduling algorithm, the primary user

agents will collaborate in-order to make a joint scheduling decision about allocating the resource blocks to each one of them, then the secondary user agents will compete among themselves to use the remaining resource blocks. In the Competitive Competitive scheduling algorithm, the primary user agents will compete among themselves over the available resources, then the secondary user agents will compete among themselves over the remaining resources.

6.2 Problem definition

Scheduling two types of users, the primary users over the available radio resource blocks, and the secondary users over the remaining resources. The scheduling process is done every Transmission Time Interval (TTI), which equals 1 ms. Each user whether its a primary or secondary is considered an agent. The primary user agents will use the collaborative approach in-order to make a jointly decision about allocating the resource blocks to them, or the competitive approach depending on the scheduling algorithm that is used. And the remaining resource blocks will be sensed by the secondary user agents, and then to be used. The secondary user agents will use the competitive approach to compete among themselves to use these remaining resource blocks. Both the primary and the secondary users can access the network pool of radio resources, that is provided by the macro-cell. However, the secondary users have lower priority than the primary users, and they are transparent to primary users, which means that the primary users will consider that the whole resource blocks are available for them only, and they will access these resources as if the secondary users don't exist. And in the case if a secondary user is using an available radio resource at a current time slot, but a primary user is about to use the same radio resource at the next time slot, the secondary user has to withdraw and free this resource to be used by the primary user.

6.3 Collaborative Competitive scheduling algorithm

The first scheduling algorithm that is proposed and implemented in Matlab is the Collaborative Competitive scheduling algorithm, Algorithm 1. In this algorithm the scheduling process is divided into two stages; the first scheduling stage is performed for the primary users, and the second one, which comes after is performed for the secondary users. It combines two Q-learning approaches, the collaborative approach that is based on modifying the work proposed by [44] for primary users, and the competitive approach that is based on the work proposed by [81] for secondary users.

State set S

The set S represent all the observed states of all the Resource Blocks (RBs) at all the running time.

$S = \{s_0, s_1, ..., s_{t-1}, s_t, s_{t+1}, ..., s_{no.epoch}\}$

$s_t = \{RB_1, ..., RB_x\}$, where $x = no.RBs$

$s_t \in S$, s_t is a sub-set of the set S that represent the states of all the available RBs at time t. And it is the same for all users agents, the primary users agents, and the secondary users agents. Each resource block has three states, free, or busy for a primary user, or busy for a secondary user.

Primary users scheduling stage

The primary users scheduling stage starts by each primary user agent taking an action from the primary users action set, then these actions will form one joint action. Then the scheduler will calculate the obtained reward from executing this joint action. Then the scheduler will update the PUs shared Q-table.

Algorithm 1 Collaborative Competitive Scheduling Algorithm

Input: no. PUs, no. SUs, no. RBs, no. epoch, exploration parameter e

Output: PUs shared Q-table, SUs Q-tables

Initialize all parameters: Q-tables, PU Actions set A_{PU}, SU Actions set A_{SU}, state of RBs set S

for $t = 1$ to no. epoch **do**

  for $i = 1$ to N, where N = no. PUs **do**

    if no. available RBs > 0 **then**

      if rand $<= e$ **then**

        PU agent i will explore by taking an action a^i randomly from A_{PU}

      else

        PU agent i will exploit by taking an action a^i from A_{PU} based on the Expectation Values table

      end if

      $A_{-i} = A_{PU} - \{a^i\}$

    end if

    Mark the used RBs in the sub-state s_t as busy for PU agent i

  end for

  Form the joint action $(a^{-i} \cup a^i)$ to be executed in the following state

  Calculate the obtained reward r_{t+1} after executing the joint action $(a^{-i} \cup a^i)$ according to Jain's fairness index: $r_{t+1} = ((\sum_{i=1}^{N} T_i)^2)/(N \sum_{i=1}^{N} {T_i}^2)$

  T_i denotes the throughput obtained for primary user i. N is the number of primary users which is 5

  Update the shared Q-table according to the following Q-learning formula:

  $Q(s_t, (a^{-i} \cup a^i)) \leftarrow (1-\alpha)Q(s_t, (a^{-i} \cup a^i)) + \alpha[r_{t+1}(s_t, (a^{-i} \cup a^i)) + \gamma V(s_{t+1})]$

  for $i = 1$ to N **do**

    PU agent i will update its counters about other PU agents taking their actions

    PU agent i will calculate the product of probabilities of other PU agents taking their actions: $\prod_{j \neq i}\{Pr^i_{a^{-i}[j]}\}$

    PU agent i will update the Expectation Value of its individual action a^i in its Expectation values table: $EV(a^i) = \sum_{a^{-i} \in A_{-i}} Q(a^{-i} \cup a^i) \prod_{j \neq i}\{Pr^i_{a^{-i}[j]}\}$

  end for

  for $k = 1$ to no. SUs **do**

    if no. free RBs in the sub-state $s_t > 0$ **then**

      if rand $<= e$ **then**

        SU agent k will explore by taking an action a^k randomly from A_{SU}

      else

        SU agent k will exploit by taking an action a^k on a greedy basis from A_{SU}

      end if

      SU agent k will calculate the reward of executing action a^k

      SU agent k will update its Q-table based on the Q-Learning formula:

      $Q(s_t, a^k) \leftarrow (1-\alpha)Q(s_t, a^k) + \alpha[r_{t+1}(s_t, a^k) + \gamma V(s_{t+1})]$

    end if

    $A_{-k} = A_{SU} - \{a^k\}$

  end for

end for

Actions and Action set

The primary users action set A_{PU} consists of multiple actions, each action has a different number of resource blocks with unique indexes. This will avoid collisions between primary users agents since they all have access to this actions set.

$A_{PU} = \{a_1^{PU}, ..., a_n^{PU}\}$, a^{PU} is an action to be taken by primary user agent, n is the number of actions in A_{PU}.

In regard to the decision policy that is deployed for choosing an action, it is based on either exploration or exploitation, and this is determined based on the value of the exploration parameter e. The value of this parameter determines the probability of exploration and the probability of exploitation. For example, if $e = 0.5$, then there is a 50% probability of an agent to explore, and 50% probability of an agent to exploit.

In the case of exploration, the agent will make a random choice in taking an action from the primary users action set. In the case of exploitation, the agent will make its choice to take an action based on the expectation formula values in the joint Q-table, to execute an individual action which form with other agents actions the best joint action that exists in the shared Q-table. The best joint action will be associated with the highest reward.

After the first primary user agent takes an action, the scheduler will update the primary users action set as, $A_{-i} = A_{PU} - \{a^i\}$, so that each agent will take a different action, this will help in avoiding any collision between primary users. Then the next primary user agent will enter the same loop, and this loop will be repeated until all primary user agents takes actions. The result of all the individual actions that were taken by the five primary user agents will contribute in forming one joint action, in which we denote to it by $(a^{-i} \cup a^i)$.

Rewards and Rewards set

The reward set R_{PU} consists of all the obtained rewards at all the running time. $R_{PU} = \{r_1, ..., r_{t-1}, r_t, r_{t+1}, ..., r_{no.epoch}\}$. r_{t+1} is the reward that is obtained after executing the joint action $(a^{-i} \cup a^i)$ in state s_{t+1}.

The reward function for the primary user agents is chosen to optimize the primary user's average throughput for all the users while at the same time maintaining a fair share of the radio resources to each user. So in this work, the scheduler calculates the obtained reward r_{t+1} according to jain's fairness index:

$$r_{t+1} = ((\sum_{i=1}^{N} T_i)^2)/(N \sum_{i=1}^{N} {T_i}^2) \tag{6.1}$$

T_i denotes the throughput obtained for primary user i. N is the number of primary users which is 5.

Q-table and Expectation values

After executing the joint action and calculating the obtained reward, the scheduler will update the shared Q-table. The Q-learning formula that is used to update an entry in the Q-table is as follows:

$$Q(s_t, (a^{-i} \cup a^i)) \leftarrow (1-\alpha)Q(s_t, (a^{-i} \cup a^i)) + \alpha[r_{t+1}(s_t, (a^{-i} \cup a^i)) + \gamma V(s_{t+1})] \tag{6.2}$$

$V(s_{t+1})$ is determined by the policy of choosing an action at time t.

After the scheduler updates the shared Q-table, each PU agent will do the following:

First, it will update its counters about other PU agents taking their actions. The primary user agent is a Joint Action Learner (JAL), which means that the agent learns about other agents actions and their effect, in addition to its actions effect. In-order for the agent i to learn about other agents actions and their effects, it keeps a count ${C^{-i}}_{a^{-i}}$ for the number of times other agents "which we denote to any one of them by $-i$" has taken action a in the past. Then agent i calculates the probability of agent $-i$ to take an action a^{-i} as ${Pr^i}_{a^{-i}} = {C^{-i}}_{a^{-i}} / (\sum_{b^{-i} \in A_{-i}} {C^{-i}}_{b^{-i}})$, where b^{-i} represent all the previous actions taken by agent $-i$.

Second, it will calculate the product of probabilities of other PU agents taking their actions as: $\prod_{j \neq i} \{Pr^i_{a^{-i}[j]}\}$.

Third, it will update the expectation value $EV(a^i)$ of its individual action a^i that it took in its Expectation Values table according to the following formula:

$$EV(a^i) = \sum_{a^{-i} \in A_{-i}} Q(a^{-i} \cup a^i) \prod_{j \neq i} \{Pr^i_{a^{-i}[j]}\} \tag{6.3}$$

These expectation values help the PU agent in implementing its exploitation strategy.

Secondary users scheduling stage

The secondary users scheduling stage dose not include any cooperation between the secondary user agents. On the contrary, the secondary user agents compete on the remaining resource blocks that are left after scheduling the primary users. The secondary users scheduling loop of taking an action, then obtaining a reward based on executing this action, and then updating the Q-table, is repeated for every secondary user agent.

Actions and Action sets

The secondary users actions set A_{SU} is different from the primary users action set. It is accessed by all the secondary user agents. It consists of multiple actions, and each action has a different number of resource blocks in order to avoid collision between secondary users.

$A_{SU} = \{a_1^{SU}, ..., a_m^{SU}\}$, a^{SU} is an action to be taken by a secondary user agent, m is the number of actions in A_{SU}.

These actions are designed with an upper limit on how many resource blocks the agent can get. This upper limit is equal to the number of the remaining resource blocks over the number of secondary users. This will prevent the secondary user agent who enters the scheduling loop first in getting all the remaining resource blocks.

The secondary user agent will start by sensing the remaining resource blocks that are left after scheduling the primary users. If there are remaining resource blocks, the agent will take an action from the secondary users actions set. But, if there aren't any remaining resource blocks, the agent will not take any action.

The secondary user agent deploys two types of decision policies in choosing an action. It will either explore or exploit depending on the value of the exploration parameter e.

In the case of exploration, the agent will make a random choice in taking an action from the secondary users actions set. In the case of exploitation, the agent will make a greedy choice of what action to take from the secondary user actions set. The goal of the greedy choice is to take the action that will yield with the highest reward. In-order for the agent to do so, it will look through its Q-table.

Rewards

After executing an action, the secondary user agent will calculate the reward. The reward function for each secondary user agent is chosen to optimize the secondary user's average throughput. In this work, it was assigned to be the actual user's average throughput.

Q-tables

After calculating the reward, the secondary user agent will associate this reward with the action that resulted in this reward. Then the secondary user agent will build or update its own Q-table. The agent builds its Q-table, by creating new entries as a result of exploring new actions. And the agent updates these entries as a result of choosing a pre-existing entries in the process of exploitation. The agent does these operations according to the following formula:

$$Q(s_t, a^k) \leftarrow (1-\alpha)Q(s_t, a^k) + \alpha[r_{t+1}(s_t, a^k) + \gamma V(s_{t+1})] \tag{6.4}$$

$V(s_{t+1})$ is determined by the policy of choosing an action at time t.

6.4 Competitive Competitive scheduling algorithm

The second scheduling algorithm that is proposed and implemented in Matlab is the Competitive Competitive scheduling algorithm, Algorithm 2. In this algorithm the scheduling process is also divided into two stages; the first scheduling stage is performed for the primary users, and the second one, which comes after is performed for the secondary users. It uses the competitive Q-learning approach that is based

on the work proposed by [81] for both types of users, the primary and secondary users.

State S

The set S represent all the observed states of all the Resource Blocks (RBs) at all the running time.

$S = \{s_0, s_1, ..., s_{t-1}, s_t, s_{t+1}, ..., s_{no.epoch}\}$

$s_t = \{RB_1, ..., RB_x\}$, where $x = no.RBs$

$s_t \in S$, s_t is a sub-set of the set S that represent the states of all the available RBs at time t. And it is the same for all users agents, the primary users agents, and the secondary users agents. Each resource block has three states, free, or busy for a primary user, or busy for a secondary user.

Primary users scheduling stage

The primary scheduling stage in the Competitive Competitive scheduling algorithm does not include any cooperation between the primary user agents. On the contrary, the primary user agents compete on the available resource blocks. The primary users scheduling loop of taking an action, then obtaining a reward based on executing this action, and then updating the Q-table, is repeated for every primary user agent. After the first primary user agent finishes its scheduling loop, the scheduler will update the primary users action set to make sure that each agent will take a different action.

Algorithm 2 Competitive Competitive Scheduling Algorithm

Input: no. PUs, no. SUs, no. RBs, no. epoch, exploration parameter e
Output: PUs Q-tables, SUs Q-tables
Initialize all parameters: Q-tables, PU Actions set A_{PU}, SU Actions set A_{SU}, state of RBs set S
for $t = 1$ to no. epoch **do**
  for $i = 1$ to no. PUs **do**
    if no. available RBs > 0 **then**
      if rand $<= e$ **then**
        PU agent i will explore by taking an action a^i randomly from A_{PU}
      else
        PU agent i will exploit by taking an action a^i on a greedy basis from A_{PU}
      end if
      PU agent i will calculate the reward of executing action a^i
      PU agent i will update its Q-table based on the Q-Learning formula:
      $Q(s_t, a^i) \leftarrow (1 - \alpha)Q(s_t, a^i) + \alpha[r_{t+1}(s_t, a^i) + \gamma V(s_{t+1})]$
    end if
    $A_{-i} = A_{PU} - \{a^i\}$
  end for
  for $k = 1$ to no. SUs **do**
    if no. remaining RBs in the sub-state $s_t > 0$ **then**
      if rand $<= e$ **then**
        SU agent k will explore by taking an action a^k randomly from A_{SU}
      else
        SU agent k will exploit by taking an action a^k on a greedy basis from A_{SU}
      end if
      SU agent k will calculate the reward of executing action a^k
      SU agent k will update its Q-table based on the Q-Learning formula:
      $Q(s_t, a^k) \leftarrow (1 - \alpha)Q(s_t, a^k) + \alpha[r_{t+1}(s_t, a^k) + \gamma V(s_{t+1})]$
    end if
    $A_{-k} = A_{SU} - \{a^k\}$
  end for
end for

Actions and Actions set

The primary users action set A_{PU} consists of multiple actions, each action has a different number of resource blocks with unique indexes. This will avoid collisions between primary users agents since they all have access to this actions set.

$A_{PU} = \{a_1^{PU}, ..., a_n^{PU}\}$, a^{PU} is an action to be taken by primary user agent, n is the number of actions in A_{PU}. Each action has a different number of resource blocks with distinct indices, and they were set in a way to create an upper limit on how much resource blocks a primary user can get, in which a primary user can get almost fifth of the available resources at max.

The primary user agent deploys two types of decision policies in choosing an action. It will either explore or exploit depending on the value of the exploration parameter e. In the case of exploration, the agent will make a random choice in taking an action from the secondary users actions set. In the case of exploitation, the agent will make a greedy choice of what action to take from the secondary user actions set.

Rewards

After executing an action, the primary user agent will calculate the reward. The reward function for each primary user agent is chosen to optimize the primary user's average throughput. In this algorithm, it was assigned to be the actual user's average throughput.

Q-tables

After calculating the reward, the primary user agent will associate this reward with the action that resulted in this reward. Then the primary user agent will build or update its own Q-table. The agent builds its Q-table, by creating new entries as a result of exploring new actions. And the agent updates these entries as a result of choosing a pre-existing entries in the process of exploitation. The agent does these

operations according to the following formula:

$$Q(s_t, a^i) \leftarrow (1 - \alpha)Q(s_t, a^i) + \alpha[r_{t+1}(s_t, a^i) + \gamma V(s_{t+1})] \tag{6.5}$$

$V(s_{t+1})$ is determined by the policy of choosing an action at time t.

Secondary users scheduling stage

The secondary users scheduling stage in the Competitive Competitive scheduling algorithm is done exactly as the secondary users scheduling stage in the Collaborative Competitive scheduling algorithm.

6.5 Experiments

6.5.1 Experiments set-up

Experiments variables

The Network deployment of the experiments' set-up consists of one macro-cell which serves 5 PUs and 5 SUs. The macro-cell has a range of 1Km of diameter, and it is served with an eNodeB of 43 dB power. The bandwidth of the Macro-cell is 15 MHz. Which means there will be a total of 75 Resource Blocks, each with a bandwidth of 0.2 MHz. The Number of Epochs was set to 100. The exploration parameter e was set to 0.5. The learning rate α was set to 0.8. The discount factor γ was set to 0.9. And each experiment was run 200 times and their results were averaged.

Experiments scenario

In the main experiment scenario which was applied to both algorithms, the group of all the primary users had a full access to 100% of the total spectrum at any time, and the secondary users were allowed to access what is left of the available resource blocks of the spectrum after scheduling the primary users.

Experiments objective

The aim of these experiments is to test and compare the performance of both scheduling algorithms, and to measure how much of the spectrum each will utilize when there is 100% demand on the spectrum. The performance measurements were based on the throughput percentages that each user acquired from the total macro-cell bandwidth, and the fairness level of sharing the spectrum among users.

6.5.2 Experiments results

The results are displayed in Figures 6.1 and 6.2. In these figures, the simulation results displays the throughput percentages on the Y-axis, and the Number of Epochs on the X-axis. The "PUs percentages" are five curves, in which each curve represent the percentage that each primary user obtained of the spectrum. The "SUs percentages" are five curves, in which each curve represent the percentage that each secondary user obtained of the spectrum. The Total percentages is a one curve that represent the sum of all the ten percentages.

As regards to the use of the Collaborative Competitive scheduling algorithm, its performance results are displayed in figure Figure 6.1. As results shows, the algorithm converged very quickly to 91% utilization of the spectrum total throughput. This utilization of the spectrum consisted of the sum of all the users' percentages. All of

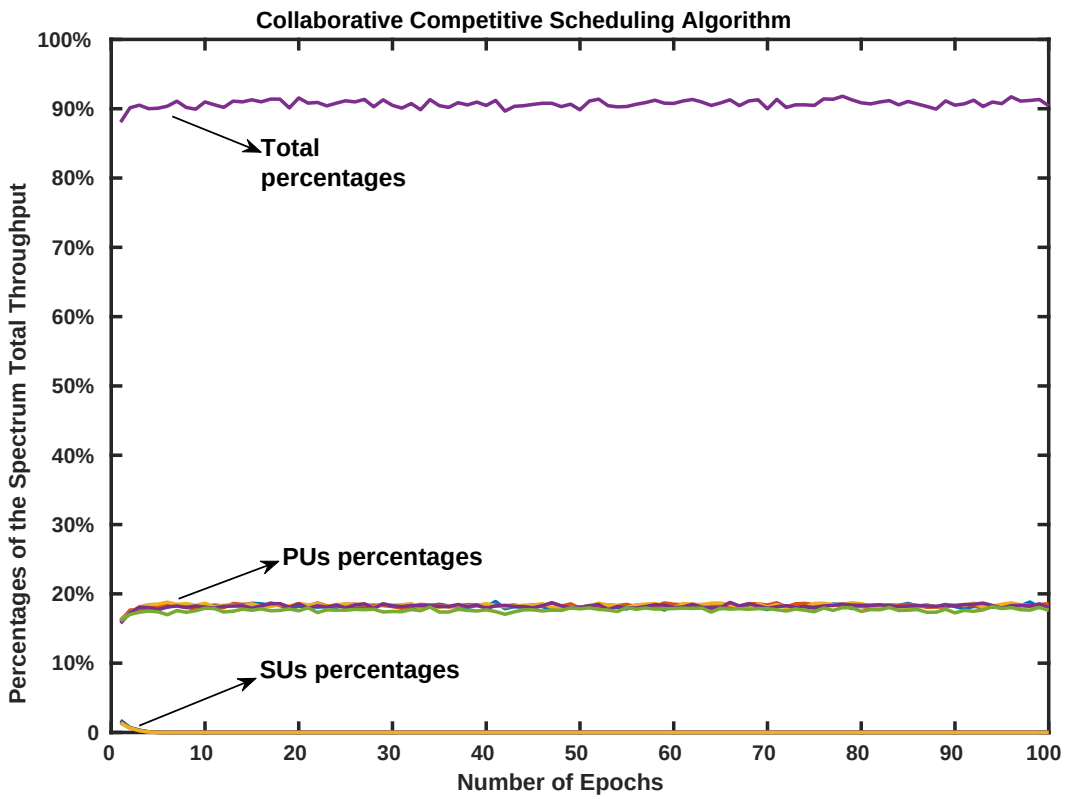

Figure 6.1: Percentages of the total system throughput usage while using the Collaborative Competitive scheduling algorithm

this spectrum utilization resulted from what the primary users acquired, in which it was distributed among them in fair shares. The distribution of the available resources followed a fair approach in which each primary user of the five had almost 18% of the spectrum, and this is because the scheduling process was based on actions that were influenced by the reward that is based on the Jain's fairness index. This helps the primary user agents to make a better joint action of how the available resources should be shared. And eventually lead to a fair distribution of the available resources and higher utilisation of the spectrum. As regard to the secondary users, they got

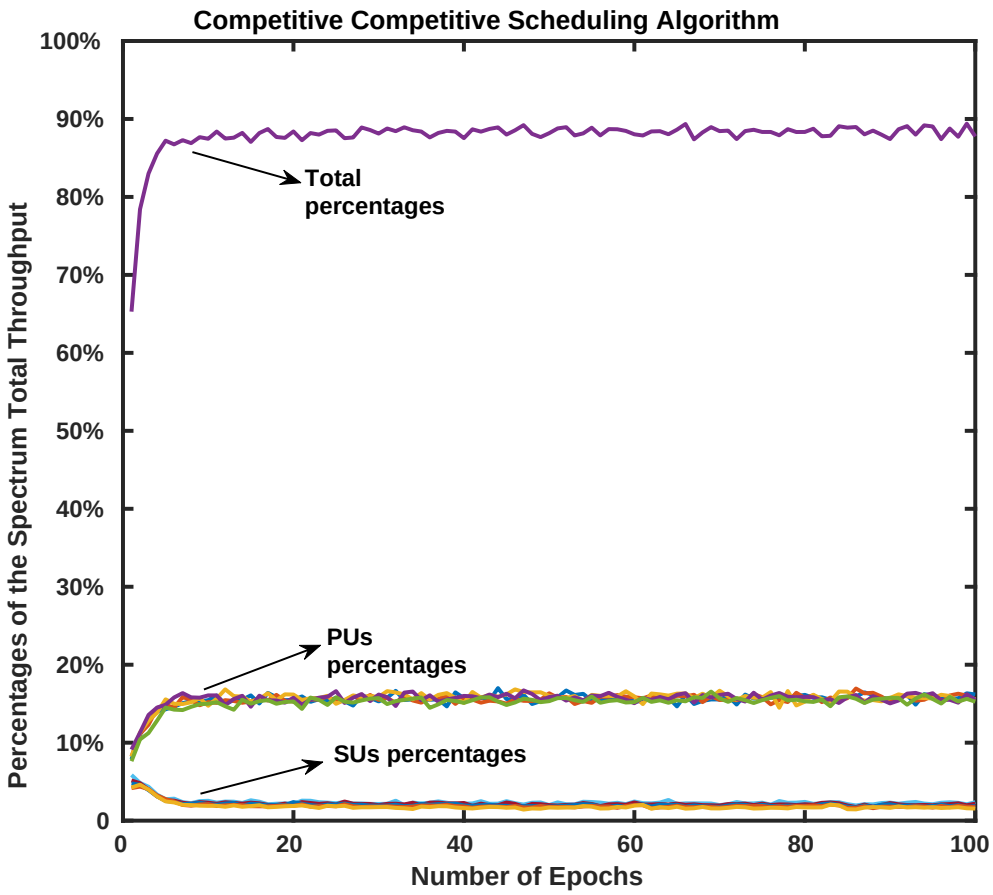

Figure 6.2: Percentages of the total system throughput usage while using the Competitive Competitive scheduling algorithm

low percentages, and this is because they had to compete over 9% of the spectrum.

As regards to the use of the Competitive Competitive scheduling algorithm, its performance results are displayed in Figure 6.2. As results shows, the algorithm also converged very quickly to 88% utilization of the spectrum total throughput. This utilization of the spectrum consisted of the sum of all the users' percentages. The PUs percentages resulted in a 75% of the spectrum, each primary user obtained 15% of the spectrum. The distribution of the resources followed a fair approach without

the use of Jain's fairness as the function reward because there was an upper limit on how much resources each primary user can get by controlling the amount of resources that the actions in the actions sets can provide, in which each primary user can get almost fifth of the spectrum resources at max. In regard to the secondary users, they got 25% of the spectrum to compete over. And they were able to obtain 15% of the spectrum, each secondary user obtained 3% of the spectrum. The fair way of distributing the remaining resources was also due to forcing a limit on how much each secondary user can get at max, in which each one of them can get almost fifth of the remaining resources at max.

6.6 Conclusion

In this chapter we proposed, implemented, and tested two novel scheduling algorithms. The Collaborative Competitive scheduling algorithm, and the Competitive Competitive scheduling algorithm. These algorithms schedule two types of users; the primary users which represent the licensed subscribers, and the secondary users which represent the unlicensed subscribers. The implementation and testing was done using Matlab. Testing the performance measurements was based on the throughput percentages that each user acquired from the total macro-cell bandwidth, and the fairness level of sharing the spectrum among users. Experiments results showed that both scheduling algorithms converged to almost 90% utilization of the spectrum. However, the Collaborative Competitive scheduling algorithm provided all this utilization of the spectrum to the primary users, in which they pay for their service. In terms of distributing the resources in fair shares among users, both algorithms provided an equal degree of fairness. However, they differed in their mechanism of doing so. The Collaborative Competitive scheduling algorithm forced the fairness by using the jains fairness index as the reward calculation for the joint action. The

Competitive Competitive scheduling algorithm forced the fairness among the users by creating an upper limit on how much each user can get by controlling the amount of resources that the actions in the actions sets can provide. In conclusion, it is recommended to use the Collaborative Competitive scheduling algorithm due to the high utilization of the spectrum which it can provide to the primary users, and due to the high fairness degree of distributing the resources among the primary users without the need of using any upper limit on how much each users can get.

Chapter 7

Summary of the Dissertation and Research Directions

In the following, we summarize the main aspects and contributions of this dissertation, and propose possible research direction that can be addressed in future work.

7.1 Summary of the Dissertation

In Chapter 2, we provided a detailed explanation of the main features that are included in the evolution process of LTE Release 8/9 to LTE-A release 10/11. This explanation covered carrier aggregation, LTE-A heterogeneous networks, relays and backhaul, coordinated multi-point operation, inter-cell interference coordination, and enhanced inter-cell interference coordination. Then, we briefly explained the road map beyond LTE-A to 5G cellular networks. The importance of this chapter to begin this dissertation with, is to provide a laying foundation to understand the technologies which were further studied and modelled in the dissertation following chapters.

In Chapter 3, we provided a QoS performance study of channel-aware/QoS-aware scheduling algorithms, the modified largest weighted delay first, Log-Rule, and Exp-Rule. We started by modifying the LTE-Sim simulator to allow it to support the use of the intra-band continuous case of carrier aggregation. Then, we run experiments with different scenarios and different parameters. These experiments aimed to study the behaviour of these three algorithms when the network is congested. The network model included a macro-cell to operate as an LTE Release 8/9, and a macro-cell that is supported by the CA feature to operate as LTE-A Release 10/11. In addition, there was a comparison among the scheduling algorithms in both cases. The QoS performance evaluation was in terms of the QoS parameters, the system's average throughput, Packet Loss Rate, average packet delay, and fairness among users. Finally, we provided the detailed experiments results, and explained them.

In Chapter 4, we provided another QoS performance study of Disjoint Queue Scheduler (DQS) for video-applications over LTE-A HetNets on the users' QoS, in which users were classified into macro-cell users or pico-cell users based on their location and service coverage. We further modified the LTE-Sim to support the use of DQS for an LTE-A HetNet deployment of a macro-cell and a variable number of pico-cells. Then, we run experiments with different scenarios and different parameters. These experiments aimed to study the QoS performance of a three cross carrier aggregation scenarios on each users' class separately. The first aggregation scenario included the use of the DQS that is based on the MLWDF scheduling algorithm (DQS MLWDF). The second aggregation scenario included the use of the DQS that is based on the EXP-Rule scheduling algorithm (DQS EXP-Rule). The third aggregation scenario included the use of the MLWDF and the use of a single carrier only (SC MLWDF). The QoS parameters which were studied include user average throughput, packet loss rate, and average packet delay. Finally, we provided the detailed experiments results, and explained them.

In Chapter 5, we provided a detailed explanation of how Q-learning is a good technique to be used for packet scheduling in LTE cellular networks. We did this by explaining the concept of machine learning and how it is being used in cognitive radio, the concept of reinforcement learning, and the approach of using Q-learning in an LTE radio environment. The importance of this chapter to be part of this dissertation, is in laying the foundation of understanding this technique, in which it was used in the implementation of two novel scheduling algorithms that were proposed in the following chapter of this dissertation.

In Chapter 6, we proposed two novel multi-agent Q-Learning-based scheduling algorithms for LTE cellular networks. The first one is the Collaborative Competitive scheduling algorithm, and the second one is the Competitive Competitive scheduling algorithm. These two scheduling algorithms were proposed as a solution to the problem of scheduling two types of users, the primary users over the available radio resource blocks, and the secondary users over the remaining resources "spectrum holes". Then, we implemented these algorithms using Matlab. Then, we run experiments to test the performance of these algorithms in terms of the throughput percentages that each user acquired from the total macro-cell bandwidth, and the fairness level of sharing the spectrum among users. Finally, we provided the detailed experiments results, and explained them.

7.2 Future Research Directions

The research work which was done in Chapter 6 could be extended to support more scenarios, and to include the new features of LTE-A and LTE-A pro, and to build different network models, and to apply different machine learning techniques.

References

[1] 3gpp, "about 3gpp home," [online]. available:. http://www.3gpp.org/about-3gpp/about-3gpp.

[2] 3gpp, "carrier aggregation explained." [online]. available:. http://www.3gpp.org/technologies/keywords-acronyms/101-carrier-aggregation-explained.

[3] 3gpp, "lte." [online]. available:. http://www.3gpp.org/technologies/keywords-acronyms/98-lte.

[4] 3gpp, "a new logo for 5g specifications," [online]. available:. http://www.3gpp.org/news-events/3gpp-news/1825-5g-logo_news.

[5] 3gpp, "ericson mobility report. on the pulse of the networked society," [online]. available:. http://www.ericsson.com/res/docs/2015/ericsson-mobility-report-june-2015.pdf.

[6] 3gpp, "lte-advanced pro ready to go," [online]. available:. http://www.3gpp.org/news-events/3gpp-news/1745-lte-advanced_pro.

[7] A. basir, "icic and eicic," [online]. available:. http://4g-lte-world.blogspot.com/2012/06/icic-and-eicic.html.

[8] Agilent technologies, "introducing lte-advanced," [online]. available:. http://cp.literature.agilent.com/litweb/pdf/5990-6706EN.pdf.

[9] Anritsu, "lte resource guide." [online]. available:. http://www.3gpp.org/technologies/keywords-acronyms/98-lte.

[10] Anritsu, "understanding lte-advanced carrier aggregation." [online]. available:. http://downloadfile.anritsu.com/RefFiles/en-GB/Promotions/Understanding-Carrier-Aggregation-web.pdf.

[11] F. rayal, “unleashing the power of hetnets: Interference management techniques for lte-advanced networks,” [online]. available:. https://communities.cisco.com/community/solutions/sp/mobility/blog/2013/03/18/unleashing-the-power-of-hetnets-interference-management.

[12] Fcc, "700 mhz public safety spectrum" [online]. available:. https://www.fcc.gov/general/700-mhz-public-safety-spectrum-0.

[13] Fcc, "auction 92: 700 mhz band" [online]. available:. http://wireless.fcc.gov/auctions/default.htm?job=auction_summary&id=92.

[14] Federal communications commission spectrum policy task force, "report of the spectrum efficiency working group" [online]. available:. https://transition.fcc.gov/sptf/files/SEWGFinalReport_1.pdf.

[15] Fujitsu, “enhancing lte cell-edge performance via pdcch,” [online]. available:. http://www.fujitsu.com/us/Images/Enhancing-LTE-Cell-Edge.pdf.

[16] Huawei, “the second phase of lte-advanced lte-b: 30-fold capacity boosting to lte” [online]. available:. http://www.google.com/url?sa=t&rct=j&q=&esrc=s&source=web&cd=1&ved=0CCsQFjAA&url=http%3A%2F%2Fwww.huawei.com%2Filink%2Fen%2Fdownload%2FHW_259010&ei=9EtfUvnkD4OtigLzp4CICw&usg=AFQjCNGqWt91brhtxabWq_-Zqb0QJqOTew&bvm=bv.54176721,d.cGE.

[17] Long term and scripting tutorials, “enhacement inter-cell interference coordination (eicic),” [online]. available:. http://tweet4tutorial.com/tutorial/enhancement-inter-cell-interference-coordinationeeicic/.

[18] Mark lee, "1.3 elements of reinforcement learning." [online]. available:. https://webdocs.cs.ualberta.ca/~sutton/book/ebook/node9.html.

[19] Nokia networks, “lte release 12 and beyond,” [online]. available:. http://networks.nokia.com/sites/default/files/document/nokia_lte_a_evolution_white_paper.pdf.

[20] Pool david, "artificial intelegence, foundations of computational agents" [online]. available:. http://artint.info/html/ArtInt_265.html.

[21] Radio-electronics.com, "lte frequency bands and spectrum allocations" [online]. available:. http://www.3gpp.org/technologies/keywords-acronyms/98-lte.

[22] Rohde and schwarz, “lte-advanced (3gpp rel.11) technology introduction,” [online]. available:. http://cdn.rohde-schwarz.com/dl_downloads/dl_application/application_notes/1ma232/1MA232_1E_LTE_Rel11.pdf.

[23] Stefan parkvall, "release 14 - the start of 5g standardization" [online]. available:. https://www.ericsson.com/research-blog/lte/release-14-the-start-of-5g-standardization/.

[24] Tata consultancy services, "radio resource management - radio admission control and bearer control." [online]. available:. http://www.tcs.com/SiteCollectionDocuments/White%20Papers/Telecom-Whitepaper-Radio-Resource-Management.pdf.

[25] Telecom abc, "telecom abc," [online]. available:. http://www.telecomabc.com/.

[26] Wikipedia, "radio resource management." [online]. available:. https://en.wikipedia.org/wiki/Radio_resource_management.

[27] Ian F Akyildiz, Won-Yeol Lee, Mehmet C Vuran, and Shantidev Mohanty. Next generation/dynamic spectrum access/cognitive radio wireless networks: a survey. Computer networks, 50(13):2127–2159, 2006.

[28] Ian F Akyildiz, Won-Yeol Lee, Mehmet C Vuran, and Shantidev Mohanty. A survey on spectrum management in cognitive radio networks. IEEE Communications magazine, 46(4):40–48, 2008.

[29] Ali Alfayly, Is-Haka Mkwawa, Lingfen Sun, and Emmanuel Ifeachor. Qoe-based performance evaluation of scheduling algorithms over lte. In Globecom Workshops (GC Wkshps), 2012 IEEE, pages 1362–1366. IEEE, 2012.

[30] Salman A AlQahtani and Mohammed Alhassany. Comparing different lte scheduling schemes. In Wireless Communications and Mobile Computing Conference (IWCMC), 2013 9th International, pages 264–269. IEEE, 2013.

[31] Jeffrey G Andrews, Holger Claussen, Mischa Dohler, Sundeep Rangan, and Mark C Reed. Femtocells: Past, present, and future. IEEE Journal on Selected Areas in Communications, 30(3):497–508, 2012.

[32] Matthew Andrews, Krishnan Kumaran, Kavita Ramanan, Alexander Stolyar, Phil Whiting, and Rajiv Vijayakumar. Providing quality of service over a shared wireless link. IEEE Communications magazine, 39(2):150–154, 2001.

[33] ChiSung Bae and Dong-Ho Cho. Fairness-aware adaptive resource allocation scheme in multihop ofdma systems. Communications Letters, IEEE, 11(2):134–136, 2007.

[34] Riyaj Basukala, Huda Adibah Mohd Ramli, and Kumbesan Sandrasegaran. Performance analysis of exp/pf and m-lwdf in downlink 3gpp lte system. In Asian Himalayas Regional International Conference on INTERNET, 2009.

[35] Mario Bkassiny, Yang Li, and Sudharman K Jayaweera. A survey on machine-learning techniques in cognitive radios. IEEE Communications Surveys & Tutorials, 15(3):1136–1159, 2013.

[36] Francesco Capozzi, Giuseppe Piro, Luigi Alfredo Grieco, Gennaro Boggia, and Pietro Camarda. Downlink packet scheduling in lte cellular networks: Key design issues and a survey. Communications Surveys & Tutorials, IEEE, 15(2):678–700, 2013.

[37] V Chandrasekhar, J Andrews, and A Gatherer. Femtocell networks: A survey, ieee communications magazine, 2008.

[38] Li Chen, Wenwen Chen, Xin Zhang, and Dacheng Yang. Analysis and simulation for spectrum aggregation in lte-advanced system. In Vehicular Technology Conference Fall (VTC 2009-Fall), 2009 IEEE 70th, pages 1–6. IEEE, 2009.

[39] Yuan Chen and Bernhard Walke. Analysis of cell spectral efficiency in 3gpp lte systems. In Personal Indoor and Mobile Radio Communications (PIMRC), 2013 IEEE 24th International Symposium on, pages 1799–1804. IEEE, 2013.

[40] Zhe Chen and Robert C Qiu. Cooperative spectrum sensing using q-learning with experimental validation. Proceedings of the IEEE SoutheastCon, Nashville, TN, USA, pages 17–20, 2011.

[41] Xiaolin Cheng, Gagan Gupta, and Prasant Mohapatra. Joint carrier aggregation and packet scheduling in lte-advanced networks. In Sensor, Mesh and Ad Hoc Communications and Networks (SECON), 2013 10th Annual IEEE Communications Society Conference on, pages 469–477. IEEE, 2013.

[42] Yao-Liang Chung, Lih-Jong Jang, and Zsehong Tsai. An efficient downlink packet scheduling algorithm in lte-advanced systems with carrier aggregation. In Consumer communications and networking conference (CCNC), 2011 IEEE, pages 632–636. IEEE, 2011.

[43] Yao-Liang Chung and Zsehong Tsai. A quantized water-filling packet scheduling scheme for downlink transmissions in lte-advanced systems with carrier aggregation. In Software, Telecommunications and Computer Networks (SoftCOM), 2010 International Conference on, pages 275–279. IEEE, 2010.

[44] Caroline Claus and Craig Boutilier. The dynamics of reinforcement learning in cooperative multiagent systems. AAAI/IAAI, (s 746):752, 1998.

[45] Ioan S Comşa, Mehmet Aydin, Sijing Zhang, Pierre Kuonen, and Jean-Frédéric Wagen. Reinforcement learning based radio resource scheduling in lte-advanced.

In Automation and Computing (ICAC), 2011 17th International Conference on, pages 219–224. IEEE, 2011.

[46] Ioan Sorin Comsa, Sijing Zhang, Mehmet Aydin, Pierre Kuonen, and Jean-Frederic Wagen. A novel dynamic q-learning-based scheduler technique for lte-advanced technologies using neural networks. In Local Computer Networks (LCN), 2012 IEEE 37th Conference on, pages 332–335. IEEE, 2012.

[47] Erik Dahlman, Stefan Parkvall, Johan Skold, and Per Beming. 3G evolution: HSPA and LTE for mobile broadband. Academic press, 2010.

[48] Dahlman E and Skold J. 4G LTE/LTE-Advanced for Mobile Broadband. Elseiver, 2011.

[49] A. Toskala H. Holma. LTE Advanced: 3GPP Solution for IMT-Advanced. Wiley, 2012.

[50] Simon Haykin. Cognitive radio: brain-empowered wireless communications. IEEE journal on selected areas in communications, 23(2):201–220, 2005.

[51] Zhongqiu He and Fei Zhao. Performance of harq with amc schemes in lte downlink. In Communications and Mobile Computing (CMC), 2010 International Conference on, volume 2, pages 250–254. Ieee, 2010.

[52] C Henrique and C Ribeiro. A tutorial on reinforcement learning techniques. In Proc. International Conference on Neural Networks, 1999.

[53] Harri Holma and Antti Toskala. LTE for UMTS-OFDMA and SC-FDMA based radio access. John Wiley & Sons, 2009.

[54] Josep Colom Ikuno, Martin Wrulich, and Markus Rupp. System level simulation of lte networks. In Vehicular Technology Conference (VTC 2010-Spring), 2010 IEEE 71st, pages 1–5. IEEE, 2010.

[55] Mauricio Iturralde, Tara Ali Yahiya, Anne Wei, and A-L Beylot. Performance study of multimedia services using virtual token mechanism for resource allocation in lte networks. In Vehicular Technology Conference (VTC Fall), 2011 IEEE, pages 1–5. IEEE, 2011.

[56] Dhananjay Kumar, NN Kanagaraj, and R Srilakshmi. Harmonized q-learning for radio resource management in lte based networks. In ITU Kaleidoscope: Building Sustainable Communities (K-2013), 2013 Proceedings of, pages 1–8. IEEE, 2013.

[57] Haeyoung Lee, Seiamak Vahid, and Klaus Moessner. A survey of radio resource management for spectrum aggregation in lte-advanced. Communications Surveys & Tutorials, IEEE, 16(2):745–760, 2014.

[58] Husheng Li. Multi-agent q-learning for competitive spectrum access in cognitive radio systems. In Networking Technologies for Software Defined Radio (SDR) Networks, 2010 Fifth IEEE Workshop on, pages 1–6. IEEE, 2010.

[59] Yang Li, Sudharman K Jayaweera, Mario Bkassiny, and Chittabrata Ghosh. Learning-aided sub-band selection algorithms for spectrum sensing in wide-band cognitive radios. IEEE Transactions on Wireless Communications, 13(4):2012–2024, 2014.

[60] Bin Liu, Hui Tian, and Lingling Xu. An efficient downlink packet scheduling algorithm for real time traffics in lte systems. In Consumer communications and networking conference (CCNC), 2013 IEEE, pages 364–369. IEEE, 2013.

[61] David Lopez-Perez, Ismail Guvenc, Guillaume De la Roche, Marios Kountouris, Tony QS Quek, and Jie Zhang. Enhanced intercell interference coordination challenges in heterogeneous networks. IEEE Wireless Communications, 18(3):22–30, 2011.

[62] Wang Miao, Geyong Min, Yuming Jiang, Xiaolong Jin, and Haozhe Wang. Qos-aware resource allocation for lte-a systems with carrier aggregation. In Wireless Communications and Networking Conference (WCNC), 2014 IEEE, pages 1403–1408. IEEE, 2014.

[63] Joseph Mitola. Cognitive Radio Architecture The Engineering Foundations of Radio XML. John Wiley & Sons, 2006.

[64] Andrew Y Ng. Shaping and policy search in reinforcement learning. PhD thesis, University of California, Berkeley, 2003.

[65] Sinh Chuong Nguyen, Kumbesan Sandrasegaran, and Faisal Mohd Jamal Madani. Modeling and simulation of packet scheduling in the downlink lte-advanced. In Communications (APCC), 2011 17th Asia-Pacific Conference on, pages 53–57. IEEE, 2011.

[66] Christantus Obinna Nnamani, Chidera Linda Anioke, and Cosmas Ikechukwu Ani. Improved mlwdf scheduler for lte downlink transmission. International Journal of Electronics, (just-accepted), 2016.

[67] novel mobile radio (nomor). Lte-a hetnets using carrier aggregation. [online]. available:. `http://www.nomor.de/uploads/db/a3/dba3e71e617a0ab4b7d3821afd59cc5e/Newsletter_CA_HetNet_2013-06.pdf`.

[68] Emmanouil Pateromichelakis, Mehrdad Shariat, Atta ul Quddus, and Rahim Tafazolli. On the evolution of multi-cell scheduling in 3gpp lte/lte-a. IEEE Communications Surveys & Tutorials, 15(2):701–717, 2013.

[69] Giuseppe Piro, Luigi Alfredo Grieco, Gennaro Boggia, Francesco Capozzi, and Pietro Camarda. Simulating lte cellular systems: an open-source framework. Vehicular Technology, IEEE Transactions on, 60(2):498–513, 2011.

[70] K Tuyls PJ't Hoen, L Panait, S Luke, and H la Poutré. An overview of cooperative and competitive multiagent learning. Learning and Adaptation in Multi-Agent Systems, pages 1–50.

[71] Huda Adibah Mohd Ramli, Riyaj Basukala, Kumbesan Sandrasegaran, and Rachod Patachaianand. Performance of well known packet scheduling algorithms in the downlink 3gpp lte system. In Communications (MICC), 2009 IEEE 9th Malaysia International Conference on, pages 815–820. IEEE, 2009.

[72] Daniel Robalo, Fernando J Velez, Rui R Paulo, and Giuseppe Piro. Extending the lte-sim simulator with multi-band scheduling algorithms for carrier aggregation in lte-advanced scenarios. In Vehicular Technology Conference (VTC Spring), 2015 IEEE 81st, pages 1–6. IEEE, 2015.

[73] JS Roessler. Lte-advanced (3gpp rel. 12) technology introduction white paper, 2015.

[74] Stuart Russell, Peter Norvig, and Artificial Intelligence. A modern approach. Artificial Intelligence. Prentice-Hall, Egnlewood Cliffs, 25:27, 1995.

[75] Bilal Sadiq, Ritesh Madan, and Ashwin Sampath. Downlink scheduling for multiclass traffic in lte. EURASIP Journal on Wireless Communications and Networking, 2009:14, 2009.

[76] Rony Kumer Saha. Modified proportional fair scheduling for resource reuse and interference coordination in two-tier lte-advanced systems. International Journal of Digital Information and Wireless Communications (IJDIWC), 3(2):149–168, 2013.

[77] Stefania Sesia, Matthew Baker, and Issam Toufik. LTE-the UMTS long term evolution: from theory to practice. John Wiley & Sons, 2011.

[78] Najem N Sirhan, Gregory L Heileman, and Christopher C Lamb. Traffic offloading impact on the performance of channel-aware/qos-aware scheduling algorithms for video-applications over lte-a hetnets using carrier aggregation. International Journal of Computer Networks & Communications (IJCNC), 7(3):75–90, 2015.

[79] Najem N Sirhan, Gregory L Heileman, Christopher C Lamb, and Ricardo Piro-Rael. Qos-based performance evaluation of channel-aware/qos-aware scheduling algorithms for video-applications over lte/lte-a. Computer Science & Information Technology (CS & IT), 5(7):49–65, 2015.

[80] Najem N Sirhan, Manel Martínez-Ramón, Gregory L Heileman, Nasir Ghani, and Christopher C Lamb. Qos performance evaluation of disjoint queue scheduler for video-applications over lte-a hetnets. In Proceedings of the 7th International Conference on Computing Communication and Networking Technologies, page 4. ACM, 2016.

[81] Richard S Sutton and Andrew G Barto. Reinforcement learning: An introduction, volume 1. MIT press Cambridge, 1998.

[82] Hui Tian, Songtao Gao, Jianchi Zhu, and Lan Chen. Improved component carrier selection method for non-continuous carrier aggregation in lte-advanced systems. In Vehicular Technology Conference (VTC Fall), 2011 IEEE, pages 1–5. IEEE, 2011.

[83] Pavithra Venkatraman and Bechir Hamdaoui. Cooperative q-learning for multiple secondary users in dynamic spectrum access. In IWCMC, pages 238–242, 2011.

[84] Yuanye Wang, Klaus I Pedersen, Preben E Mogensen, and Troels B Sørensen. Resource allocation considerations for multi-carrier lte-advanced systems operating in backward compatible mode. In Personal, Indoor and Mobile Radio Communications, 2009 IEEE 20th International Symposium on, pages 370–374. IEEE, 2009.

[85] Yuanye Wang, Klaus I Pedersen, Troels B Sørensen, and Preben E Mogensen. Carrier load balancing and packet scheduling for multi-carrier systems. Wireless Communications, IEEE Transactions on, 9(5):1780–1789, 2010.

[86] Fan Wu, Yuming Mao, Supeng Leng, and Xiaoyan Huang. A carrier aggregation based resource allocation scheme for pervasive wireless networks. In Dependable, Autonomic and Secure Computing (DASC), 2011 IEEE Ninth International Conference on, pages 196–201. IEEE, 2011.

[87] Minjie Xue, Kumbesan Sandrasegaran, Huda Adibah Mohd Ramli, and Cheng-Chung Lin. Performance analysis of two packet scheduling algorithms in downlink 3gpp lte system. In Advanced Information Networking and Applications Workshops (WAINA), 2010 IEEE 24th International Conference on, pages 915–919. IEEE, 2010.

[88] Kok-Lim Alvin Yau, Peter Komisarczuk, and Paul D Teal. Applications of reinforcement learning to cognitive radio networks. In 2010 IEEE International Conference on Communications Workshops, pages 1–6. IEEE, 2010.

[89] Su Yi and Ming Lei. Backhaul resource allocation in lte-advanced relaying systems. In Wireless Communications and Networking Conference (WCNC), 2012 IEEE, pages 1207–1211. IEEE, 2012.

[90] William Zame, Jie Xu, and Mihaela Van Der Schaar. Cooperative multi-agent learning and coordination for cognitive radio networks. IEEE Journal on Selected Areas in Communications, 32(3):464–477, 2014.

[91] Lei Zhang, Fei Liu, Lin Huang, and Wenbo Wang. Traffic load balance methods in the lte-advanced system with carrier aggregation. In Communications, Circuits and Systems (ICCCAS), 2010 International Conference on, pages 63–67. IEEE, 2010.

[92] Leiqi Zhang, YY Wang, Liwen Huang, HL Wang, and WB Wang. Qos performance analysis on carrier aggregation based lte-a systems. In Wireless Mobile and Computing (CCWMC 2009), IET International Communication Conference on, pages 253–256. IET, 2009.

[93] Leiqi Zhang, Kai Zheng, W Wang, and Liwen Huang. Performance analysis on carrier scheduling schemes in the long-term evolution-advanced system with carrier aggregation. Communications, IET, 5(5):612–619, 2011.

[94] Qing Zhao and Brian M Sadler. A survey of dynamic spectrum access. IEEE signal processing magazine, 24(3):79–89, 2007.